Experimental investigation & thermodynamic modeling of a diesel engine to analyze performance, energy, emission and exergy using edible and inedible biodiesel blends

Thesis submitted

by

Abhishek Samanta

DOCTOR OF PHILOSOPHY (ENGINEERING)

DEPARTMENT OF MECHANICAL ENGINEERING
FACULTY COUNCIL OF ENGINEERING & TECHNOLOGY
JADAVPUR UNIVERSITY
KOLKATA- 700 032
INDIA

2021

FACULTY COUNCIL OF ENGINEERING & TECHNOLOGY

JADAVPUR UNIVERSITY

KOLKATA- 700 032, INDIA

Index No. 207/16/E

1. Title of the thesis : **Experimental investigation & thermodynamic modeling of a diesel engine to analyze performance, energy, emission and exergy using edible and inedible biodiesel blends**

2. Name, Designation & Institution of the Supervisor :

Dr. Prokash Chandra Roy
Associate Professor
Department of Mechanical Engineering
Jadavpur University
Kolkata- 700 032, India

3. List of Publications : **Journal Publications:-**

1. Samanta, A. and Roy, P.C., **Pragmatic analysis on performance & emission and a single zone engine model development with inedible neem & waste vegetable oil biodiesel blend (B10)**, *International Journal of Energy for a Clean Environment*, vol. 22, Issue 1, pp. 53-89, 2021.
2. Samanta, A., Goswami, S. and Roy, P.C., **Producing Biodiesel and Optimized by Taguchi Design against Palm Oil as Sustainable Alternative Fuels in Bangladesh**, *International Energy Journal*, vol. 20, Special Issue 3A, pp. 411-420, 2020.
3. Samanta, A. and Roy, P.C., **An Empirical Investigation of Biodiesel Engine Fuelled with Palm Oil Methyl Ester Biodiesel Blends**, *International Journal of Vehicle Structures and Systems*, vol. 12, Issue 1, pp. 85-88, 2020.
4. Samanta, A. and Roy, P.C., **Repercussion of Neem Oil & Palm Oil Biodiesel Blends (B5 & B10) and Diethyl Ether & 1-Butanol with Palm Oil Biodiesel Blends On**

Performance of a Unmodified Diesel Engine, *International Journal of Mechanical and Production Engineering Research and Development*, vol. 10, Issue 3, pp. 1685-1692, 2020.

5. Samanta, A., Adhikary, A. and Roy, P.C., **Waste Cooking Oil Biodiesel: Its Testing, Performance and Emission in an Unaltered Diesel Engine**, *IOP Conf. Series: Materials Science and Engineering*, 1080 012034, 2021. ICAMEI 2021. DOI:10.1088/1757-899X/1080/1/012034.
6. Abhisek Samanta and Prokash C. Roy, Experimental and theoretical assessment of a diesel engine using different palm oil methyl ester (POME) blends at different compression ratio. **Under review, final version sent to Journal of The Institution of Engineers (India): Series C (published by Springer)**
7. Abhisek Samanta and Prokash C. Roy, Experimental investigation on a VCR using biodiesels obtained from different edible and inedible oils: comparisons. (**under preparation and to be communicated to Energy Journal (Elsevier)**)

4. List of Patents : NIL

5. List of Presentations in National/ International Conferences:

Paper presentation:-

International Conference

1. Samanta, A. and Roy, P.C., Combustion and performance characteristics of a VCR engine using palm oil methyl ester (POME) blended with diesel, International Conference on Energy and Sustainable Development 2020 (ICESD 2020), during 14-15 February 2020 at Jadavpur University, Kolkata 700032.
2. Samanta, A. and Roy, P.C., An empirical investigation on the combustion, performance characteristics and a single zone biodiesel engine model development of a compression ignition engine fuelled with palm oil methyl ester biodiesel blends, International Conference on Recent Developments in Mechanical Engineering (ICRDME 2019), during 21-22 March 2019 at S.A. Engineering College, Chennai 600 077.
3. Samanta, A. and Roy, P.C., Biodiesel from Palm oil as an alternative fuel for diesel engine", International Conference on Bioprocess for Sustainable Environment and Energy (ICBSEE 2018), during 6-7 December 2018 at National Institute of Technology Rourkela, Odisha 769001.

National Conference

1. Samanta, A. and Roy, P.C., Modeling and Performance Analysis of Compression ignition Engines using Biodiesel as Fuel, National Conference on Recent Trends in Emerging Science and Technology (NCRTEST 2016) during 29-30 March 2016, Camellia Institute of Technology, Kolkata 129.

“Statement of Originality”

I **Abhishek Samanta** registered on 3rd February, 2016 do hereby declare that this thesis entitled “**Experimental investigation & thermodynamic modeling of a diesel engine to analyze performance, energy, emission and exergy using edible and inedible biodiesel blends**” contains literature survey and original research work done by the undersigned candidate as part of Doctoral studies.

All information in this thesis have been obtained and presented in accordance with existing academic rules and ethical conduct. I declare that, as required by these rules and conduct, I have fully cited and referred all materials and results that are not original to this work

I also declare that, I have checked this thesis as per the “Policy on Anti Plagiarism, Jadavpur University, 2019”, and the level of similarity as checked by iThenticate software is **04** %.

Signature of Candidate:

Date:

Certified by Supervisor:

(Signature with date, seal)

FACULTY COUNCIL OF ENGINEERING & TECHNOLOGY

JADAVPUR UNIVERSITY

KOLKATA- 700 032, INDIA

CERTIFICATE FROM THE SUPERVISOR

This is to certify that the thesis entitled "**Experimental investigation & thermodynamic modeling of a diesel engine to analyze performance, energy, emission and exergy using edible and inedible biodiesel blends**" submitted by Shri **ABHISHEK SAMANTA,** who got his name registered on 3rd February, 2016 for the award of Ph. D. (Engineering) degree of Jadavpur University is absolutely based upon his own work under the supervision of Dr. PROKASH CHANDRA ROY and that neither his thesis nor any part of the thesis has been submitted for any degree/ diploma or any other academic award anywhere before.

……..

Signature of the Supervisor

and date with Office Seal

This thesis is dedicated to

my Parents

Mr. Satyajit Samanta, Mrs. Madhabi Samanta

my Wife

Debjani Santra Samanta

and my Parents-in-law

Mr. Ashok Kumar Santra, Mrs. Sukla Santra

ACKNOWLEDGEMENTS

Undertaking this research work, is a both pain and enjoyable life-changing experience. It's like climbing a high crest, step by step, accompanied with many hardship, frustration, bitterness, encouragement, trust and with so many assistances. During last five years I have been engaged in the field of engine research with biodiesel, and I find unique and exciting experience in my life. At the end of journey, when I discover the completeness of the present work with fruitful research outcomes, I realize that it is teamwork.

With immense pleasure I sincerely like to express my deepest gratitude and indebtedness to my respected supervisor Dr. Prokash Chandra Roy for guiding, teaching and inspiring me through the various phases of my research work. Dr. Roy's encouragement, trust on my work, unwavering support and patience have been helpful for overcoming difficult stages throughout the research work. I am in debt a lot to my supervisor to finish this dissertation.

I would like to takes this opportunity to express his profound gratitude and deep regards to the Head of The Department Prof Sumanta Neogi and all teachers in Mechanical Engineering Department, Jadavpur University.

I also wish to thank Dr. Shubhangi Gupta, Executive Director, Budge Budge Institute of Technology and Mr. Mayukh Nath Mishra, Officer-in-charge, Ranaghat Government Polytechnic, for their cooperation to carry out research parallel with teaching during the various stages of this research work.

I would also wish to express thanks to all the Laboratory In-charge and Technical Assistant in Heat Power laboratory, Chemical Engineering laboratory, Power Engineering and School of Energy Studies laboratory.

I would also like to thank all his other lab mates Sampad K. Das, Debashis Biswas, Anindya Adhikary and Sourav Goswami for their co-operation, help and motivation.

Finally, there are several people who deserve my appreciation for making this hard journey success. I would not forget to pay my gratitude to my father Mr. Satyajit Samanta and mother Mrs. Madhabi Samanta for their pathway to reach here to fulfill their dream in reality. I would also like to express my gratitude to my parents-in-law Ashok Kumar Santra and Sukla Santras for their unfailing emotional support. Thanks must also be given to my wife, Debjani Santra Samanta, who deserves special mention for being my best friend and my most ardent supporter and an endless source of inspiration during my research tenure. I am very much thankful for her compromise, faith, consistency, mildness, kindness, encouragement, word of confidence and eternal love.

Date …….. *……*

(Abhishek Samanta)

Synopsis

The demand for energy alternatives other than conventional fossil fuel is growing in the modern era as the rise in depleting fossil fuel prices and thriving interest in the environment. Most developing countries are primarily dependent on the supply from the volatile international market that affects their socio-economic growth. Non-renewable resources, such as fossil fuels, can be substituted by renewable resources such as biofuels obtained in liquid (biodiesel) and gaseous form (hydrogen, biogas, producer gas). By adopting new policies, generations of biodiesel have expanded in the modern era in numerous countries. Biodiesel is acknowledged as a 'green fuel' with diverse superiority compared to petroleum diesel. It is non-toxic, renewable, and safe to handle. Also, biodiesel is biodegradable. The low sulfur content with an increased flashpoint compared to petroleum diesel makes the biodiesel a promising suitable automotive fuel in the near future. According to FAO (Food and Agricultural Organization) Italy, the rapid escalation in biodiesel generation is alarming as biodiesel's extensive use would develop greater constrain on food supply, and adverse social and environmental consequences could arise. Though no possible unanimity can be validated, the high food price does not correlate with edible seed oil production. However, more significant investments in the agricultural sector offer probable everlasting convenience for agriculture and rural development.

In Malaysia, the palm tree was popularized since 1870 as an exquisite plant. In 2014 the universal production of oil had expanded about 155.8 million tons. Only in Malaysia, there was 60% growth of palm agricultural land by 2005. The fruit of the palm tree is produced two or three years after being planted. Palm trees produce fruit for twenty-five years. The amount of oil produced per hectare is more as compared to other oilseed crops. In 2014, Malaysia's government had mandated the adoption of 5% palm oil methyl ester biodiesel (B5) with petroleum diesel in

the transport sector entire nationwide. In 2018 researchers have claimed that industrial palm oil can yield sufficient biodiesel (POME) to balance Malaysia's total diesel consumption effectively. Diesel engine manufacturers provide engine warranties on biodiesel's consumption up to B7 in Malaysia, and the fact that without any significant modification, the diesel engine can handle biodiesel-diesel blends up to B100 (100% biodiesel) can promise a better future environment.

Global biodiesel generation is based on edible oil such as Palm, Sunflower, etc. However, in India, Bangladesh, and Pakistan, where scarcity of food is a prime concern, biodiesel production from edible oil is not very welcome. Some inedible oils are accessible in these countries, which are prescribed for biodiesel generation. Azadirachta Indica (neem) thrives in different regions of Asia (India, Bangladesh, etc.) in the genre 'maliaceae'. This herbal and holy tree can grow up to 18 meters with 40% oil content seed. Triglycerides and other triterpenoid composites are found in neem oil with mainly palmitic acid and stearic acid. Waste vegetable oil (WVO) indicates the oil after cooking, which is a waste product and is produced by food industries at the time of food formation. A noticeable hefty amount of WVO is spawned by the hotel, restaurant, and food chain industries and ditched into illicit dumping ground and river. The use of WVO in biodiesel production can cut down the production cost and hazardous waste dump.

In the long run, pure biodiesel directly in the engine can cause complications of injector & delivery valve clogging, severe engine deposits, and a sticky piston ring. Inedible vegetable oil biodiesel blend can be applied to compensate for the total consumption of petroleum diesel. Due to high viscosity, flash point, density, and low heating value, raw vegetable oil cannot be straightly used in an unmodified diesel engine. Vegetable oil is required to be transformed into biodiesel to achieve the required properties as engine fuel. The neem oil and waste cooking oil biodiesel from inedible sources can be utilized commercially as a counterfeit for petroleum diesel. Also, the esterifies product maintain tolerable fuel properties according to the American Society for Testing and Materials (ASTM), European Committee for standardization (EN) & Bureau of

Indian Standards (BIS). There are a thriving amount of works dedicated to the generation and application of various biofuels. In the modern era, the utmost prevailing substitute to Petroleum-based diesel is biodiesel; chemically, it was known as an alkyl ester of fatty acids from various plant and animal sources. Biodiesel has more oxygen in its structure cause of its organic nature, which allows widespread oxidation of fuel, resulting in complete combustion. Due to biodiesel's more significant cetane number, it has good self-ignition characteristics, which benefits in its combustion and permits achieving comparable thermal efficiency values regarding engine powered by diesel fuel. Biodiesel also reduces the formation of CO, HC, and soot particles in the engine. However, the NOx emission from the engine with biodiesel is found to be higher.

IC engines' exergy and energy analysis has been considered for almost decades to estimate the various losses developing during the CI engine operation. The value of useful work is represented by exergy, which a system can provide when moving toward the reference environment by a reversible process. Analysis of exergy can assess the location, type, and magnitude of energy losses in various engine areas. Hence, analysis of exergy provides a context to take necessary action for reducing the losses in different parts of the engine.

Numerous research works have been done on CI Engines in various capacities. Most of the works are cited based on the experimental investigation to find out the engine performance. Researchers are recently showing more interest in simulating the engine performance to get optimum engine operating parameters instead of build and test method that requires more time and expense. Commonly simulation of the engine can be done considering the engine cylinder volume as 'single zone," multi-zone,' and 'multidimensional'. Generally, single-zone thermodynamic models are used to have a fast and primary analysis of engine combustion and performance. In the single-zone model, it is assumed that the cylinder charge is a uniform or homogeneous mixture with the same temperature and composition for all the time during the engine cycle. The model must be based on empirical heat-release laws to use a single-zone model

in diesel engines. A multidimensional model sets the cylinder's space on a fine grid, but it requires detailed information of many phenomena inside the combustion chamber. This kind of approach has its disadvantage in computational time and the need for massive storage space. The multi-zone model is an intermediate step between single-zone and multidimensional models. Multi-zone models can be effectively used to model diesel engine combustion systems. However, Multi-zone models are generally not any good than single-zone models since the phenomena of zone characteristics and interactions inside the combustion chamber are unknown. Single-zone models are one of the simplest and fastest methods to model engine combustion processes.

Based on the above discussions, the present work deals with biodiesel production from three different vegetable oil. Biodiesel production from edible palm oil, inedible neem oil, and waste vegetable oil was executed, and biodiesel's characteristics were studied. Palm oil has been established as a suitable biodiesel resource in various countries. Neem oil (considered inedible but herbal tree) is available in India and tropical regions. Waste vegetable oil is a waste product produced by food industries and available in plenty throughout the world. The optimal parameters as catalyst concentration, the molar ratio of methanol and oil, reaction time, and temperature for high biodiesel yield of palm oil biodiesel were determined by the Taguchi method. An experimental investigation to study the combustion, performance, emission characteristics of biodiesel fired C. I. engine were carried out with different biodiesel blends (B5, B10, B15, B20) under various engine load conditions at three different compression ratios. The energy in terms of shaft energy and associated energy loss and exergy as exergetic efficiency were analyzed based on experimental data. Also, the CI engine model was developed in an in-house code using a single zone approach fueled with biodiesel blends. The combustion product model was incorporated in the model. Finally, the CI engine simulation model was validated with the experimental results fueled with biodiesel blends.

Contents

List of Figures

List of Tables

Nomenclature

4-S	Four Stroke
ASTM	American Society For Testing And Materials
B0	100% Petroleum Diesel
B10	10% Biodiesel +90% Petroleum Diesel
B15	15% Biodiesel +85% Petroleum Diesel
B20	20% Biodiesel +80% Petroleum Diesel
B5	5% Biodiesel +95% Petroleum Diesel
BP	Shaft Power
BSEC	Brake-Specific Energy Consumption
BTE	Brake Thermal Efficiency
CA	Crank Angle
CCD	Central Composite Design
CD	Combustion Duration
CI	Compression Ignition
CO	Carbon Monoxide
CP	Cylinder Pressure
CR	Compression Ratio
EBP	Ethanol Blending Programme
EE	Exergetic Efficiency

A	Valve Area
A_{ch}	Surface Area Of Cylinder Head
A_p	Cross Sectional Area Of A Flat Topped Piston
B	Bore
C_{pe}	Specific Heat Of Exhaust
C_{pw}	Specific Heat Of Water
E^0_1	Transfer Rate Of Exergy Of Incoming Air
E^0_2	Transfer Rate Of Exergy Of Incoming Fuel
E^0_3	Transfer Rate Of Exergy Of Exhaust
E^0_4	Transfer Rate Of Exergy Of Shaft Work
E^0_5	Transfer Rate Of Exergy Of Heat Transfer To Coolant
E^0_6	Transfer Rate Of Exergy Of Heat Transfer To Atmosphere
E^0_{ch}	Chemical Rate Of Exergy
E^0_{ds}	Rate Of Exergy Destruction
E^0_{ph}	Physical Rate Of Exergy
h	Heat Transfer Coefficient
k	Ratio Of Specific Heat
k	Adiabatic Index
l	Connecting Rod Length

EN	European Standard
EOC	End of Combustion
FFA	Free Fatty Acid
GC	Glycerol Column
HC	Unburnt Hydrocarbon
HHV	Higher Heating Value
ICE	Internal Combustion Engine
IEO	International Energy Outlook
KOH	Potassium Hydroxide
LF	Loss Function
LHV	Lower Heating Value
LTB	Larger The Better
M/O	Methanol to Oil Ratio
MFB	Mass Fraction Burned
NaOH	Sodium Hydroxide
NDIR	Nondispersive Infrared
NHR	Net Heat Release Rate
NO	Oxides of Nitrogen
NOME	Neem Oil Methyl Ester
NOx	Oxides of Nitrogen
NTB	Nominal The Better
OA	Orthogonal Arrays
OECD	Organisation for Economic Co-Operation and Development
OEM	Original Equipment Manufacturer

$\boldsymbol{m}$	Mass Flow Rate
$\boldsymbol{M}$	Mass
$\mathbf{m_a}$	Air Flow Rate In Engine
$\mathbf{m_{cw}}$	Water Flow Rate In Calorimeter
$\mathbf{m_f}$	Fuel Mass Flow Rate
$\mathbf{m_w}$	Water Flow Rate In Engine
N	Rotation Speed Per Minute
Ø	Equivalence Ratio
P	Engine Cylinder Pressure
$\boldsymbol{P}$	Cylinder Pressure
$\mathbf{P_0}$	Dead State Pressure
$\boldsymbol{Q}$	Quantity Of Heat Supplied To The System
Qe	Energy Loss By Exhaust Gases
Qin	Heat Energy Of Fuel
$\boldsymbol{Q_l}$	Heat Loss
$\mathbf{Q_{loss}}$	Heat Loss
Qs	Shaft Power
Qu	Unaccounted Losses
Qw	Energy In Cooling Water
R	Arm Length In Dynamometer
$\boldsymbol{r}$	Crank Radious
R	Ratio Of Connecting Rod Length To Crank Radius
$\boldsymbol{r_c}$	Compression Ratio
$\boldsymbol{S}$	Position Of Piston Pin From Crank Pin

OVAT	One Variable At a Time
POME	Palm Oil Methyl Ester
PPM	Parts Per Million
RPM	Rotation Per Minute
RSM	Response Surface Methodology
BSFC	Brake Specific Fuel Consumption
SNR	Signal to Noise Ratio
SOC	Start of Combustion
STB	Smaller The Better
TBO	Tree-Borne Oilseed
UHC	Unburned Hydrocarbon
Vs	Versus
w.r.t	With respect to
WC	Wash Column
WVO	Waste Vegetable Oil
WVOME	Waste Vegetable Oil Methyl Ester
τ_{id}	Ignition delay
θ	Crank angle
ϑ_{pis}	Average piston speed
T_0	Environment /Dead State Temperature
T_{atm}	Ambient Temperature
T_{cie}	Exhaust calorimeter inlet
T_{cio}	Exhaust calorimeter inlet temperature
T_{ciw}	Calorimeter water inlet
T_{coe}	Exhaust calorimeter outlet
T_{cow}	Calorimeter water outlet
T_g	Gas temperature
T_w	Wall temperature
T_{wie}	Engine cooling water inlet temperature
T_{woe}	Engine cooling water outlet temperature
U	Uncertainty
u	Internal energy
V	Engine cylinder volume
V_c	Clearance volume
V_d	Displacement volume
W	Load (kg)
x_b	Mass fraction burned
$z(\theta)$	Vertical piston position relative to TDC

Chapter 1

Introduction and Literature review

1.1 General Description and Applications

Significant dependency on the Internal Combustion Engine (ICE) for the transport and energy generation sector nowadays has entered over the past few decades. With an increase of 50% compared to the last 100 years, 60 million cars were produced globally only in 2012 **(Reitz, 2013)**. Wherein 2019, the number had increased to 67 million in car segments, and only in India, the total engine operated vehicle production was about 5 million in 2019[1]. ICE is used in the conventional approach for developing mechanical power using the chemical energy of fuel. Energy can be utilized from the resources of three categories, e.g., fissile, fossil, and renewable. The fundamental approach that described the durability & constancy of humanity's environmental, economic, and social aspects was termed 'sustainability' **(Das *et al.*, 2020)**. In the time of abrupt transformation in the environment appearing globally, it has been unavoidable to explore renewable energy resources with sustainability. As claimed by IEO (International Energy Outlook)-2019, fossil-based petroleum energy consumption has been raised in Asia. In non-OECD (Organisation for Economic Co-operation and Development) countries, India and other parts of Asia & Africa, where the average growth rate was about 4% and the population was about two-thirds of the global population in 2018; energy utilization would rise by nearly 70% between

[1] Source: International Organization of Engine Vehicle Manufacturers. Available in (at:http://www.oica.net/category/production-statistics/2019-statistics/). Accessed on June 30, 2020.

2018 and 2050 compared to a 15% rises in OECD regions[2]. It had been forecasted that the oil reserves would be depleted within some decades if the consumption increased at a rate of 3% annually **(Sharma and Singh, 2009)**. The amount of increased energy demand was 6.5% annually in India, but 80% of the crude oil demand was compensated by imports **(Suresh** *et al.***, 2018**). Hence energy security will be a significant factor shortly. The increase in energy utilization globally and nationally demands renewable resources for energy before the current conventional resources are crippled. In this context, biofuels have emerged, such as biodiesel. **Wan Ghazali** *et al.* **(2015)** reported that biodiesel specified as methyl ester was substantial to nature and consisted of fatty acids. Biodiesel was formed from triglycerides by the approach of transesterification. It is an alternative renewable fuel that lessens the heavy reliance on petroleum diesel. Biodiesel also has enormous considerable accomplishments in the global climate. Biodiesel is sulfur-free, oxygenate, and biodegradable. Investigators observed that biodiesel leads to a reduction in emissions, notably in the case of carbon monoxide, unburnt hydrocarbons, and soot emissions.

Bhuiya *et al.* **(2016)** reported that in the case of worldwide cumulative GHG emissions and energy consumption, petroleum products-based transportation occupied the third spot. This degree of usage of petroleum products would rise by 60% by 2030, primarily cause of industrialization, populace increment, and better ways of life. Biofuels are important cause of their supportability with petroleum derivatives, and it is renewable. Biofuels could be used on various kinds of diesel engine vehicles irrespective of climatic conditions. Improving the production of liquid biofuels, such as biodiesel, would provide accessibility to a cleaner, less expensive resource of energy rather than petroleum products. **Ghadge and Raheman (2005)** reported that various seed or grain oils had been utilized in a few nations as biodiesel resources

[2]Source: U.S. Energy Information Administration. "International Energy Outlook 2019 with projections to 2050". Available in (at: https://www.eia.gov/ieo). Accessed on June 30, 2020.

as per their accessibility. Oil from soybean seed is regularly used in Brazil, the United States, and Argentina. When oil from rapeseed is used generally in various European nations, palm oils are utilized for biodiesel in Indonesia and Malaysia. In India, Jatropha curcas (**Martínez** *et al*.**, 2014**) are used as acceptable biodiesel fuel. Vegetable oil resources, soybean oils, and rapeseed are usually utilized. However, different harvests, for example, palm oil, mustard, sunflower, hemp, and microalgae, are also promising (**Singh** *et al*.**, 2019**).

Edible vegetable oil, fats, and inedible oils, such as jatropha, and castor oil, were the resources being utilized (**Demirbas, 2008**). A few current investigations focused on using inedible oils to create biodiesel locally and economically (**BankovicIlic** *et al*.**, 2012; Kumar** *et al*.**, 2021**). Palm, Rapeseed, and soybean oils remained the established resources when neem, cotton, and mustard were now new oil plants (**Demirbas** *et al*.**, 2016**). The creation of biodiesel from inedible oilseeds has been considerably investigated throughout the most recent couple of years. Examples of inedible oil seeds that had been broadly utilized for biodiesel creation incorporated Jatrophacurcas, Madhucaindica, Pongamiapinnata and Azadirachtaindica (**Oyelade** *et al*.**, 2017**). There was an increase in the extraction of oils from inedible oil seeds utilized in creating biodiesel, which had the standard engine fuel properties and required no significant modification in the engine (**Avhad** *et al*.**, 2016**).

Naylor and Higgins (**2017**) reported that from an overall perspective, biodiesel was anticipated to shape 70% of transport fuel by 2040. Current policy and research have generally influenced the biodiesel industry's progress in various countries.

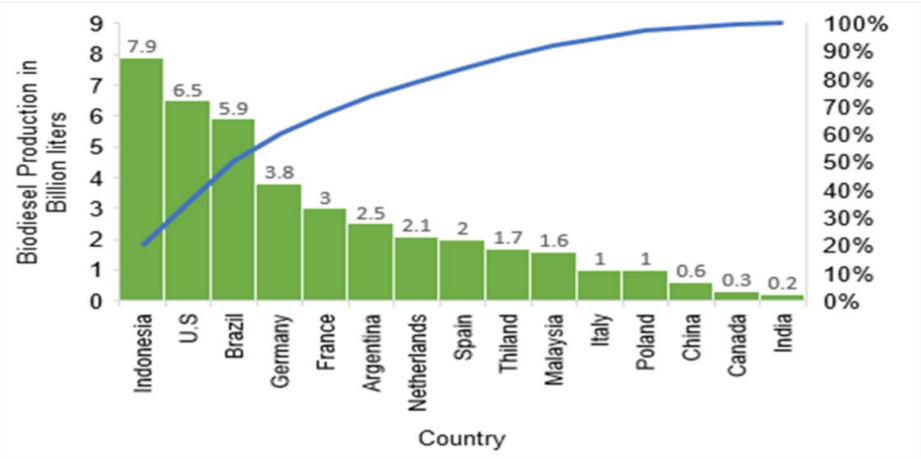

Figure 1.1: Biodiesel Production in 2019, worldwide in Billion liters[3].

Figure 1.1 shows the most raised 15 biodiesel making countries in 2019 as sustainable power organizations, but the biodiesel production in India is the least compared to other countries. The reason was discussed by **Saravanan** *et al.* (**2018**) as eight barriers; Economic, Technical, Trade, Infrastructure, Ethical, Knowledge, Political barriers and Conflict of interest. Economic barriers were associated with biodiesel production costs, whereas Technical and Trade barriers were mainly due to suitable conservation technology and quality standards. Still, the most serious ones were Knowledge, Ethical and Political barriers. There are many debates on food verse fuel thought, but on the other side, governments are providing subsidies for kerosene (petroleum-based fuel). If the developing countries can follow the leading biodiesel creators' improved design, biodiesel creation and vehicle engine application will continue increasing.

[3]Source: Leading biodiesel producers worldwide in 2019, by country (https://www.statista.com/). Accessed on November 26, 2020.

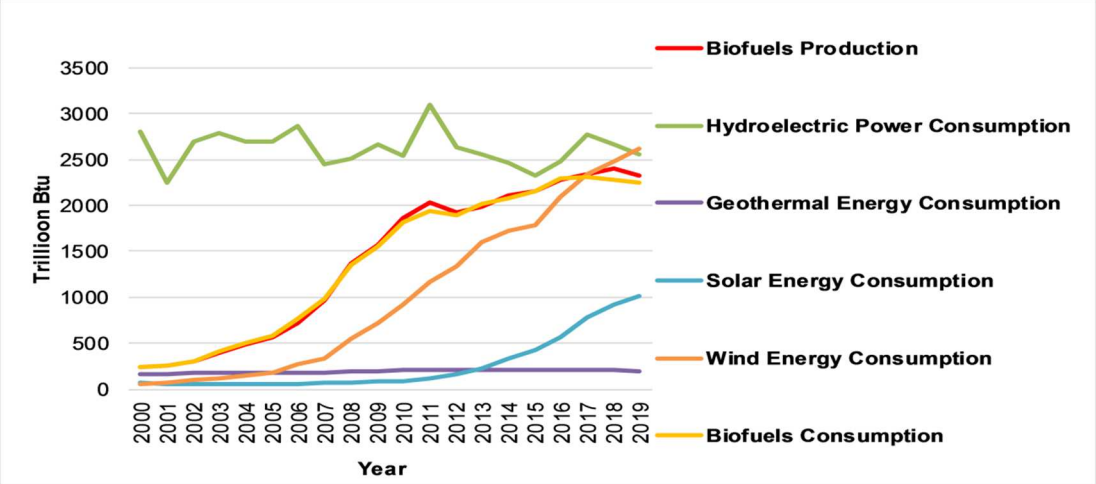

Figure 1.2: Renewable Energy Production and consumption in U.S, (EIA, 2020)[4]

As shown by EIA 2020 projections (figure 1.2) of the Annual Energy Viewpoint review, extended biofuel production should compensate for an increase in energy usage[5]. **Rosha** ***et al.*** **(2019)** suggested that a considerable degree of biodiesel blending with fossil diesel (up to B20) was needed to sustain the transport region's current energy demand and supply. This fuel blending can be maintained by the existing formative estimation that focuses on engine execution using higher blends of biodiesel–diesel. Engine research also needs the engine performance and emission investigation, demonstrating improved usage of higher biodiesel blends with no enormous engine modification. The most established conflict for biodiesel usage is the production rate similar to its consumption (figure 1.2).

[4]U.S Energy Information Administration, (https://www.eia.gov)
[5]U.S. Energy Information Administration, (https://www.eia.gov)

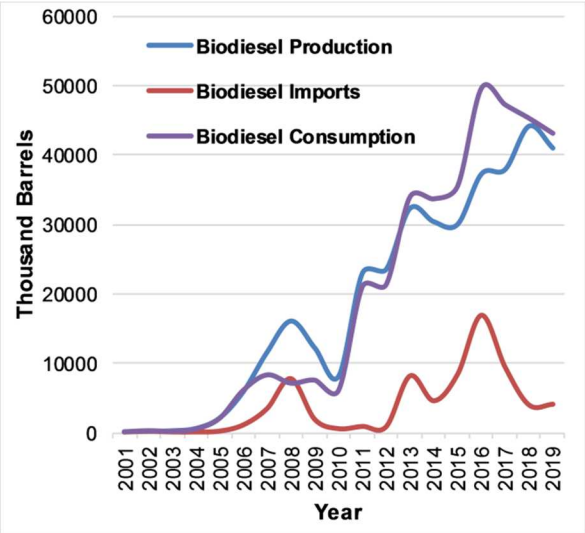

Figure 1.3: Biodiesel Production and consumption in U.S, (EIA, 2020)[6]

Still, hopefully, the scenario has changed for biodiesel in the current time (figure 1.3). In any case, biodiesel use could experience a lack of higher blending rates that were not acceptable in the transportation zone. Most biofuel usage in enormous quantities in developed countries happens at a low level of blending with petroleum-based products. Another limitation that can restrain the replacement of petroleum diesel is biodiesel's commercialization because biodiesel's advanced formation in the U.S. and E.U. comes primarily from palm oil or edible oil, which is limited in the resource since it is required as food in various countries. In this manner, the above discussion demonstrates that locally biodiesel production is so far falling behind. **Ogunkunle and Ahmed** (**2019**) suggested that the growing advancement could be a factor adding to biodiesel fuel's creation on a large scale. As production increases, the interest in transportation increases

[6]U.S Energy Information Administration, (https://www.eia.gov)

and the prerequisite for sustainable fuel comes. The circumstance will improve with the current industrialization and commercialization of biodiesel creation from inedible feedstocks.

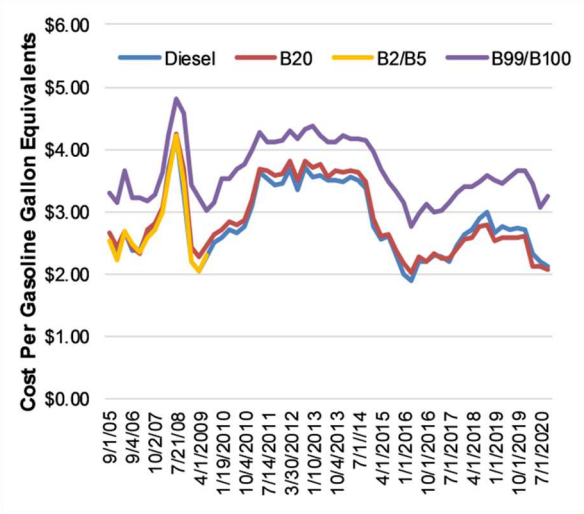

Figure 1.4: Biodiesel cost compared to Diesel in U.S.[7]

The diesel fuel utilized in a diesel engine is refined from crude petroleum, known as petroleum diesel. Biomass-based diesel fuels are biofuels produced using biomass or biomass materials and incorporated as renewable diesel or biodiesel. However, biodiesel can likewise utilize as a heating fuel (**Kumar** *et al*.**, 2016**). The fuels that can be used as immediate substitutes for petroleum diesel and give a similar vehicle efficiency are the biodiesel with ASTM standards, particularly ASTM D6751, and are recommended blends with diesel. Prices in figure 1.4 were presented in the units in which they are typically sold, dollars per gasoline gallon equivalent (GGE), and it was observed that the price of B20 and petroleum diesel were similar. Still, the price for B100 was higher compared to diesel. However, it could be said that the price difference

[7] Clean Cities Alternative Fuel Price Reports (https://afdc.energy.gov/fuels/prices.html)

would reduce in the future (**Setyawan, 2014**). In 2019, the U.S. consumed around 43 million barrels (1.8 billion gallons) of biomass-based diesel fuel, practically biodiesel blended with petroleum diesel[8]. The U.S. Environmental Protection Agency report for 2019 demonstrated that U.S. biodiesel utilization was around 900 million gallons. Government organizations in the U.S use biodiesel blends, usually B20, with school and travel buses, military vehicles, snowplows, etc. Fuel stations that sell biodiesel blends of B20 to the general public are accessible in practically every state[9].

1.2 Biodiesel as Engine Fuel

In the current era, diesel engine application is growing in various sectors, like construction, agriculture, power generation, and transport, cause of better thermal efficiency. Therefore, the pursuit of fossil-based petroleum diesel has increased at a sufficient rate. However, the various emissions are the prime concern of the diesel engine. The significant reduction of nitrogen oxide (NOx) and particulate matter (PM) in the conventional diesel engine is troublesome. There is an urgency for a suitable solution to minimize the PM and NOx to grab the benefit of good fuel economy with low carbon dioxide emission **(Yamaki** *et al.***, 1994)**. Diesel engine fueled with vegetable oil was approved on the requisition of the Government of France to build self-reliance in the energy sector in the provinces in Africa, which envisioned low-cost energy without relying on imported coal fossil fuel. Peanut oil for the initial test was selected as it was available in plenty in the tropical region. The French organization 'Otto' presented the peanut oil-powered diesel engine in 1900, Paris Exhibition. During this era, animal oil and castor oil-powered locomotive was tested by Rudolph Diesel **(Rodrigo** *et al.***, 2012)**.

[8]U.S Energy Information Administration, (https://www.eia.gov)
[9] U.S Energy Information Administration, (https://www.eia.gov)

Amid different alternative renewable fuels, biodiesel is considered the diesel engine's acceptable fuel for its better ignition quality, renewability, absence of aromatic and sulfur content, and biodegradability with low greenhouse gas emissions **(Semwal *et al.*, 2011)**. The application of biodiesel on a diesel engine can be adapted by small or without any modification. Moreover, the biodiesel properties are very close to diesel, but it has oxygen content bounded in fuel, and it has high miscibility with diesel without any blending agent. Also, biodiesel has magnificent lubricity to lessen wear and prolong the fuel injection pump life (**Tamilselvan *et al., 2017*).**

Biodiesel in any percentage can be mixed with diesel for a biodiesel blend, and it improves the mechanical efficiency of engines and cuts down the emissions of sulfur oxides **(Kumar, 2007)**. Due to biodiesel's high flashpoint, the operation safety is also enhanced, and anyone can apply it directly without any significant modification to the diesel engine **(Singh and Gu, 2010)**. Various car producers have recognized the idea that biodiesel is an energy source that is adaptable with their diesel vehicles **(Atabani *et al.*, 2013; Ashraful *et al.*, 2014)**.

Expanding industrialization demands energy and definite fossil fuel reserves, with tightening emission norms have created a demand to identify petroleum diesel substitutes. Global biodiesel generation is based on edible oil such as palm, sunflower, etc. However, in India, Bangladesh, and Pakistan, where scarcity of food is the prime concern, biodiesel production from edible oil is not very welcome. Some inedible oils are accessible in these countries prescribed for biodiesel generation (**Dhamodaran *et al.*, 2017**). **Neto Da Silva *et al.* (2006)** reported using sunflower methyl ester in a high-capacity diesel engine, which did not alter engine performance and fuel consumption more than diesel. Also, exhaust gas opacity did not change. However, there was no clear indication of a reduction in CO emission. A novel approach of rapeseed oil methyl ester fueled diesel engine with additional ethanol injection in inlet port was developed and suggested by **Kowalewicz (2007)**. In this approach, ethanol can be evaporated. During suction,

fresh air enters the engine cylinder with evaporated ethanol, which reduces the combustion period with a reasonable reduction in CO & HC emission at high loads and a reduction in NOx emission at low loads. Also, in the long run, pure biodiesel directly in the engine can cause complications of injector & delivery valve clogging, heavy engine deposits, and sticky piston rings.

Anyone can apply an inedible vegetable oil biodiesel blend to compensate for the total consumption of petroleum diesel. Due to high viscosity, flash point, density, and low heating value, raw vegetable oil can not be straightly used in an unmodified diesel engine. A combustion burner for highly viscous waste oil was developed by **Kawaguchi** *et al.* **(2004)** for proper oil atomization and emission reduction. In that burner, luminous flames with reduced NOx and CO emissions were observed, along with no black exhaust smoke. The study indicated the possibility of high combustion efficiencies of waste oil with less energy consumption in their study. The neem oil and waste cooking oil biodiesel from inedible sources can be utilized commercially as a counterfeit for petroleum diesel as the esterified product maintains tolerable fuel properties, according to the American Society for Testing and Materials (ASTM), European Committee for standardization (EN) & Bureau of Indian Standards (BIS) (**Singh** *et al.***, 2019**). The literature accessible on inedible oil biodiesel is finite. **Ramadhas** *et al.* **(2004)** reported that vegetable oil biodiesel could be applied in unmodified diesel engines. Also, the author recommended various advantages of biodiesel. Some authors have concluded the benefits of inedible oil biodiesel over petroleum diesel, specifying the operations required to improve the fuel properties of inedible oil biodiesel **(No** *et al.***, 2011)**. **Markov *et al.*** (**2019**) proposed a method with various criteria for composition optimization of blended biofuels. Mustard, linseed, and camelina oils were considered to reduce exhaust gas toxicity indicators in the diesel engine. It was reported that the application of B10 biodiesel-diesel blends reduces 4-10 % nitrogen oxide emission and 11-16% smoke opacity along with a 5-15% reduction in carbon monoxide and 11-17% light hydrocarbon

emission. Also, during the experiments, it was observed that the change in engine efficiency did not surpass 3% throughout the runtime.

Conventional engine emission products, PAH (polycyclic aromatic hydrocarbons), ketone, and aldehyde emission were also considered in the report. Concerning emission, the potential of methyl ester and different untreated oil against fossil diesel were advised before and after the treatment of exhaust emission with oxidation catalyst **(Koelch** *et al.***, 2005)**. There were various economic and substantial benefits of inedible oil for biodiesel production; researchers have defined the importance of pretreatment in inedible oil for biodiesel production **(Araújo** *et al.***, 2013)**. **Fernandes** *et al.* **(2013)** estimated the suitable arrangement for biodiesel production from inedible oil and waste recycling.

However, biodiesel also has particular deficiencies, like cold flow properties, inferior storage stability, and unsatisfactory spray characteristics with low heating value (**Misra and Murthy, 2011**). Though, these deficiencies can be conquered with suitable feedstock for biodiesel and processing techniques.

1.3 Biodiesel feedstock

Bart *et al***.** (**2010**) reported more than 350 oil-bearing feedstock as expected hotspots for biodiesel yield (**Bart** *et al***., 2010**). The feedstock should meet two fundamental prerequisites: low creation cost and huge maximum yield. The accessibility of feedstock for delivering biodiesel relies upon the provincial atmosphere, topographical areas, neighborhood soil culture, and agricultural policy.

Biodiesel feedstocks only contribute to 75% of biodiesel creation cost, as shown in figure 1.5.

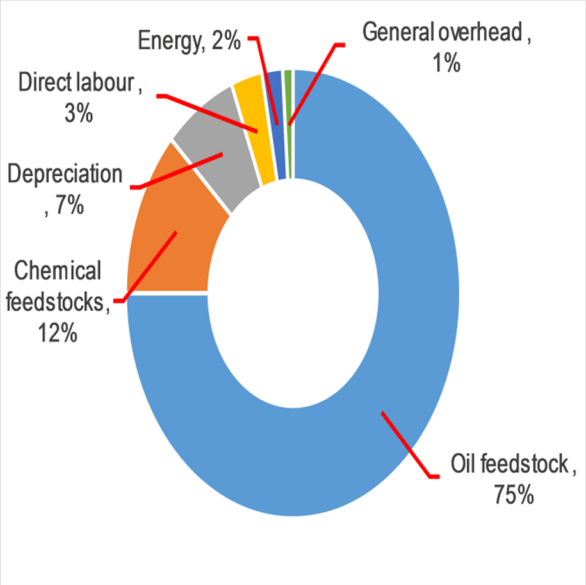

Figure 1.5: Common cost for biodiesel production (**Ahmad** *et al*.**, 2011**)

Therefore, choosing the least expensive resources is essential to guarantee the minimum creation expense of biodiesel. Table 1.1 presents the primary biodiesel resources.

Table 1.1: Primary feedstocks of biodiesel

Edible oils	Non-edible oils	Animal Fats	Other Sources
Palm (Elaeisguineensis)	Neem (Azadirachtaindica)	Fish oil	Algae (Cyanobacteria)
Soybeans (Glycine max)	Mahua (Madhucaindica)	Pork lard	Bacteria
Rice bran oil (Oryzasativum)	Jatropha (Jatropha curcas)	Poultry Fat	Fungi
Rapeseed (Brassica napus L.)	Pongamia (Pongamiapinnata)	Beef tallow	Latexes
Safflower (Helianthus annuus)	Castor (Ricinuscommunis)		

Balat (2011) suggested some conditions when looking at biodiesel feedstock. Every feedstock should be assessed dependent on a full life-cycle examination. This investigation

includes accessibility of land, development in agriculture, energy supply, the emission of ozone-depleting substances, soil disintegration, cost, water necessities, water availability, and feedstock impacts on air quality.

In 2017, the feedstock of worldwide biodiesel was palm oil, 31%, rapeseed oil and soybean oil contributed 20% and 27%, waste vegetable oil, 10%, and waste fats contributed 7% and 5% for other sources**.** As indicated by the Department of Agriculture of the United States, Asian nations, such as Indonesia, Thailand, and Malaysia, could deliver a generally high biodiesel measure contrasted with other Asian countries. The status of biodiesel and petroleum-based diesel in chosen Asian nations in 2018 was reported as Indonesia, Thailand and Malaysia, which produced 5600, 1567, and 1245 million liter biodiesel from Palm oil. China and Japan had produced 834 and 17 million liters of biodiesel from waste vegetable oil. In contrast, India had made 185 million liters of biodiesel from waste vegetable oil, inedible industrial oil, and animal fats. Still, the petroleum base diesel consumption was 2 to 5 times higher than other Asian countries except for China[10].

India began a program known as the National Biodiesel Mission in 2003, which included Jatropha curcas and a self-supporting extension of the program prompting bio-diesel creation to meet 20% of the nation's diesel necessities by 2011–2012[11]**.** Nonetheless, the application was troublesome due to a few issues, for example, nonattendance of establishment uphold, innovation upholds, and monetary help (**Kumar and Chaube, 2012**). Scientists in the nation have likewise been searching for new crude materials of biodiesel. India delivered 185 million liters of biodiesel in 2018, which depended on waste vegetable oil, inedible oil, and creature fats, while the

[10] UFOP, 2018. UFOP report on global market supply 2018/2019. https://www.ufop.de/files/4815/4695/8891/WEB_UFOP_Report_on_Global_Market_Supply_18-19.pdf.
[11] Gonsalves, J.B., 2006. An assessment of the biofuels industry in India. https://unctad.org/system/files/official-document/ditcted20066_en.pdf.

utilization of petroleum-based diesel was 102,079 million liters. Also, the government has altered the allowable emission levels of BS6 from 2020.

Oil-based palm is gleaned from palm fruit sapling, native Western Guinea. The palm tree was later introduced to different states. The palm tree was popularized in 1870 as a beautiful plant in Malaysia. In 2014 the universal production of oil had expanded by about 155.8 million tons. There was only a 60% growth of palm agricultural land in Malaysia by 2005 (**Ibragimov** *et al.***, 2019**). The fruit of the palm tree is produced two or three years after being planted. The palm tree had fruit for twenty-five years. The amount of oil yield per hectare is more as compared to other oilseed crops. In 2014, Malaysia's government mandated the adoption of 5% palm oil methyl ester (B5 POME) with petroleum diesel in the entire transport sector[12]. In 2018 researchers have claimed that industrial palm oil could yield sufficient biodiesel (POME) to effectively balance Malaysia's total diesel consumption. Diesel engine manufacturers provide engine warranties on biodiesel consumption up to B7 in Malaysia. Without any significant modification, diesel engines can handle biodiesel-diesel blends up to B100 (100% biodiesel) and promise a better future environment (**Szulczyk** *et al.***, 2018**). **Araby** *et al.* **(2018)** estimated the essential fuel requirements of Palm oil and POME blend with diesel, and results indicated that blended fuel values were very adjacent to petroleum diesel till 30% (B30). About 91.07% Palm oil Biodiesel yield was reported at 70°C with 2 to 3 hours reaction time at a 1:15 molar ratio of palm oil to methanol with catalyst concentration of 3 to 6 wt% KOH along with the support of heterogeneous catalysts. However, potassium-based species consumption was observed in both spent catalysts

[12]Adnan, H., 2014. Palm oil biodiesel program to cover all of Malaysia by July. The star online; 2014. https://www.thestar.com.my/business/business-news/2014/04/26/b5-goes-nationwide/ (accessed 15 July 2020).

(**Adeyemi** *et al.***, 2011**). Tables 1.2 represent the comparison between palm, neem, and jatropha vegetable oil sources.

Table 1.2: Comparison among Palm, Neem and Jatropha vegetable oil source (**Atabani*et al.*, 2013**)

Name	Distribution	Plant type	Plant part	Oil content		Yields		Uses
				Seed (wt%)	Kernel (wt%)	kg oil / ha	litres oil / ha	
Elaeis Guineensis (Palm)	Malaysia, Indonesia, Thailand, Brazil, Singapore, Argentina, USA	Tree	seed, kernel	30-60	30-60	5950	-	Edible oil., biodiesel
***Azadirachta Indica* (neem)**	Native to India, Burma, Bangladesh, Sri-Lanka, Malaysia Pakistan and Cuba, growing in tropical and semitropical regions	Tree	seed, kernel	20-30	25-45	2670	-	Oil-illuminant, timber, firewood, biodiesel
***Jatropha Curcas* (Jatropha)**	Indonesia, Thailand, Malaysia, Philippines, India, Pakistan, Nepal	Tree	seed, kernel	20-60	40-60	1590	1892	oil-Illuminant, lubricant, biodiesel

Enthusiastic researchers from Bangladesh have taken the initiative to develop biofuels (**Baeyens and Kang, 2015**). The introduction of a 5% bioethanol blend with conventional fuel in the transport sector has been planned by Bangladesh Government[13], though; no such activity has been reported in Bangladesh. Feedstock resources for biodiesel in Bangladesh have been

[13]Biofuels International, 2018. Bangladesh to Allow 5% Ethanol Blend. Biofuels Int Mag. BPDB, 2017. Annual Report: 2016-2017. Dhaka.

reviewed (**Habibullah** *et al.***, 2015**). However, the production of bioethanol from renewable feedstock has been overlooked. Among the various feedstock, palms retain high relevance. In the ancient world, people used the palm for sugar-producing. In addition to that, the palm can flourish in grim habitats, and its sap consists of about 10-20% sugar. The collector can collect the fluid without destroying the palm tree, and it can be aged approximately 5-100 years. A male palm tree could produce a 140.42 kg sugar-based mass with 29.85% sugar concentration per annum; however, a female tree could provide a 195.56 kg sugar-based mass (**Swaraz** *et al.***, 2019**). **Nabi** *et al.* **(2010)** from Bangladesh reported 96 vol% biodiesel yield at 60 °C with 22 vol% methanol and 0.45 wt% catalyst concentration from a vegetable feedstock. Also, the reduction in carbon monoxide emission and engine noise and smoke with all biodiesel blends was reported.

Azadirachta Indica (neem) thrives in different regions of Asia (India, Bangladesh, etc.) in the genre' maliaceae'. This herbal and holy tree can grow up to 18 meters with a 40% oil content seed. Triglycerides and other triterpenoid composites are found in neem oil, mainly palmitic acid and stearic acid (**Ali** *et al.,* **2013**). Waste vegetable oil (WVO) indicates the oil after cooking, a waste product produced by food industries at food formation. A noticeable hefty amount of WVO is spawned by the hotel, restaurant, and food chain industries and ditched into illicit dumping grounds and rivers. WVO use in biodiesel production can reduce production costs and hazardous waste dumps (**Capuano** *et al***., 2017**). Biodiesel production, only by alkaline esterification, the neem oil, and waste cooking oil, is challenging as these oils have high free fatty acids (FFA). However, acid catalyst esterification followed by alkali catalyst transesterification is used to transform large amounts of FFA oil into suitable methyl esters. Biodiesel leads to less emission as an oxygenated fuel.

There are various economic and substantial benefits of inedible oil for biodiesel production; researchers have defined the importance of pretreatment in inedible oil for biodiesel production (**Araújo** *et al.*, **2013**). **Fernandes** *et al.* **(2013)** have estimated the suitable arrangement for biodiesel production from inedible oil and waste recycling.

1.4 Availability of Biodiesel in India

In India, biofuel legislation could track the first biofuel legislation in 1948. Then the Parliament executed Act No. 22, Indian Power Alcohol Act, 1948. The Act's initial intention was to administer a fundamental approach to advancing the Indian 'power alcohol' production unit. However, Parliament abolished the Act in the year 2000. Finally, in 2002, the EBP was furnished by the Ministry of Petroleum and Natural Gas, which mandated with petrol 5% blending of ethanol. The Ethanol Blending Programme (EBP) was the ineffective cause of the deficiency of sugar molasses, non-observance to embrace ethanol pricing, technical set back by State agencies, obstruct procurement, and other reasons (**Saravanan** *et al*., **2018**).

India has empowered itself to produce roughly a quarter of the net fossil fuel demand (**Dhar and Shukla, 2015**). Though, to satisfy the deficit, resources are imported that exhaust a considerable sum of the country's foreign currency. Therefore, improving convenient technology and renewable energy can be treated as an assuring decision to the current ecological and energy difficulty (**Singh Pali** *et al.,* **2020**). Biodiesel importunity as 20% blending objective is predicted to increase by 19.8 liters in 2020 whereas 31.1 billion liters in 2030. In India, the biodiesel generation primarily concentrated on jatropha oilseed and other prospective tree brone oils have to be examined effectively (**Scarlat** *et al.,* **2015**). Therefore, for biodiesel generation and extensive endeavor, application of different unrealized edible & inedible oil feedstock to identify the complex challenges in biodiesel production as per the government's biofuel policy (**Kumar** *et*

al., **2012**). As suggested by India's biofuel policy, no solo feedstock can satisfy the pressure of 20% blending.

India's way of dealing with the biofuel program is described by a mix of reality and curiosity and the severe extent of aspiration inside them. It is novel because it did not depend on increasing or broadening traditional agriculture, regardless of whether for ethanol creation or biodiesel creation. On the other hand, various food grains like rapeseed, sugarcane, soybean, etc., are used by the USA, Brazil, and Germany. Furthermore, an unfavorable effect on edible oil accessibility may rise, which may increase food prices (**Pohit** *et al*.**, 2010**).

Biswas and Pohit (**2013**) reported that Indian producers were looking for a few oleic seeds-bearing plants in the forest developed in barren lands. Out of these, jatropha and Pongamia were chosen to create biodiesel to a small degree. The biodiesel mission partitioned it into two stages, Phase I and Phase II. For Phase I, the timeline was 2003 to 2007. Where initial time frame for phase II was 2007-2012. The main objective of this mission was to blend 20% biofuel within 2012. More or less 400 oil-bearing inedible crops are discovered in India. The use of jatropha gained much appreciation cause about 40% oil content with a low incubation time is extraordinary. Also, the decision was influenced because Latin America and Africa utilized jatropha for a similar reason. The mission went voluntarily with a few colleges and exploration establishments to create and select suitable vegetable feedstock. Very few oil marketing companies (OMC) are assigned to purchase and distribute biofuel under a settled value. Furthermore, only 700,000 hectares were assigned for jatropha cultivation which essentially little to satisfy the 20% blending objective across the nation. The mission lost interest by 2008 because of agricultural constraints and fluctuating production from jatropha.

Consequently, another strategy was acquainted with receiving a more extensive arrangement of plants creating inedible oils that could likewise be developed on barren land. The

legislature received in 2009 was the National Policy on Biofuels. Again, this activity's objective of a 20% blend with petroleum fuel was estimated by 2017. However, inedible and waste vegetable oil and variety in agroclimatic circumstances were promoted reasonably for explicit zones. It was an intelligent choice to enlarge the selection of plants instead of confining them to jatropha, as it were. Even though the nation has not made any exceptional achievement in biodiesel creation over nearly twenty years of experimentation, it has given various important outputs that may manage the future course of activities.

1.5 State of the Art of the Present Work

Internationally, over 350 oil-bearing feedstocks are recognized as expected resources for biodiesel production (**Bart** *et al.***, 2010**). Edible oil resources are considered the 1st generation of biodiesel feedstock. As of now, over 95% of the world's biodiesel is delivered from edible oils. However, their utilization raises numerous worries, such as food versus fuel crisis and significant ecological issues, such as real destruction of soil, deforestation, and a considerable part of the accessible farming land. Over the past ten years, vegetable oil plants' costs have increased significantly, influencing the commercial reasonability of the biodiesel industry (**Deng** *et al***., 2011**). Moreover, the utilization of such eatable oils to deliver biodiesel is not attainable in the long run due to the developing gap among such oils' applications and flexibility in numerous nations. For example, investing all U.S. soybean in biodiesel creation would meet just 6% of diesel requests (**Chapagain** *et al.***, 2009**). Inedible oils are accessible in numerous places, particularly in barren lands that are not feasible for food crops. They wipe out rivalry for food, lessen the deforestation rate, are more proficient, naturally welcoming, and produce beneficial side effects. They are similar to edible oils. India's main resources for biodiesel creation from inedible oils are Azadirachta Indica (neem) and Waste vegetable oil. Inedible oils are viewed as the 2nd generation of biodiesel feedstocks (**Jena *et al.*, 2010; Sarin *et al.*, 2009**).

High viscosity and low instability are the principal obstructions that prevent the utilization of raw vegetable oils in conventional diesel engines. The common problems are carbon deposition, piston ring sticking and injector clogging. Subsequently, numerous attempts were made to improve vegetable oil properties to meet diesel fuel properties (**Singh and Singh, 2010**). These issues can be reduced by transesterification. Transesterification is the most well-known technique to decrease the viscosity of vegetable oils. Transesterification has been acknowledged worldwide as the best strategy. Among different methodologies, transesterification was preferred because of its minimal effort. A catalyst is utilized to begin the response. Catalyst is also fundamental as methanol is hardly dissolvable in oil or fat, improves the solvency of methanol, and expands the reaction rate (**Shahid and Jamal, 2011**). Transesterification depends on several factors. There always exists a high level of disagreement about the transesterification method among researchers regarding the process's reliability (**Kant Bhatia** *et al.***, 2021**). The biodiesel conversion reactor system's performance will vary with biodiesel resources' physical and chemical properties. Engines run with biodiesel require much more periodic attention than diesel-fuelled engines cause of clogging in the injector and delivery valve of the fuel system. The properties and suitable design provide reliable operation for long runs in the case of diesel. Getting biodiesel is not much difficult, but obtaining excellent quality and yielding for the long run is challenging. With the increase in energy demand, petroleum products' cost increases as their inventory are overwhelmed by a couple of nations. Reliance on imported non-renewable energy sources represents a genuine danger to any nation's energy security and financial steadiness. The World may run out of oil in the following 50 years (**Mujtaba** *et al.***, 2020**). Numerous countries have started to search for alternative renewable fuel sources (**Bian** *et al.***, 2020**). Even though biodiesel's burning properties are like petroleum products, it tends to be utilized in an unmodified engine with no adjustment (**Bhatia** *et al.***, 2017**). Feedstock determination is a significant errand as over 70% of the expense of biodiesel creation is credited to feedstock (**Jamil** *et al.***, 2017**).

Biodiesel creation is founded on eatable oils (palm oil) and is liable for expanding food costs (**Guo** *et al*.**, 2020**). Using second-generation non-consumable feedstocks, such as Neem oil and waste vegetable oil, can help manage food security and diminish creation costs. Since Neem oil and Waste vegetable oil have a high substance of free unsaturated fats, biodiesel is profoundly viscous. However, Acid catalyst esterification, followed by alkali catalyst transesterification, is utilized to decrease FFA.

However, this technology does not flourish satisfactorily even though biodiesel resources are available in large quantities everywhere around the World. In many cases, the government is taking part in making policies, providing subsidies, and developing awareness to make it reliable and acceptable technology. Biodiesel has been acknowledged worldwide as a prompt answer to the weighty reliance on diesel fuel. Be that as it may, the drawn-out dependence on edible oils as feedstock for biodiesel creation has undermined edible oil's suitability and raised some natural issues. Besides, over the most recent ten years, the costs of vegetable oil plants have expanded drastically. Because of these components, it is vital to discover other inedible oil feedstock to substitute edible oil to create biodiesel. This study's real target is to derive biodiesel from the different inedible feedstock, Neem, and waste vegetable oil available in India, then study biodiesel's combustion, performance, and emission characteristics, and afterward contrast the experimental data with edible palm oil. Also, analyze energy and exergy from experimental data.

Engine performance will also vary with the biodiesel type and blend quantity. In these circumstances, the built and test method is not proper concerning time and cost to find suitable operating parameters and performance. The modeling of engine systems for diesel and biodiesel blend applications based on engine geometry, thermodynamics, heat transfer principle, and emission simulation can provide adequate guidelines to efficiently and economically design the system. Models can predict engine operating parameters for available fuels. Based on the above

discussions, it is prudent to study the state of research on methodologies that are practiced in modeling a single zone engine based on different biodiesel blends.

1.5.1 Modeling of engine

Commonly, the CI engines are intended for diesel fuel. Utilizing a similar engine for biodiesel activity needs minor alterations in the engine working conditions (**Sayin and Gumus, 2011**). Researchers are recently showing more interest in simulating the engine performance to get optimum engine operating parameters instead of building and testing method that requires more time and cost. Also, engine makers are consistently searching for approaches to improve engine functions with reduced expenses and time-efficient development. Naturally, the engine's multidimensional mathematical model will play an undeniably significant part in engine development. Demonstrating engine simulation activity gives the essential comprehension of the physical and chemical changes during the engine cycle (**D'Errico** *et al.***, 2011**). The improvement of numerical programming tools or software builds its capacity to settle more chaotic conditions. Two types of diesel engine models are common: thermodynamic models and multidimensional models. Thermodynamic models are grouped into two subgroups: single and multizone models. A multidimensional model sets the cylinder's space on a fine grid, but it requires detailed information about many phenomena inside the combustion chamber. This kind of approach has its disadvantage in terms of computational time and the need for massive storage space. The multi-zone model is an intermediate step between single-zone and multidimensional models. Multi-zone models can be effectively used to model diesel engine combustion systems. However, multi-zone models are generally not any good as single-zone models since the phenomena of zone characteristics and interactions inside the combustion chamber are unknown.

A single-zone model is frequently utilized if there are a quick response requirement and less computational time. In single-zone models, the chamber charge is thought to be uniform in

temperature and composition. The thermodynamics first law computes the energy because of fuel injection. The fuel-injected is expected to blend quickly with the chamber charge, which is accepted to carry on as an ideal gas (**Awad** *et al.***, 2013**). The model should be founded on empirical heat-release law to utilize a single zone model in the diesel engine scenario. This methodology needs a comprehensive recognizable proof examination. Single zone thermodynamic models are used in very few studies to analyze the new biodiesel-diesel blend fuel and give a speedy investigation of execution (**Ramadhas** *et al.***, 2006**). **Rakopoulos and Giakoumis (1998)** developed a single zone thermodynamic model. They analyzed naturally aspirated indirect injection diesel engine operation and tested at steady state condition against experimental results. **Descieux and Feidt (2007)** proposed a single zone thermodynamic model for an air standard diesel engine. Using a one-zone model, he analyzed the thermodynamic performance, heat transfer, and friction term. **Gogoi and Baruah (2010)** presented a single zone simulation model for compression ignition to predict the model's performance with alternative fuels such as biodiesel. The ignition delay was considered a function of cetane no equivalence ratio, cylinder pressure, and universal gas constant. **Payri** *et al.* **(2011)** had developed a zero-dimensional single-zone model. The model solved instantaneous pressure and temperature inside the combustion chamber, mass, and energy conversion equation to obtain the combustion chamber's immediate gas state. The Woschni correlation had been modified by considering the swirl effect was different from conventional. **Abou Al-Sood** *et al.* **(2012)** had developed a thermodynamic simulation model of a four-stroke, direct injection compression ignition engine. This simulation model included the sub-model for fuel-burning rate, combustion product calculation, heat transfer, and the working fluid's thermodynamic properties. The model was based on a single zone combustion model with a rapid premixed burning phase. This research has established an in-house compression ignition, single-zone biodiesel engine model based on engine geometries (stroke, cylinder diameter, connecting rod length and diameter of the crank).

Deviation in specific heat ratio of engine cylinder charge and burned gases has been established to anticipate the pressure fluctuation relative to the crank angle, engine output and mean effective pressure relevant for palm oil methyl ester (POME), neem oil methyl ester (NOME) and waste vegetable oil methyl ester (WVOME) biodiesel. The predicted model for biodiesel engine has been verified using diesel and POME blended biodiesel (B5 &B10), NOME & WVOME (B10) blended biodiesel. Also, a simple model was introduced to predict the carbon monoxide and oxide of nitrogen emission in terms of mole fraction. It was observed that the performance of engine varies with different biomass biodiesel and different blends.

1.6 Scope and Objectives of Present Work

Broad usage of biodiesel can lessen the reliance on fossil fuel, which is now the primary energy source for the world. For nations without or restricted fossil-based energy resources, the utilization of biodiesel can prompt a decrease in imports of energy supply. In this manner, developing countries can save lots of foreign exchange. Different feedstocks have been found for making biodiesel. The decision of which feedstock is selected by a nation relies upon accessibility, cost, and edible nature. Argentina likes to utilize soybean oil. However, Indonesia, China, and Malaysia favour palm oil because soybean is famous for food arrangements. Palm oil is liked in Asian nations since they have a surplus quantity. However, oil from rapeseed is generally utilized in Europe. For example, a few countries, India, are attempting to pick their favoured feedstock since it is insufficient for any of the oils (edible or inedible). Regardless of biodiesel creation innovation advances, no significant (OEM) Original Equipment Manufacturer guarantees B100 use. The OEM position is because only one out of every odd biodiesel is the equivalent. Indeed, biodiesel's physiochemical properties from a similar feedstock may vary contingent upon the species, production method, water substance, type or catalyst concentration, methanol to oil ratio, and even time utilized for the production. The nature of feedstock is not

ensured. This is why to protect buyers from purchasing low standard fuel, the OEMs have officially expressed that the biodiesel should meet ASTM D-6751 (American Culture for Testing and Materials) or/and EN14214 (European Board of trustees for Normalization). Many engine examinations are consequently needed at different compression ratios and engine loading conditions for a lower biodiesel presence blend (B5, B10, B15 & B20). On the other hand, the engine research build and test method require more time and cost. Also, engine makers are consistently searching for approaches to improve engine functions with reduced expenses and time-efficient development. In this regard, Single-zone model incorporation in diesel engine modeling could be useful. The diesel engine model with the single-zone model approach is simple, but it is also efficient and requires less computational time.

This examination means to accomplish the following objectives:

- To derive biodiesel (POME, NOME, WVOME) from edible palm oil, inedible neem oil & waste vegetable oil and study the characteristics of those biodiesel.
- To determine optimal parameters of catalyst concentration and the molar ratio of methanol and oil, reaction time and temperature for high yield production of biodiesel.
- To carry out an experimental investigation to study the combustion, performance and emission characteristics of biodiesel fired C. I. engine with different biodiesel blends (B5, B10, B15, B20) under 0%, 25%, 50%, 75% and 100% load conditions at different compression ratios 16:1, 17:1 and 18:1.
- To analyse the energy in terms of shaft energy and associated energy loss and exergy in terms of exergetic efficiency.

- To develop a single zone C.I. Engine model and validate the model with experimental results and also to predict the engine performance and CO, NO exhaust emission in mole fraction using different biodiesel blends.

1.7 Contribution of the Thesis

Over 350 oil-bearing seeds were perceived for biodiesel production (**Bart** *et al*.**, 2010**). Given this reality, this exploration's extent was to recognize and choose some potential oil-bearing plants (eatable and inedible) for biodiesel creation in India. These feedstock incorporated; inedible Neem (Azadirachta Indica), waste vegetable oil, and edible palm (Elaeisguineensis). Essential fuel properties, such as kinematic viscosity, calorific value, density and flash point, have been explored and contrasted with the ASTM D6751 standard. Additionally, the Taguchi method optimised four critical parameters for maximum biodiesel yield. Contributions of various parameters were evaluated using ANOVA. A biodiesel engine model was developed in an in-house code to predict engine combustion, performance, and CO & NO emission. The engine model was validated with experimental results using edible Palm oil biodiesel blends (B5 and B10) and inedible Neem oil & Waste vegetable oil biodiesel blends (B10). Finally, Engine combustion nature and performance, emission, and energy-exergy analyses of some selected feedstock at B5, B10, B15, and B20 fuel blends were investigated at three different compression ratios and various engine loading conditions.

1.8 Organization of the Thesis

This dissertation is comprised of five chapters. The organization of the chapters is listed as follows:

The first chapter gave an introduction and review of the research topic. It began by providing a prologue to the significance of energy, emission discharges, environmental change,

expanding costs and anticipated exhaustion of petroleum derivatives, biofuels' value, and biodiesel to answer the current world energy emergency. This discussion was followed by a foundation that showed biodiesel's significance and gave a few instances of biodiesel feedstocks around the planet and the potential techniques to overcome the high viscosity and low volatility of vegetable oils against petroleum-based diesel.

The second chapter discussed the biodiesel production methodology, principle, and procedure used for this study. Fuel characterization methods were explained regarding American and European standards. Also, the critical parameters in the transesterification process were optimized by the Taguchi method. Among those parameters, which were most critical for maximum yield, were determined along with their contributions.

The third chapter presents the combustion, performance, and emission results obtained from the experimental work for all the test fuels. Energy and exergy analysis was also discussed in this chapter.

The fourth chapter presented a single-zone thermodynamic model of a CI engine fueled with biodiesel blends. The model was validated with the experimental results from chapter three. The predicted performance and emission of the engine with different biodiesel blends have been discussed in detail.

General conclusions have been drawn, and the future work scope has been highlighted in **chapter five**.

Chapter 2

Biodiesel Production and Optimization

2.1 Introduction

In this chapter, two distinct types of tree-borne oilseeds (TBO) (palm oil and neem oil) were studied as possible renewable fuels for direct injection diesel engines compared with waste vegetable oil. Methyl ester derived from palm oil (POME), neem oil (NOME), and waste vegetable oil (WVOME) were described in detail in this chapter. The relevant fuel properties for produced POME, NOME, and WVOME were examined and compared with the literature's data. Also, the optimal conditions of the experiment in POME production were determined by the Taguchi method.

2.2 Material & Method for Biodiesel production

Vegetable oils were not appropriate as fuel for CI engines (diesel). Subsequently, a suitable conversion process must alter the fuel properties nearer to petroleum-based diesel. The main objective of vegetable oil conversion was to diminish the viscosity and ignition-related issues. Significant attempts have been made to create biodiesel from vegetable oil to achieve the diesel engine's fuel properties. **Zahan and Kano** (**2018**) reported four biodiesel conversion options, particularly microemulsion, pyrolysis, blending, and the alcoholysis process, commonly known as transesterification. Among these, transesterification was recognized as the best due to the lower cost and straightforwardness. Regardless of the method of biodiesel conversion, biodiesel properties should meet the ASTM D6751 standards.

Table 2.1 records biodiesel and diesel properties with their guidelines individually (**Deka and Basumatary, 2011**).

Table 2.1: Biodiesel and Petroleum diesel standards (**Deka and Basumatary, 2011**)

Properties	Petroleum diesel	Biodiesel
Standard	ASTM D975	ASTM D6751
Density (kg/m^3)	880	860-900
Flash point (℃)	93 min	120 min
Acid value (mg KOH/g)	0.5 max	0.5 max
High calorific value (MJ/kg)	44.2	35

Transesterification was used to convert the raw vegetable oil with an alcohol to separate esters and glycerol, as demonstrated in figure 2.1.

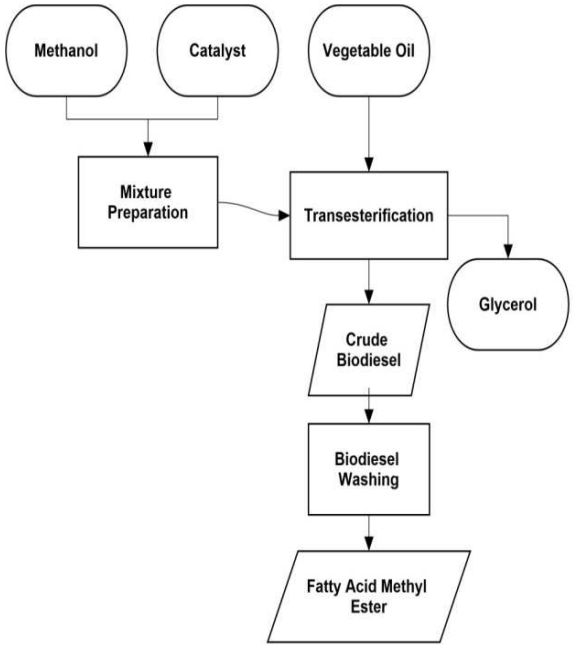

Figure 2.1: Biodiesel production with transesterification

The presence of a catalyst quickened the reaction rate significantly. The essential constituent of vegetable oil was triglyceride. Vegetable oils involved 90 to 98% triglyceride and limited mono-glycerides, di-glycerides, and free unsaturated fats (**Ganesan *et al.*, 2009**). The general cycle comprised three successive and reversible responses where di-glycerides and monoglycerides were framed as intermediates.

Three types of catalysts, soluble base, acid, or an enzyme, could be utilized in the transesterification. Practically, biodiesel was produced by utilizing a base-catalyzed transesterification process. It was simple and required low temperature (**Kalbande and Vikhe, 2008**), less reaction time, and lesser required catalyst (**Lin and Lin, 2006**). Among the alkali catalysts KOH and NaOH, KOH was generally used to produce biodiesel because of its ease in transesterification and dissolved a bit easier in methanol than NaOH (**Agarwal, 2007**). 1 to 0.5% KOH by weight of the oil was generally used for biodiesel production, but more catalyst was needed if the acid value was greater than 1, (**Bala, 2001**). **Veljkovic et al. (2006)** portrayed a two-step process in which the alkali-catalyzed transesterification was followed by the acid-catalyzed esterification for the biodiesel creation from tobacco seed oil. The initial step decreased the free fatty acid (FFA) level to under 2% in 25 minutes for the molar proportion of 18:1. In the 2nd step, alkali-catalyzed transesterification, the initial step's result was changed into methyl ester and glycerol. **Malaya et al. (2008)** utilized a two-step method to deliver biodiesel from Pongamia Pinnata oil and considered the impact of FFA level on biodiesel production. **Holser and Kuru (2006)** examined milkweed seed oil as an alternative feedstock to create biodiesel fuel. They concluded that converting unsaturated oil into methyl ester was more straightforward than transformation it into its ethyl ester.

Mehar et al. (2006) reported that the transesterification process depends on factors such as alcohol, catalyst, response temperature, and reaction time. A molar proportion of 6:1 was typically utilized in the transesterification process to get ester yields higher than 98% by weight

because a lower molar proportion requires more reaction time. However, the transformation was enhanced with higher molar proportions, but the yield was reduced due to difficulty in glycerol separation. Generally, methanol was utilized in this reaction because of the quick reaction rate and high dissolvability in oil (**Lin and Lin, 2006**).

2.2.1 Feedstock and Materials

The three primary feedstock utilized in this investigation were edible palm oil, inedible neem oil and waste vegetable oil (WVO). WVO was collected from the guesthouse kitchen at Jadavpur University, situated in Kolkata, India. Edible palm oil and inedible neem oil were bought from local suppliers. At first, pre-treatment measures were applied by the need for feedstock. For instance, WVO was filtered through a 5 μm filtration paper to eliminate any leftover cooking particles. The collected oil was tested for its free fatty acid (FFA) content by titration. In Acid catalyst esterification, sulfuric acid (Mahaveer surfactants Pvt. Ltd, purity 98%) was applied as a catalyst along with methanol. In alkali catalyst transesterification, potassium hydroxide (Merck & Co., min assay 84%) was used as a catalyst along with methanol (Make Finar, min assay 99%).

2.2.2 Titration of selected vegetable oil

Titration was performed at Jadavpur University, Chemical Engineering Dept. lab. Titration arrangement and oil test are as follows;

- Readiness of titration arrangement: 1 gram of KOH mixed into 1 litre of distilled water to prepare a solution.
- Planning of oil test: 1 ml of oil, 10 ml of isopropyl alcohol, and several phenolphthalein droplets were added and blended in a test tube.

- Titration: the prepared liquid titration arrangement was introduced into the test tube till the shading was transformed into pink colour, and the solution spent was recorded at that point.

Titration results determined the catalyst needed for the transesterification, FFA, and acid value estimation of every feedstock. FFA and acid value esteem were determined by utilizing conditions 2.1 and 2.2 (**Masera and Hossain, 2017**).

$$AV(mg \cdot KOH/g) = \frac{V_{titration} \cdot M_o \cdot N_{KOH}}{m} \quad (2.1)$$

$$Acidity(\%) = \frac{V_{titration} M_o N_{KOH}}{m} 0.1 \quad (2.2)$$

V_{titre} - volume of titre in millilitre,
M_o - molar mass of the oleic acid,
m - mass of oil in grams and
N_{KOH} -concentration of KOH solution in mole/millilitre.

Vegetable oils are composed primarily of the fatty esters of glycerol. The transesterification of vegetable oils constitutes an efficient method to provide fuel with chemical properties that are similar to those of diesel fuel. The fatty acid composition of the oils seems to have an important role in the performance of biodiesel in diesel engines. Alkali catalyzed transesterification was permitted with FFA of vegetable oil estimated under 2%. **Ramadhas et al. (2005)** prescribed the acid-catalyzed esterification to reduce FFA before alkali catalyzed transesterification, if FFA was higher than 2%. In table 2.2 FFA of selected feedstock are shown.

Table 2.2. FFA of selected feedstock

Selected Feedstock	FFA (wt.%)
Refined Palm Oil	0.60
Neem oil	3.90
Waste vegetable oil	2.10

2.3. Biodiesel Production Experimental Setups

The different sorts of transesterification techniques were applied to separate biodiesel from vegetable oil. For the most part, FFA was exceptionally high for unconventional oil. Likewise, the process of getting biodiesel from high FFA should be customizable to adjust quality as per engine fuel. A plausible biodiesel creation arrangement (figure 2.2 & figure 2.3) was utilized for economical but scattered with small scale production in the rural area to avoid lavish and complicated installation to achieve quality biodiesel.

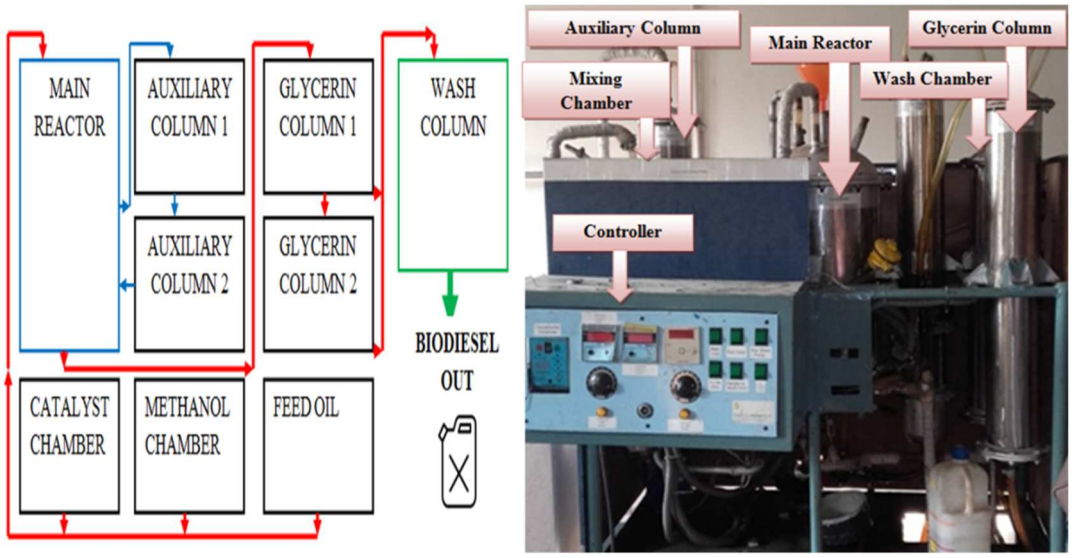

Figure 2.2: Biodiesel Production Experimental Set-Up

Moreover, the properties of high FFA oil would modulate depending on climate and storage conditions. The FFA of oil increases with storage duration, and sometimes it decays depending on oil quality (**Dhar** *et al.*, **2012**).

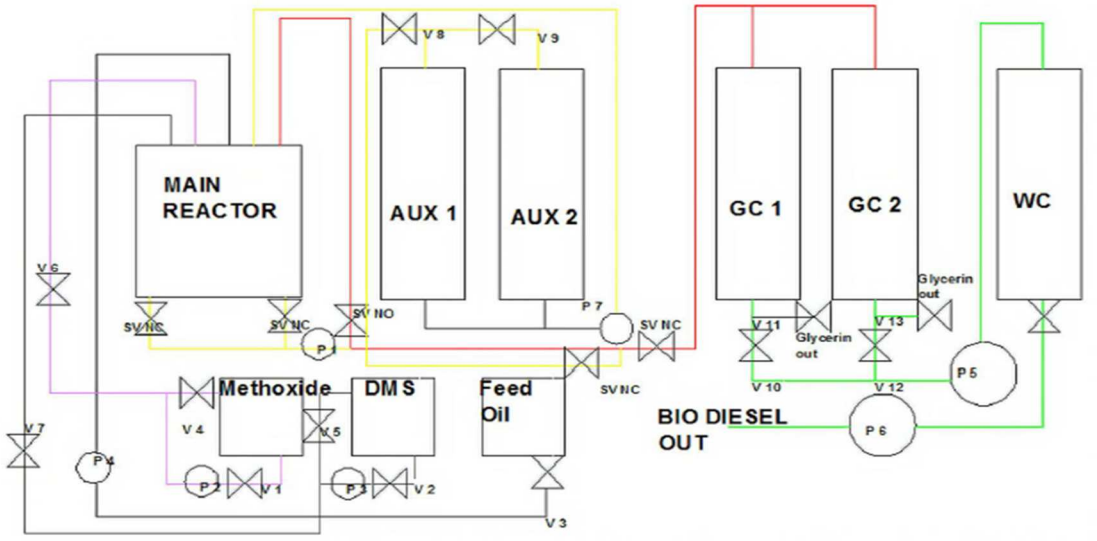

Figure 2.3: Biodiesel production experimental set-up schematic diagram (10-25 litres/batch).

2.3.1 Biodiesel from Palm oil

The experiment setup consisted of nine cylinders. Out of them, five were useful for the preparation of biodiesel. In the schematic diagram as shown in figure 2.3, in the lower part, out of three chambers, the first chamber from the left was for catalyst, the second one was for alcohol like methanol, ethanol, and the last one was for mixing. A pump connected these chambers, which helped pump alcohol and catalyst mixture to the main reactor cylinder. Also, three valves were there, which control the rate of flow. The acceleration of the chemical reaction in the main reactor chamber was improved by a fan, which helps appropriately mix reactants. Temperature control was essential for higher-yielding and the minimum time requirement. That was why temperature sensors and controllers maintain the required temperature inside the cylinder. A pump linked the main reactor chamber to the glycerol column (GC). Here, the mixture remained for some time, and due to different molecular weights, the upper portion was filled with biodiesel and the lower

part with glycerol. At the bottom-most part of the GC chamber, a valve was there that opened, and glycerol came out. The rest of the biodiesel product was taken later into the wash column (WC) chamber. Biodiesel at that time was not pure. Further purification was necessary. For that, washing should be done repeatedly with water until the pH value of water came to 7. The transesterification reaction is shown in the following equation 2.3.

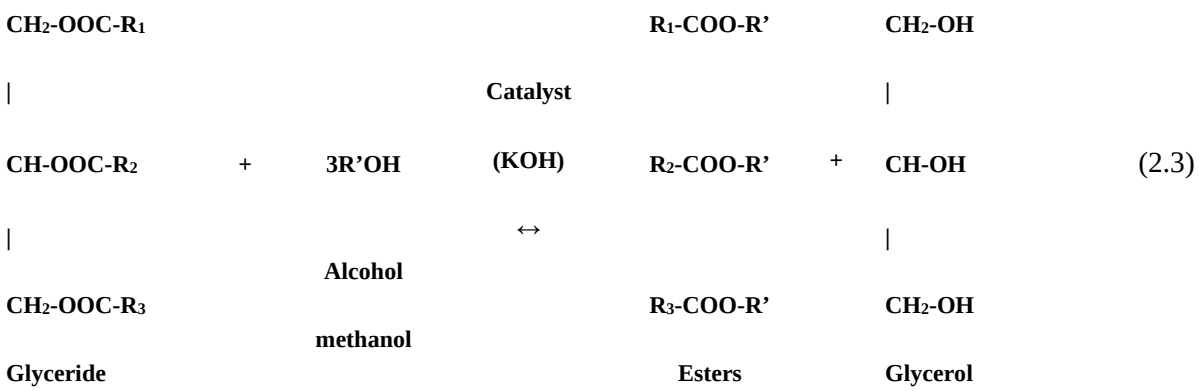

(2.3)

2.3.2 Biodiesel from Neem oil and Waste Vegetable oil

Since neem oil and waste vegetable oil had a high FFA, biodiesel was profoundly viscous. In this investigation, Acid catalyst esterification followed by alkali catalyst transesterification was utilized. At the initial stages of biodiesel production, oil was treated at 80 degrees Celsius for about two hours to remove moisture content (**Das** *et al.***, 2018**). However, in the latter stages of the reaction, the temperature was reduced as the methanol's boiling point was around 65 degrees Celsius. During acid catalyst esterification, 2 % sulfuric acid (20ml/ litre of oil) was added with a stirred solution of oil and methanol at 1.3:1 proportion at 600 rpm and 50 degrees Celsius for around one hour at the atmospheric pressure (**Ali** *et al.***, 2013**). On finalizing the reaction, the entire arrangement was taken into a different chamber and permitted to rest for two hours. The

excess methanol and sulfuric acid went to the upper layer, and the lower layer was then removed for the next alkali catalyst transesterification. The separated ester was again treated with a potassium hydroxide solution (10g/ litre) and methanol (250ml/ litre) at 600 rpm and 50 degree Celsius for around one hour at atmospheric pressure. Again, the whole solution was taken into a separate chamber and allowed to rest for about twenty-four hours to complete the reaction. The ester and glycerol were separated after twenty-four hours, and the upper layer of ester was extracted. The extracted ester consists of surplus methanol, which could be evacuated by heating the ester at 80 degrees Celsius, and the vaporized methanol could be recycled for another batch reaction.

2.3.3 Finalizing biodiesel for engine application

The biodiesel needed to be cleaned by a wash in warm water to improve the quality (10%/litre) consistently for 24 hours to pull out catalyst, glycerin, methanol, and soap. Ultimately the washed biodiesel should be warmed to clean the moisture content before blending with petroleum diesel. After the separation of phases, purification of biodiesel was necessary and attended by washing to nullify the catalyst in biodiesel. This process should be continued until the pH value of water come to 7. Free fatty acids could be recovered from the ester phase by distillation at 30-50 °C. Finally, wash biodiesel should be kept at 50 °C for eight hours in a heater oven, and then biodiesel was ready for use. The biodiesel obtained after washing and treatment was measured based on literature (**Sathish, 2015)** and used to evaluate the biodiesel yield using the following equation.

$$Yield(\%) = \frac{weight - of - Biodiesel}{weight - of - oil} \times 100 \qquad (2.4)$$

2.3.4 Biodiesel quality and Properties

The significant properties were tested of produced biodiesel (Table. 2.3); density was determined using the fuel volume, mass and hydrometer technique. A viscometer was used to measure the kinematic viscosity. Flashpoint was decided by a flashpoint tester (Pensky-Martens closed cup), and a bomb calorimeter measured the heating value.. The biodiesel's significant tested properties were similar and within reach with the biodiesel American standard ASTM D 6751 and European standard EN 14214. However, the qualities did not accurately match the literature (Table. 2.3); this might happen because of different biodiesel creation conditions.

Table 2.3. Properties of Biodiesel

Properties	**POME**	**POME (Araby et al., 2018)**	**NOME**	**NOME (Sing et al., 2019; Dhar et al., 2012)**	**WVOME**	**WVOME (Sing et al., 2019)**	**ASTM D6751**	**EN 14214**
Density (Kg/ m^3)	898	877	868	891	890	875	870-900	860-900
Viscosity (mm^2/ s at 40 ˚C)	4.98	4.56	5.5	6.16	5.8	4.40	1.9-6.0	3.5-5.0
Flash Point (˚C)	179.33	196	175 ˚C	144.75	160	70.6	>130 ˚C	>120 ˚C
Calorific Value (MJ/ Kg)	37.06	41.3	36.04	39.87	35.73	38.73	-	-

Synthesis of unsaturated fat (wt%) in palm oil, neem oil, and waste vegetable oil were inspected from literature (Table. 2.4).

Table 2.4. Composition of fatty acid (wt%) in Palm Oil, Neem oil & Waste vegetable oil

Generation	Oil	Linoleic	Linolenic	Oleic	Palmitic	Stearic	References
1st	Palm oil	9-12		36-44	39-48	3-6	(Sing *et al.*, 2019)
2nd	Neem oil	-	-	49.1–61.9	13.6–16.2	-	(Sing *et al.*, 2019)
3rd	Waste vegetable oil	55.2	5.9	21.2	8.5	3.1	(Sing *et al.*, 2019)

2.3.4.1 Density

The fuel flow amount into the engine cylinder is commonly constrained by volume or time. When biodiesel was utilized in an unmodified diesel engine, the volume of biodiesel entering was thought to be equivalent to diesel. Hence, it influenced the mass of fuel. In this viewpoint, the engine might want a higher density for better efficiency. However, density directly affected the atomization of fuel (**Emiroğlu** *et al*.**, 2018**). The hydrometer technique estimated the densities of biodiesels. At first, biodiesel was loaded in a graduated chamber, and a hydrometer was placed. At that point, the reading was taken.

2.3.4.2 Kinematic Viscosity

The kinematic viscosity of fuel is perhaps the most crucial parameter related to fuel flow through the fuel supply system and inside the engine. The resistance of a fluid to flow is viscosity. **Agarwal** *et al*. **(2015)** reported that high viscosity fuel was not preferred to use in the

engine as slug development in the delivery valve might cause issues. Moreover, it was harder to atomize through injectors. As per the biodiesel viscosity, a few changes on the fuel supply line might be required for better performance, for example, an additional fuel pump and preheater. In the redwood viscometer water jacket surrounded the viscometer. The water was uniformly warmed by a heater. The test was directed a few times to check the consistency of the readings.

2.3.4.3 Flash Point

A fuel flashpoint is a significant boundary for safety concerns. Fuel with low flashpoint can cause blasts during storage or transport. Flashpoint value permits the client to play it safe to maintain a strategic distance from any fire danger. The flashpoint of biodiesel should be estimated based on the standard given by ASTM D93. The base flashpoint was announced as 130 °C for biodiesels. Biodiesel tests were conducted through Pensky-Martens closed cup analyzer. Roughly 2 ml of biodiesel was put into the shut cup thermally control chamber. Then temperature value was set lower than the predicted temperature. A trigger was used to create a flash in the oil fume placed on top of the closed cup. This methodology must be replicated at reduced temperatures on account of any flash identification at this stage. If no flash was recognized, the temperature was increased until a suitable reading was achieved.

2.3.4.4 Higher heating value

Higher heating value (HHV) or calorific value expresses energy delivered by a unit mass of fuel on complete combustion. However, condensed water vapor energy is also included. Though European or American guidelines have no limit on HHV for biodiesels, it is a fundamental attribute in engine efficiency (**Piaszyk, 2012**). ASTM D4809 is one of the suggested techniques for estimating HHV. At first, the fuel mass was measured and put into a bomb enveloped by the water jacket. At that point, the bomb calorimeter began the ignition, and the

fuse wire was consumed. The water temperature increase was recorded after the combustion of fuel. The energy content was calculated as a function of the mass of the fuel consumed, temperature difference, and heat capacity.

2.4 Optimization of Biodiesel yield

2.4.1 Taguchi Method

Dr. Genichi Taguchi introduced a technique to observe the impact of various process boundaries. This technique could detect the process performance change and mean to select the peculiar working condition. This strategy for the design of experiments utilized orthogonal arrays for different parameter optimization, which influenced the process and the degree to which they could be altered. This strategy's real speciality was not to examine all the potential parameter combinations yet just a couple of sets with a few analyses to reduce the valuable time and effort.

2.4.2 Design of Experiments (DOE) Using L9 Taguchi

OVAT or one variable at a time was not practical for an organized optimization process as the other variables were also crucial for the maximum yield of biodiesel. Accordingly, software governed approximation was preferred, which covered RSM (response surface methodology) consisting of CCD (Central Composite Design) or a one-factor approach consisting of Taguchi Orthogonal Arrays (OA). An enormous quantity of experiments was usually required to develop the optimum parametric circumstance for a process (**Uslu and Aydin, 2020**). The Taguchi method was shrinking the bulky optimization method to a few runs. Taguchi OA applied orthogonal arrays to resolve the least notable runs within associated variables at different levels of each variable acceptable in anticipating the optimum response within a remarkably reduced number of experimental runs.

The flow chart portraying the overall advances associated with the Taguchi strategy is given in figure 2.4.

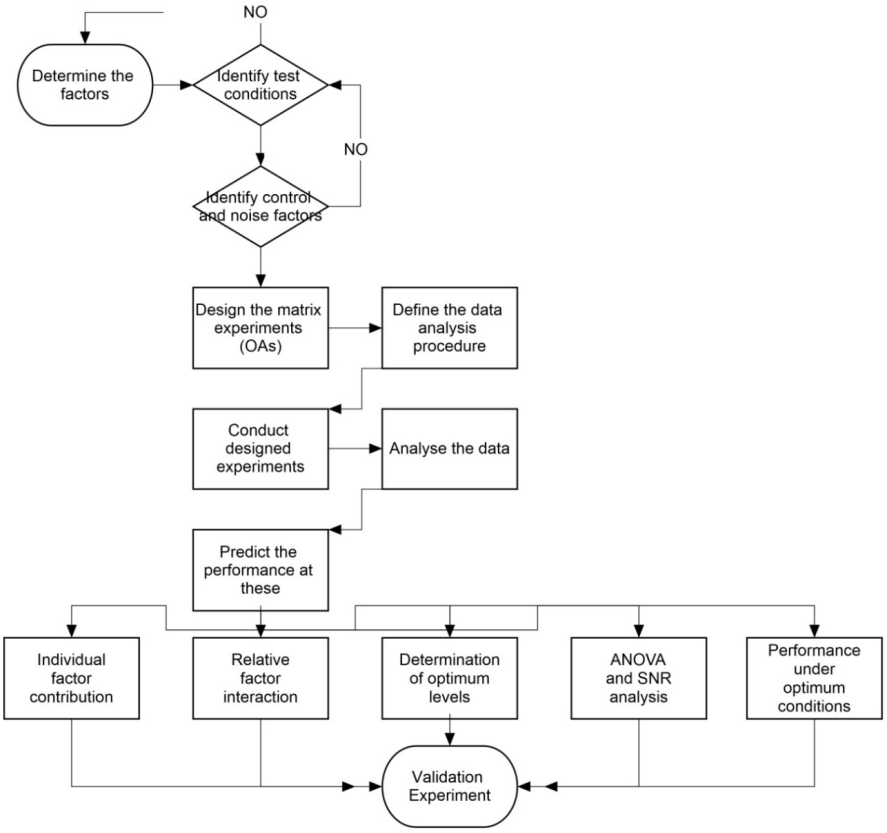

Figure 2.4: Steps in Taguchi method

Taguchi OA results in the least required runs recommended for a proper prediction of the reaction (**Sathish, 2015**). The systematically randomized runs were performed to reduce analytical errors. Traditional optimization methods for any experimental investigation were complicated and difficult to practice. Manual optimization was a challenging task because the increase in process parameters and levels of experiments increased. Taguchi method was utilized to sort out this

problem with fewer experiments (**Phadke, 1988; Park, 1996**). Only some combinations were explicitly investigated instead of all possible parameter combinations (**Sathish, 2015)**. The required number of experiments and their parameters could be finalized from the Orthogonal Arrays (OA).

In the OA configuration, precise comprehension of level and factor was crucial. Independent variables were the factor that had an impact on the dependent variable. Factor increment was described as the level. Factors were assigned at various levels in a symmetrical cluster or OA design like a net grid system. It tended to be described as a 3D shape with a 27 focus point gridding, as demonstrated in figure 2.5. A full-scale experiment took all 27 directions. The full-scale investigation would be difficult and tedious because few levels and factors were covered. The pair of combinations were spread evenly, as indicated in the red circles in figure 2.5.

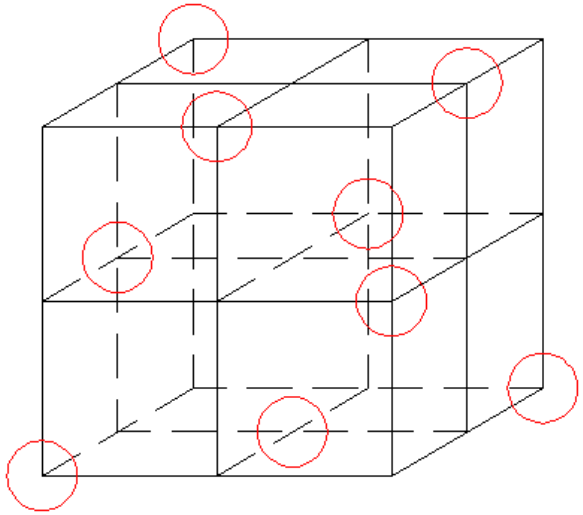

Figure 2.5: Equilibrium distribution stereogram of L9 orthogonal array design

2.4.3 Control parameters and their levels Selection

Amid different parametric criterion regulating the biodiesel yield such as methanol to oil ratio, catalyst concentration, reaction time, reaction temperature, alcohol type and quantity, catalyst type, stirring speed or agitation, moisture quantity in the reactant, and quality of the oil, only four most considerable affecting parameters with three levels (L = 3, P = 4) had been treated in this paper.

The Parameters chosen at three levels for L9 design are indicated in table 2.5.

Table 2.5. Parameters chosen at three levels for L9 design

Parameters	Variables	Levels1	Levels2	Levels3
Methanol to oil ratio	A	5:1	6:1	6.5:1
Catalyst concentration (%)	B	0.5	1	1.5
Reaction time (Hour)	C	2	2.5	3
Reaction temperature (°C)	D	50	55	60

The effects of selected parameters in three groups had been observed by attending only nine experiments as per L9 OA. All experiments were repeated three times to reduce the errors. The minimum feasible total of experiments 'N' was determined against the levels 'L' and total no design and selected control parameters 'P' adopting the correlation (**Babatunde** *et al*.**, 2020**). Transesterification depended on specific essential variables such as reaction temperature, the extent of excess alcohol, catalyst concentration, reaction time, and stirrer RPM. RPM was kept constant for present experiments RPM=1500.

Parameter level had set as:

- Methanol to oil molar ratio 5:1, 6:1, 6.5:1

- Amount of KOH (wt% of oil) 0.5, 1, and 1.5
- Reaction temperature (°C) 50, 55, 60
- Reaction time (Hour) 2, 2.5, 3

4-Parameters 3-levels experiments were considered by the Taguchi method in L9 OA to optimize the different parameters influencing the process. OA could confirm the required number of experiments and their conditions from the OA. Based on the information from the L9 orthogonal, nine experiments (see Table. 2.6) had to be conducted. Each experiment had to be conducted three times to assure repeatability.

Table 2.6. L9 OA for four parameters at three levels

Experiment no.	**Parameters and their levels**			
	M/ O (Molar ratio)	Concentration of catalyst (Wt %)	Time for reaction (Hour)	Reaction Temperature (°C)
1	5:1	0.5	2	50
2	5:1	1	2.5	55
3	5:1	1.5	3	60
4	6:1	0.5	2.5	60
5	6:1	1	3	55
6	6:1	1.5	2	50
7	6.5:1	0.5	3	55
8	6.5:1	1	2	60
9	6.5:1	1.5	2.5	50

2.4.4 Signal to Noise Ratio (SNR)

SNR was evaluated based on test data. The essential factor SNR of Taguchi design differentiates it from conventional design methods that specify the experimental responses' attributes.

This ratio expressed a test level that furnishes the optimum performance in the test factors. There were different SNR like 'larger the better' (LTB), 'smaller the better' (STB), and 'Nominal the better' (NTB). STB for a minimization problem, LTB for maximization problems, and NTB for normalization problems could be selected. In this study, 'larger is better' for biodiesel yield percentage was suitable as the objective was to define maximum biodiesel yield optimum conditions for different parameters. Taguchi suggested using loss function (LF) to determine the discrepancy among the experimental and performance parameters.

The LF amount had moreover been reformed in a signal to noise ratio (SNR). SNR based empirical data assessment was executed to recognition of optimal parameter combinations. Considering the importance of obtaining biodiesel's max yield, out of the possible distinct SNR quality characteristics, Larger-the-Better (LTB) had been adopted depending on the variables' nature. Respectively design criterion would be the level with the highest SNR. Using SNR reasoning, it was feasible to access each parameter's optimum level and optimum set of parameters producing the maximum biodiesel yield (**Sathish, 2015**). The following equations could obtain different SNR like 'larger the better,' 'smaller the better,' and 'Nominal the better'. Where 'n' was the number of trials, and 'j' was the number of design parameters.

Larger the better- $$SNRi = -10\,log\frac{1}{n}(\sum_{j=1}^{n}\frac{1}{y_j^2}) \quad (2.5)$$

Smaller the better - $$SNRi = -10\,log(\sum_{j=1}^{n} \frac{y_j^2}{n}) \quad (2.6)$$

Nominal the better- $$SNRi = 10\,log(\sum_{j=1}^{n} \frac{y_j^2}{s_j^2}) \quad (2.7)$$

Where, $y_i = \frac{1}{n}(\sum_{j=1}^{n} y_{ij})$ (Response mean)

$s_i^2 = \frac{1}{n-1}(\sum_{j=1}^{n} y_{ij} - \overline{y_i})$ (Variance)

i = experiment number, and n = number of trials.

ANOVA analytical method could be applied to identify the factor with large scattering (**Xiao** *et al***., 2014**). In this work, the results from experiments could be inspected by performing an analysis of variance based on the orthogonal arrays to exhibit the degree of influence of each factor that remarkably influenced the response variables. The comparable mathematical relations entrenched with ANOVA are given in equations (2.8), (2.9), (2.10), and (2.11) (**Xiao** *et al***., 2014)**. Equation (2.8) provides the mean value of SNR, where the number of trials is given by k. Variations of the overall mean (SS) sum of squares is expressed by (2.9). The influencing factors mean (SSi) is calculated as (2.10). The individual factors contribution percentage of the selected response variables will be treated to conclude the optimized combination and calculated through equation (2.11) as follows:

$$\overline{SNR} = \frac{1}{9}\sum_{k=1}^{9}(SNR)_k \quad (2.8)$$

$$SS = \sum_{i=1}^{9}(SNR_{ij} - \overline{SNR})^2 \quad (2.9)$$

$$SS_i = \sum_{j=1}^{3} (SNR_{ij} - \overline{SNR})^2 \quad (2.10)$$

$$Contribution\% = \frac{SS_i}{SS} \times 100\% \quad (2.11)$$

SNR was inspected for all biodiesel yield percentages. The best sequences were decided in conferment with the output, and ANOVA was practised to draft the individual contribution scale. ANOVA estimated the effect of one or more aspects by correlating the response variable means at the different aspect levels.

2.4.5 Uncertainty Analysis

Various operational and physical limitations had caused uncertainty while collecting data from experimental instruments. An uncertainty analysis was made to ensure accuracy concerning the preciseness and repeatability of the experiment results.

The uncertainties of collected data and measuring equipment accuracy were significant to substantiate the experimental data's correctness. Using the root mean square method, the analysis was organized when the total uncertainty U of a quantity Q had been predicted, relying on independent variables X_1, X_2,..., X_n (The uncertainty was estimated in the calculated result based on the uncertainties in the primary measurements. Where result 'Q' is a given function or dependent factor of the independent variables X_1, X_2,…, X_n.) carrying particular errors ΔX_1, ΔX_2,..., ΔX_n as given by the following equation (**Paul** *et al***., 2017**).

$$\Delta U = \sqrt{(\frac{\partial U}{\partial X_1}\Delta X_1)^2 + (\frac{\partial U}{\partial X_2}\Delta X_2)^2 + \ldots + (\frac{\partial U}{\partial X_n}\Delta X_n)^2} \quad (2.12)$$

In Table 2.7, percentages of uncertainty and measurement accuracy of the measured experimental values are shown.

Table 2.7. Uncertainty of the measured quantities and Measurement accuracy

Properties	Units	Uncertainty (%)	Measurement accuracy
Density	(Kg/ m^3)	± 0.01	± 0.1
Kinematic Viscosity (at 40 ˚C)	mm^2/ s	± 0.11	± 0.01
Flash Point	˚C	± 2.42	± 0.1
Calorific Value	MJ/ Kg	± 0.13	± 0.001

2.4.6 Determination of optimal condition of the experiment by Taguchi method

The yielding of biodiesel was biodiesel obtained from the amount of oil invested. The yield of biodiesel was dependent on many factors. The variable factors were applied at three levels to design the experiment at MINITAB 17.

In the investigation, it was used as a catalyst for 0.5%, 1%, and 1.5% of the total reactant. The present study established the effect of different Methanol to Oil (M/O) ratios and the time taken for biodiesel transformation from the oil-based palm. As the methanol to palm oil ratio was increased, the yield increased, and it was found that the yielding reached a maximum at 6 M/O. When the time to reach equilibrium was highest, the yield was also highest at 86.2%. The effect of reaction temperature was established along with the time taken. The yield was found to be 86.2%, and the time was taken 3 hours. It was found that yield reached a maximum at 55 °C. When the time to reach equilibrium was highest, the yield was also highest at 86.2%. It had been obtained from these experiments that the optimum conditions for the production of biodiesel were: Catalyst should be 1% of the total volume, methanol to palm oil ratio should be 6, and Wall temperature should be 55 °C.

The empirical outcomes (Table 2.8) indicated that experiment No 5 had the max value of SNRA, and experiment No 4 had the lowest value of SNRA. In this present study, the escalation of POME yield was the objective, which was why the LTB SNR model was applied.

Table 2.8. Percentage of Yield and SNR for 9 experiments

Exp. No.	M/O	Cat cons (%)	Time (hour)	Temp (°C)	Mean Yield (%)	SNRA1
1	5:1	0.5	2	50	75	37.5012
2	5:1	1	2.5	55	78	37.8419
3	5:1	1.5	3	60	80	38.0618
4	6:1	0.5	2.5	60	71	37.0252
5	6:1	1	3	55	86.2	38.7101
6	6:1	1.5	2	50	81	38.1697
7	6.5:1	0.5	3	55	83	38.3816
8	6.5:1	1	2	60	81.5	38.2232
9	6.5:1	1.5	2.5	50	81	38.1697

The effect of process control parameters on average SNR for biodiesel yield was the key to finding optimum conditions for this experiment (Table 2.9).

Table 2.9. Response Table for Signal to Noise Ratios Larger is better

Level	Methanol to oil ratio	Catalyst concentration	Reaction time	Reaction temperature
1	37.80	37.64	37.96	38.13
2	37.97	38.26	37.68	38.13
3	38.26	38.13	38.38	37.77
Delta	0.46	0.62	0.71	0.36
Rank	3	2	1	4

Thus figure 2.6 shows a plot of the process control parameter versus average SNR. It means that experiment number 5 had the maximum yield and highest value of SNRA; this would be the optimum stabilized set of parameters. Where another parameter, RPM = 1500 was kept constant.

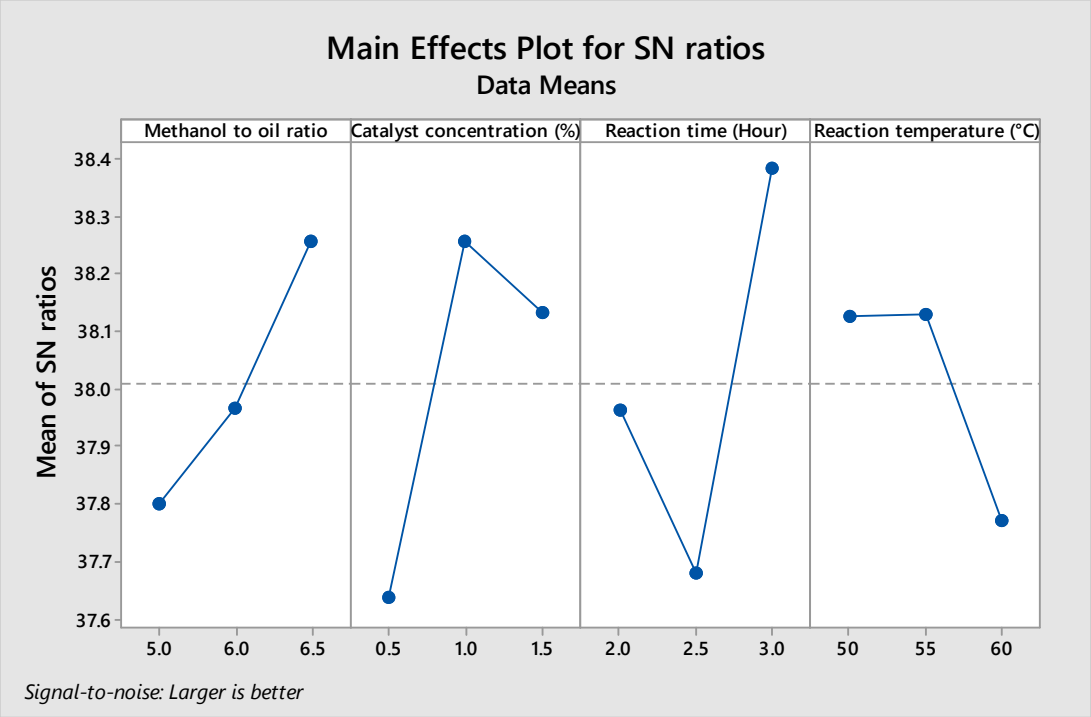

Figure 2.6. SNR of each parameter at different level

2.4.7 Analysis of variance

ANOVA was applied to gauge the response magnitude (in percentage) for each given parameter in the L9 orthogonal array. In this experimental study, ANOVA computed the relation with each parameter of biodiesel production. The utmost important parameter was determined,

and its contribution was also identified using ANOVA. Reaction time and percentage of catalyst concentration were the main vital parameters, and their contribution was 38.67% and 31.85% for POME production. The contribution percentage of biodiesel production for the other two parameters, like M/O ratio and reaction temperature, was 16.69% and 12.79%, respectively, as shown in Table 2.10.

Table 2.10. Data obtained from ANOVA (Analysis of Variance)

Source	DF	Contribution	Adj SS	Adj MS
Methanol to oil ratio	2	16.69%	27.12	13.56
Catalyst concentration (%)	2	31.85%	51.73	25.86
Reaction time (Hour)	2	38.67%	62.82	31.41
Reaction temperature(°C)	2	12.79%	20.77	10.39

2.5 Closure

This chapter discussed edible and inedible vegetable oil with a biodiesel production strategy for this study. American and European standard for biodiesel was compared with the produced biodiesel, and fuel characterization methods were explained. Also, optimizing the critical parameters of the transesterification process using the Taguchi method was performed. However, a lot of engine examination was consequently needed at different compression ratios and engine loading conditions for a lower biodiesel presence blend (B5, B10, B15 & B20). In the next chapter, an experimental setup was used to conduct experiments on the engine. Data acquisition and methods were explained. Furthermore, analytical equations to convert the observed data into results were demonstrated.

Chapter 3

Analysis of Engine Combustion, Performance, Emission and Exergy

3.1 Introduction

The shortage of fossil fuel and edible oil motivated scientists to look for appropriate inedible oil-based fuel options for engine application, particularly for unmodified diesel engines. The goal of this chapter is to utilize one edible and two inedible oil biodiesel. To be specific, the methyl ester of palm Oil (POME), neem Oil (NOME), and waste vegetable Oil (WVOME) in a blended arrangement (B5, B10, B15 & B20) was utilized in an unmodified diesel engine. The combustion nature, important performance parameter, and engine emission of a stationary single-cylinder, naturally aspirated, 4-stroke, liquid-cooled diesel engine was studied using the above test fuels and fossil petroleum-based diesel. Previous chapter exploration had demonstrated that selected methyl ester properties could fulfill biodiesel guidelines ASTM 6751 and EN14214, and utilization of this fuel should be comparable with petroleum-based diesel. In this chapter, the biodiesel properties and impacts of blends of edible & inedible oil methyl ester and petroleum-based diesel were explored on an unmodified Kirloskar made (Model-TV1) engine at different engine loads (0%, 25%, 50%, 75%, and 100%). Engine test setup compared four blends (B5, B10, B15 & B20) of selected edible & inedible oil methyl ester with petroleum-based diesel. The impacts of the four blends of POME, NOME & WVOME at different engine loads were evaluated through the experimental setup to build up suitability and aptness for an unmodified CI Engine. The evaluated parameters were cylinder pressure (CP), net heat release rate (NHR), start of

combustion (SOC), end of combustion (EOC), 5% and 10% mass fraction burned angle, Brake specific fuel consumption (BSFC), brake thermal efficiency (BTE), exergetic efficiency (EE) and emission (NOx, CO, HC).

3.2 Experimental Set-Up

An unmodified Kirloskar made stationary engine (Model-TV1) with one combustion chamber, naturally aspirated with liquid-cooled, 4-S, direct injection compression ignition engine was utilized in this examination (figure 3.1 and 3.2), which was rated 3.5 kW at 1500 rpm.

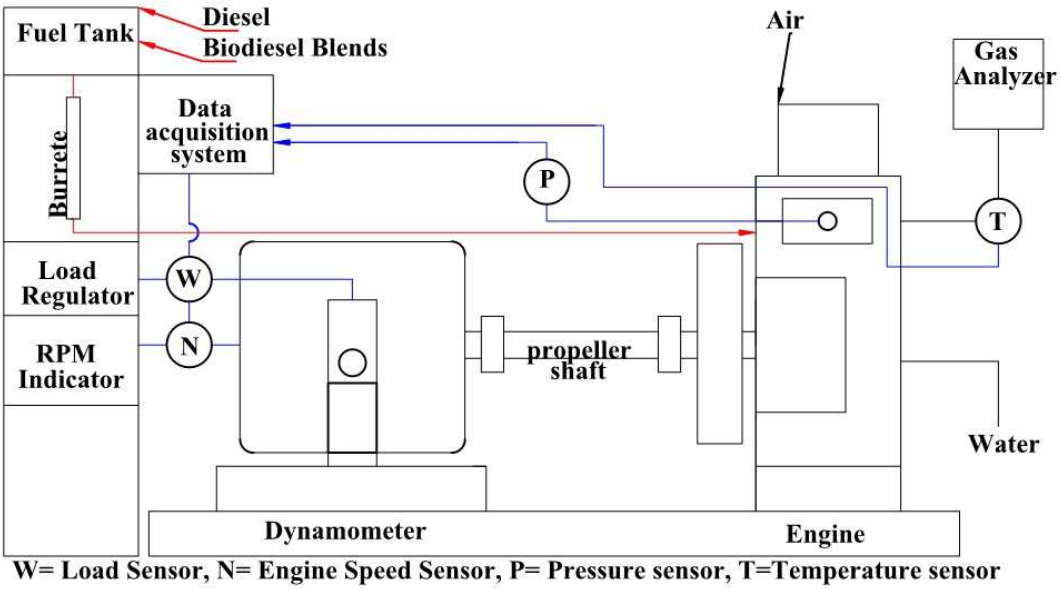

Figure 3.1: Schematic engine test rig

The ratio of compression was varied from 18:1 to 12:1 by inclining the engine block. The engine was combined with a water-cooled eddy current (Model-TMEC10, Technomech, 10 BHP @ 1500-5000 r.p.m) dynamometer with a loading unit to regulate the load on the engine through a

regulator (230V, AX155, Apex). A propeller shaft (Model-1260, Type - A, Make Hindustan Hardy Spicer) with U-joints were utilized to associate the engine with a dynamometer. A strain gauge 'S' type of load cell (Model-60001, Sensotronics make) with a range of 0 to 50 kg were utilized with the dynamometer.

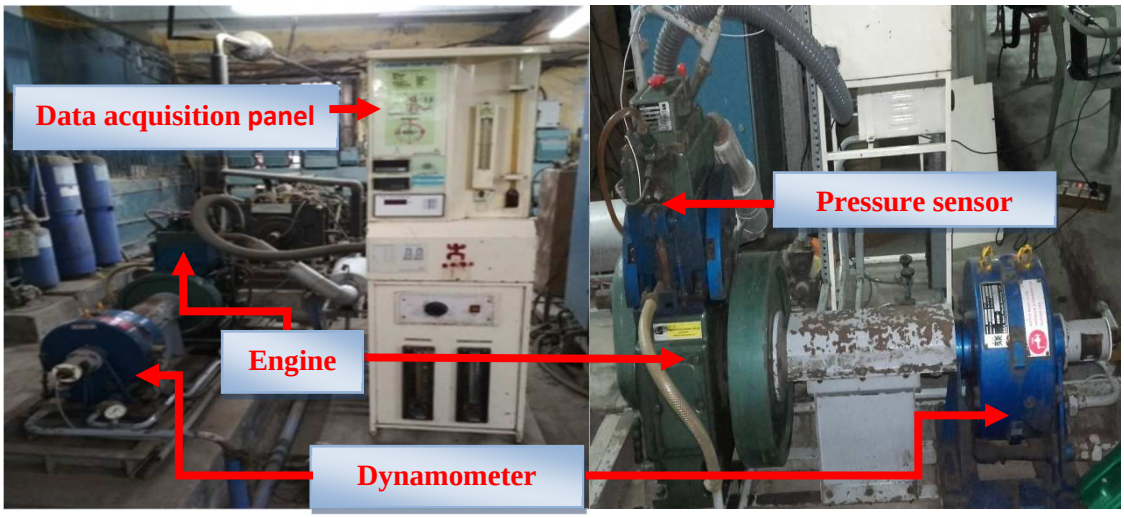

Figure 3.2: Actual view of the experiment setup with Engine

A Kubler made crank sensor (Model-8.KIS40.1361.0360, Type-cinching) had been furnished with the engine to accurately measure the crank angle alongside engine speed. Combustion pressure and mass burn fraction were detected by stainless steel with a hermetically sealed type pressure sensor (Piezotronics, Model-S111A22, up to 5000psi). An Apex made powering unit was given to control the sensors and transducers (Model-AX-409). The fuel flow was identified by a Yokogawa made transmitter (Model-EJA110E-JMS5J-912NN); the flow rate was measured by the change of pressure in the fuel pipe. The actual flow meter unit was outfitted with a 12.4 mm measurement burette tube. The auxiliary unit was furnished with a manometer and orifice meter alongside a WIKA made Airstream transmitter (Model-SL-1-A-MQA-ND-ZA4Z-ZZZ) to check the flowrate. Thermocouples (K type) with a temperature limit of 1200 degree Celsius were

utilized to measure exhaust gas alongside RTD (resistance temperature detectors) at pump output, engine water jacket output, and calorimeter water output. An information recovery framework (NI USB-6210) gathered spontaneous temperature, mass-burn fraction, pressure, airflow, fuel flow and volume information from the engine cylinder using a coaxial Teflon cable (Piezotronics, Model-002C20). All the combustion chamber data was checked utilizing a real-time software (Engine soft) interface created by Apex Innovation Pvt. Ltd.

3.2.1 Fuel Supply System

Three types of liquid fuel in the form of blends were utilized in the current examination; first, standard diesel fuel was tested for reference as a pattern (additionally referred to in the writings as B0) guideline. The test fuels were provided to the engine's fuel pump from the fuel tank under gravity feed. Fuel utilization estimations were performed on a volumetric basis utilizing a graduated glass burette. The burette was supplied with liquid fuel just before metering from the fuel tank.

3.2.2 Engine performance measurement

The engine's measure of load by the eddy current dynamometer was turned by a physically controlled knob and digital load indicator. The engine performance was estimated from the experimental setup for a given load setting. The 'Enginesoft' software programming acquired the engine data.

3.2.3 Air flow measurement

The engine's airflow was checked, bypassing the entry air through an airbox with an orifice meter and manometer. The airflow was determined and recorded in the electronic engine control board framework.

3.2.4 Pressure verses crank angle measurement

The in-chamber pressure was estimated for fuel ignition diagnostics utilizing a piezo sensor mounted on the engine cylinder. The hermetically sealed sensor (Model – S111A22) has specifications: the resolution of 0.69 kPa, Diaphragm stainless steel type, a rise time of 2 microseconds, discharge constant of 500 second, and a range of 5000 psi with a frequency of 400 kHz. A 360-degree incremental encoder detected the crank angle estimation with the push-pull interface. The encoder worked on an electro-optical examining guideline. They change mechanical developments into an electrical voltage, which was then procured on a computer at each degree crank angle.

3.2.5 Temperature measurement

A data logger was connected to Type K thermocouples. Thermocouples were introduced in various engine positions to gauge precise temperatures. For example, engine cooling water stream (in/out), calorimeter water stream (in/out), exhaust gas out from the engine, and calorimeter.

3.2.6 Emission measurement

Figure 3.3: Actual view of the Gas Analyzer setup

The engine's significant exhaust discharges are nitrogen oxides, carbon monoxide, unburned hydrocarbon (UHC), and carbon dioxide. A Manatec makes Eco Gas 100 Gas Analyzer (figure 3.3) was utilized to measure the emission. The measure of oxygen, carbon monoxide, and carbon dioxide were checked in percent volume. The UHC and oxides of nitrogen were checked

in PPM. NDIR (Nondispersive Infrared) technology detection principle was utilized in this gas analyzer for UHC, carbon monoxide, and carbon dioxide. The NOx sensor and the oxygen sensor were utilized to check oxides of nitrogen and oxygen. The experimentations were executed in different engine loading conditions (0, 25, 50, 75 and 100 %) at 1500 rpm. At first, the engine was powered with diesel at different engine load conditions to accomplish standard information. Specific consideration was given to deal with the engine speed at 1500 RPM (±10rpm) all through the engine activity. The authenticity of the information was improved by ten consecutive results of the same engine working conditions. During the test, the surrounding temperature was estimated at 34-35 °C with an RH factor of 80%. The experimental set-up specifications are given in Table 3.1.

Table 3.1: Experimental setup specifications

Engine specifications	**Make and model**	**Make Kirloskar, Model TV1, 1cylinder, 4 stroke Diesel.**
	Bore X Stroke	87.5 mm X 110 mm
	Compression ratio	18, 17, 16
	Rated power	3.5 kW
	Operating speed	1500 rpm
	Injection type & timing	Direct Injection at 23˚CA BTDC
Gas Analyzer specifications	Make and model	Make Manatec, Model Eco Gas 100.
	Technology & Operating temperature	Non dispersive Infrared (NDIR) technology, + 5℃ to + 45℃
Measurement Parameters	CO (Carbon Monoxide)	Range: 0 - 15% , Resolution: 0.01%
	HC (Hydro Carbon)	Range: 0 - 20000 PPM, Resolution: 1 PPM
	NOx (Oxides of Nitrogen)	Range: 0 - 5000 PPM, Resolution: 1 PPM

3.3. Experimental Procedures

Reference performance tests were conducted with the engine working on diesel fuel to build up a correlation of results and guarantee the experimental results' consistency. The engine load varied from at least 0.1 kg to 10 kg load. The engine tests were directed for the whole load range, i.e., 0 to 100% in an interval of 25% at a steady speed of 1500 rpm. First, the engine was heated up and run for a few moments at 1500 rpm under zero load condition to arrive at a stable working condition. The water stream was adjusted to 250 and 70 litres/hour for the engine cooling and calorimeter individually as per engine provider directions. According to the experimental plan, engine operation was set at different load levels. When the engine arrived at the steady-state condition, the engine was prepared to introduce the reference results. Manually recorded parameters were engine water, calorimeter water, and exhaust gas temperature.

The engine performance information was shown in the software interface as BTE and BSFC. An optical sensor detected the crank angle estimation and was obtained on a computer at each degree CA. The engine pressure Vs crank angle diagram was recorded for each crank angle interval.

An exhaust gas sample was drawn from the exhaust system into a gas analyzer through a collection gun during different engine load conditions for emission estimations. The examination readings were recorded from the gas analyzer.

3.3.1 Theoretical considerations of Energy Analysis

The analysis of energy was utilized to observe the energy transformation of the substantial energy of fuel into heat energy (Qin). The heat energy after the ignition was changed over into shaft power (BP) and energy loss. The energy losses were presented as by energy in cooling water (Qw), energy loss by exhaust gases (Qe), and unaccounted losses (Qu) because of

radiation, friction, and heat lost to the environment. The energy provided by the fuel in unit time could be drafted as,

$$Q_{in} = (\dot{m}_f \times LHV)kW \tag{3.1}$$

Power at the shaft could be drafted as,

$$Q_S = BP = (\frac{2\pi NWR}{60 \times 1000})kW \tag{3.2}$$

Where, N= RPM, W= Load, and R= Arm length in dynamometer.

BTE at the shaft could be drafted as,

$$BTE = (\frac{BP \times 3600 \times 100}{Q_{in}})\% \tag{3.3}$$

Brake specific fuel consumption could be drafted as,

$$BSFC = (\frac{\dot{m}_f}{BP})kgkW^{-1}s^{-1} \tag{3.4.1}$$

And specific energy consumption could be drafted as,

$$BSEC = (\frac{m_f \times \dot{} LHV}{BP})kJs^{-1}kW^{-1} \tag{3.4.2}$$

The cylinder pressure w.r.t crank angle could be drafted as,

$$\frac{dP}{d\theta} = k - \frac{1}{V}(\frac{dQ_{in}}{d\theta} - \frac{dQ_{loss}}{d\theta}) - k\frac{PdV}{d\theta} + \frac{P}{k-1}\frac{dk}{d\theta} \tag{3.5}$$

Energy present per unit time in the cooling water could be drafted as,

$$Q_w = (\dot{m}_w \times C_{pw} \times (T_{woe} - T_{wie}))kW \tag{3.6}$$

Energy present per unit time in exhaust gas could be drafted as,

$$Q_e = (\dot{m}_a + \dot{m}_f) \times C_{pe} \times (T_{cio} - T_{atm}))kW \quad (3.7)$$

Similarly, heat loss by exhaust was same as heat taken by calorimeter, so, specific of exhaust could be drafted as,

$$C_{pe} = (\frac{\dot{m}_{cw} \times C_{pw} \times (T_{cow} - T_{ciw})}{(\dot{m}_a + \dot{m}_f) \times (T_{cie} - T_{coe})} kJkg^{-1}K^{-1} \quad (3.8)$$

Unaccounted loss per unit time could be drafted as,

$$Q_U = (Q_{in} - (Q_S + Q_w + Q_e))kW \quad (3.9)$$

3.3.2 Theoretical considerations of Exergy Analysis

In this research, the 1st and 2nd thermodynamics laws were applied to analyze the quantity and quality of energy developed by diesel and biodiesel blends. The engine was operated at constant speeds and five different loads depending on different thermodynamic assumptions.

This study's reference environment corresponded to an environment temperature (T_0) of 298.15 K and an atmospheric pressure of 1 bar to conduct the exergy analysis adequately. Based on this assumption, the exergy balance could be drafted as (**Paul** *et al*.**, 2017**)

$$E_1^0 + E_2^0 = E_3^0 + E_4^0 + E_5^0 + E_6^0 + E_{ds}^0 \quad (3.10)$$

Where, $E_3^0, E_4^0, E_5^0, E_6^0, E_{ds}^0$ were the transfer rate of exergy of exhaust, shaft work, heat transfer to coolant, heat transfer to atmosphere and rate of exergy destruction. E_1^0, E_2^0 were the transfer rate of exergy of incoming air and fuel.

The rate of exergy of incoming air could be represented by,

$$E_1^0 = m_1^0[C_{p1}\left(T_1 - T_0 - T_0 \ln(\frac{T_1}{T_0})\right) + RT_0 \ln(\frac{P_0}{P_1})] \quad (3.11)$$

Where P_0, T_0 were the dead state pressure and temperature. C_{P1}, m_1 were the constant pressure specific heat and mass flow rate.

$$E_2^0 = m_2^0 \, \zeta q_{LHV} \tag{3.12}$$

The chemical exergy factor was represented by $\zeta . q_{LHV}, m_2^0$ were the lower heating value and mass flow rate of fuel (**Kotas, 2013**).

$$\zeta = 1.0401 + 0.1728\frac{H}{C} + 0.0432\frac{O}{C} + 0.2169\frac{S}{C} \times \left(1 - 2.0628\frac{H}{C}\right) \tag{3.13}$$

Where S, O, C, H were the mass fraction of sulphur, oxygen, carbon and hydrogen present in the fuel.

Aggregate of chemical and physical rate of exergy represent the rate of exergy of exhaust gas.

$$E_3^0 = E_{Ph}^0 + E_{Ch}^0 \tag{3.14}$$

The rate of exergy of shaft work could be represented by, where ω, τ were the angular velocity and torque produce by engine.

$$E_4^0 = \frac{2\pi\omega\tau}{60} \tag{3.15}$$

The important factor, exergetic efficiency could be represented by,

$$Exergetic\ Efficiency = \frac{E_4^0}{E_1^0 + E_2^0} \tag{3.16}$$

Cooling water exergy loss rate could be drafted as,

$$E_5^0 = \dot{m}_5 C_{pw} \left(T_{5\ out} - T_{5\ in} - T_{atm} \ln(\frac{T_{5\ out}}{T_{5\ in}})\right) \tag{3.17}$$

Where $\dot{m}_5, C_{pw}$ were the mass flow rate of cooling water and specific heat. T_{5out} and T_{5in} were the temperature at the outlet and inlet.

Exergy loss to the atmosphere could be drafted as,

$$E_6^0 = Q_6(1 - \frac{T_0}{T_6}) \tag{3.18}$$

Where T_6 was the mean temperature of engine body and Q_6 was the heat loss to the atmosphere.

$$Q_6 = \dot{m}_1 C_{p1}(T_1 - T_0) + \dot{m}_2 q_{LHV} - (\left(\dot{m}_1 + \dot{m_2}\right)C_{p3}(T_3 - T_0)\Big) - \dot{m}_5 C_{p5}(T_{5\,out} - T_{5\,in}) - \frac{2\pi\omega\tau}{60} \tag{3.19}$$

Exergy destruction rate was found as,

$$E_{ds}^0 = \left(E_3^0 + E_4^0 + E_5^0 + E_6^0\right) - (E_1^0 + E_2^0) \tag{3.20}$$

Entropy generation could be drafted as,

$$S_{gen} = \frac{E_{ds}^0}{T_0} \tag{3.21}$$

3.3.3 Uncertainty Analysis

Various operational and physical limitations had caused the uncertainty while collecting data from experimental instruments. An uncertainty analysis was made to ensure accuracy concerning preciseness and repeatability of the experiment results. An extensive error assessment was directed by a combined analysis of uncertainty for the performance variables. Using the root mean square method, the analysis was organized when the total uncertainty U of a quantity Q had been predicted, relying on independent variables X_1, X_2,….., X_n (The uncertainty was estimated in the calculated result based on the uncertainties in the primary measurements. Where result 'Q' is a given function or dependent factor of the independent variables X_1, X_2,…, X_n.) carrying particular errors ΔX_1, ΔX_2,….., ΔX_n as given by following equation (**Paul** *et al.***, 2017**).

$$\Delta U = \sqrt{(\frac{\partial U}{\partial X_1}\Delta X_1)^2 + (\frac{\partial U}{\partial X_2}\Delta X_2)^2 + \ldots + (\frac{\partial U}{\partial X_n}\Delta X_n)^2} \quad (3.22)$$

In Table 3.2, percentages of the uncertainty of the performance parameters are shown.

Table 3.2. Uncertainty analysis of Performance Parameters

Computed Performance Parameter	Measured Variables	Instrument Involved in Measurement	% Uncertainty of the Measuring Instrument	Calculation	Total % Uncertainty of the Computed Parameters
BP (Brake Power)	Load, RPM	Load Sensor, Load Indicator, Speed measuring Unit.	0.2, 0.1, 1.0.	$\sqrt{(0.2)^2 + (0.1)^2 + (1.0)^2}$	1.02.
Fuel flow	BSFC (Liquid Fuel)	Fuel Measuring Unit, Fuel Flow Transmitter	0.065, 1.5.	$\sqrt{(0.065)^2 + (1.5)^2}$	1.501

The measuring scope and Resolution of the MANATEC Eco Gas 100 Gas Analyzer are given in Table 3.3.

Table 3.3. Accuracy of Emission Measuring instruments

Instrument	Measuring Range	Resolution
CO (Carbon Monoxide)	0 - 15%	0.01%
CO_2(Carbon Dioxide)	0 - 19.9%	0.1%
HC (Hydro Carbon)	0 - 20000 PPM	1 PPM
O_2(Oxygen)	0 - 25%	0.01%
NOx (Oxides of Nitrogen)	0 - 5000 PPM	1 PPM

3.4 Results and discussion

3.4.0 CI Engine combustion

CI engine combustion process is primarily divided into three phases, as shown in figure 3.4.0. The first phase of combustion is called ignition delay (ID), in which the fuel droplets evaporate and mixes with high-temperature and high-pressure air. There is an interval of time in

the degree crank angle between the start of injection and the start of combustion, which is called ignition delay. The ignition delay takes place in two stages: (i) physical delay and (ii) chemical delay. In physical delay, atomization of liquid fuel jet, evaporation of fuel droplets and mixing of fuel vapour with air occur. In chemical delay, the reaction starts slowly and then accelerates until inflammation or ignition takes place (**Ganesan, 2011**).

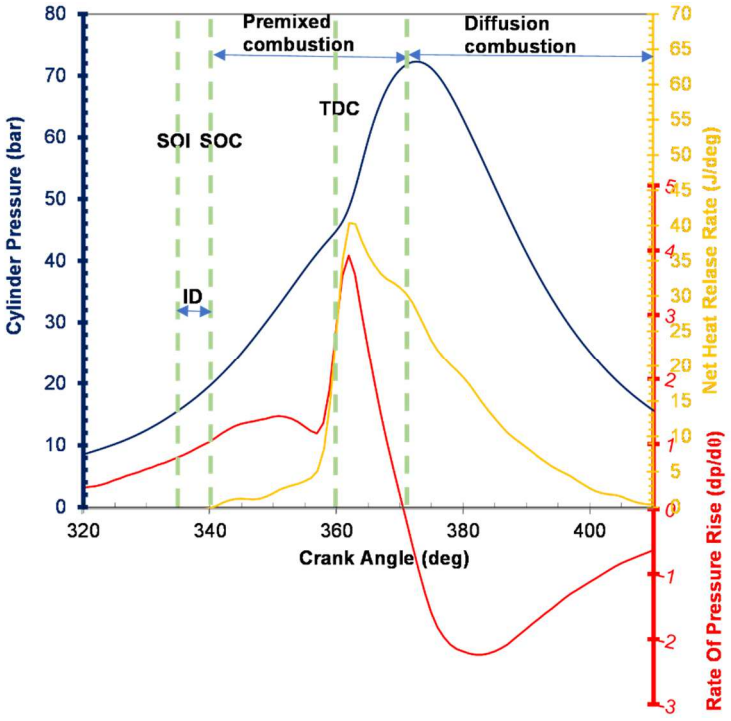

Figure 3.4.0: Curve for diesel combustion including different phases (CR 18 and peak load condition)

The second phase of combustion is called the period of rapid combustion or premixed combustion. In this phase, the air-fuel mixture undergoes rapid combustion. Therefore, the pressure rise is rapid. The combustion of the fuel, which has mixed with the air to within the flammability limits during the ignition delay period, occurs rapidly in a few crank angles. This

depends on the atomization of fuel and its quality. As a result, the peak heat release rate in the premixed combustion is generally higher than that of the subsequent stages. The consequence of the high heat release rate is more effective during this period (**Ganesan, 2011**).

The rapid combustion period is followed by the third phase, which is controlled combustion. The temperature and pressure in the second stage are already quite high. Hence, the fuel droplets injected during the second stage burn faster with a reduced ignition delay as soon as they find the necessary oxygen and any further pressure rise is controlled by the injection rate. Heat release proceeds at a lower rate later part of the expansion stroke, and this is referred to as late combustion. Combustion of any unburned liquid fuel and soot occurs during this phase (**Ganesan, 2011**).

3.4.1 Impact of biodiesel blends on cylinder pressure

The combustion chamber pressure (CP) of a CI engine mainly relied upon the fuel gathered in the ignition-delay period and the premixed burning phase's combustion rate (**Senthil** *et al.***, 2001**). The fuel-air mixture aptness influenced the ignition-delay duration. The variety of the chamber pressure with the crank angle at various loads for various blends (B5, B10, B15, B20)) of POME and diesel at CR 16 is illustrated in figures 3.4 (a). All the methyl ester blends (B5, B10, B15, B20) test fuels followed a similar chamber pressure pattern, which was marginally lower to that of petroleum-based diesel during the ignition period at five different engine load conditions (0%, 25%, 50%, 75%, 100%). This phenomenon had happened because of the poor atomization, volatility, and low biodiesel's calorific value. The tested liquid fuel was injected at high velocity through nozzles, and the droplets of fuel atomized and then vaporized by absorbing heat from the surrounding compressed air. Poor atomization and vaporization of fuel affected the rapid combustion of premixed fuel-air occurred after the ignition delay period.

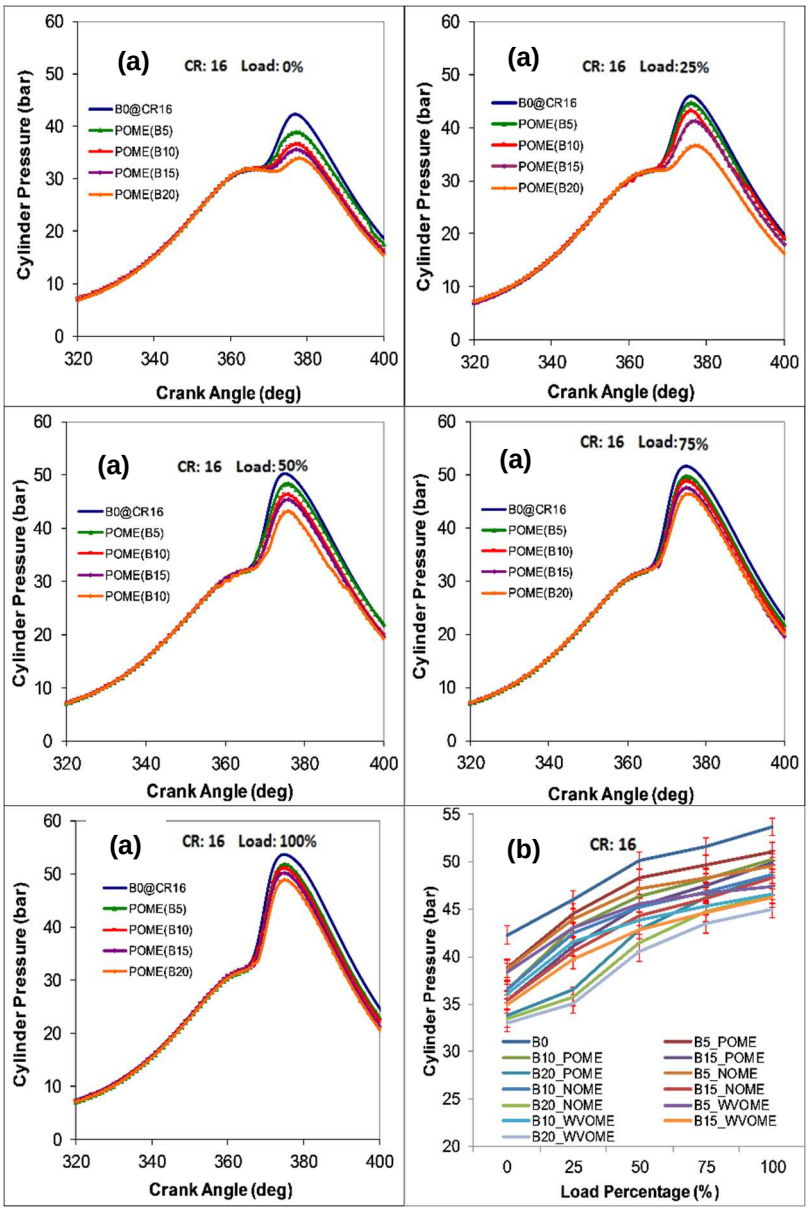

Figure 3.4: (a) Graphical illustration of the Pressure versus CA variation using diesel (B0), POME blend (B5, B10, B15, B20) with CR 16:1 at 0% to 100% Load. **(b)** Peak cylinder pressure of different test fuels & blends at different engine load conditions (CR16).

Increased CP resulting from the premixed combustion compresses and heats the charge's unburned portion, shortens the delay, and increased the remaining fuel's evaporation (volatility) rate. The combustion chamber pressure of B5 methyl esters at various loads was observed to be lower yet at short proximity than that of petroleum-based diesel at zero to 75% load conditions. However, the combustion pressure for other tested blends was observed lower than petroleum-based diesel. Surprisingly, in terms of chamber pressure, B20 performed better at 50% to top load conditions at CR 16 during combustion. This event had happened because of increased chamber temperature at mid to peak load conditions. It tended to be seen that the CP of diesel at CR 16 was observed to be 42.28 bar at zero Load, 46.03 bar at 25% load, 50.14 bar at 50% load, 51.6 bar at 75%, and 53.68 bar at 100% load conditions. Furthermore, higher CP for B5 could be observed than all other blends at all Load conditions (figure 3.4 (b)). It was also presented in figure 3.4 (b) that maximum CP for B5 reduced about 4% to 8% for POME, 4% to 8% for NOME, and 6% to 11% for WVOME compared to petroleum-based diesel. In the case of B10, the maximum CP decreased about 6% to 13% for POME, 7% to 13% for NOME, and 9% to 14% for WVOME compared to petroleum-based diesel. However, the maximum CP for B20 dropped about 9% to 19% for POME, 13% to 22% for NOME, and 16% to 23% for WVOME compared to petroleum-based diesel (figure 3.4 (b)).

From figures 3.4 (a) it was also observed that the maximum peak pressure always takes place after TDC point. Noticeable differences in peak pressure was observed at 25% engine load for B20 blends for all the biodiesels (figures 3.4 (b)).

Also, at CR 17 (illustrates in figures 3.5 (a) & (b)) all the tested methyl ester blends followed a similar chamber pressure pattern, which was marginally lower to that of petroleum-based diesel during the ignition period at same five different engine load conditions. The chamber pressure of B5 at short proximity than that of petroleum-based diesel at 75% to 100% Load

conditions. Though, in terms of chamber pressure, B15 & B20 performed better at 75% to top load conditions at CR 17. The increased chamber temperature at mid to peak load conditions was the cause of it.

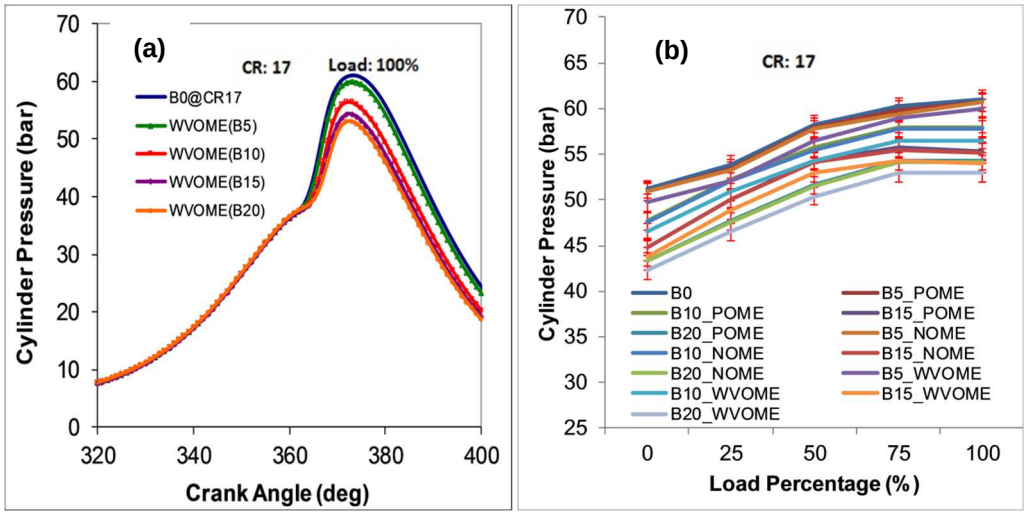

Figure 3.5: (a) Graphical illustration of the Pressure versus CA variation using diesel (B0), WVOME blend (B5, B10, B15, B20) with CR 17:1 at 100% Load. **(b)** Peak cylinder pressure of different test fuels & blends at different engine load conditions (CR17).

Likewise, the chamber pressure with the crank angle at various loads for test fuels at CR 18. All the test fuel blends followed a similar chamber pressure pattern, which was marginally lower than that of petroleum-based diesel at five different engine load conditions. The combustion chamber pressure of B5 methyl esters at various loads was lower yet at short proximity than that of petroleum-based diesel at 75% to 100% Load conditions. B15 performed better at 50% to top load conditions at CR 18. This event had happened because of increased chamber temperature at mid to peak load conditions.

The chamber pressure with the crank angle at various loads for test fuels at CR 18is illustrated in figures 3.6 (a) & (b)

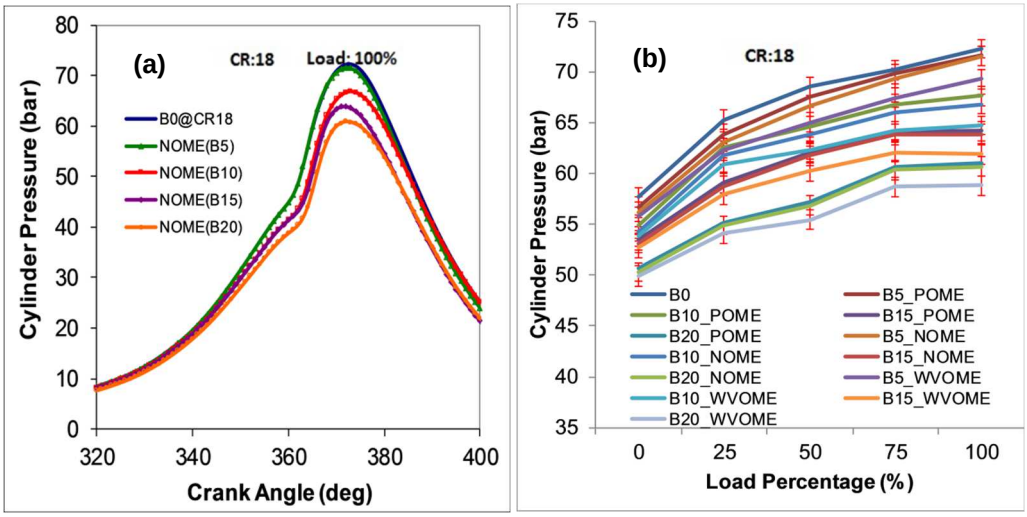

Figure 3.6: (a) Graphical illustration of the Pressure versus CA variation using diesel (B0), NOME blend (B5, B10, B15, B20) with CR 18:1 at 100% Load. **(b)** Peak cylinder pressure of different test fuels & blends at different engine load conditions (CR 18).

3.4.2 Impact of compression ratio on cylinder pressure at different blends

In this segment, the impacts of different compression ratios on the max-CP of the specific blend were discussed at different loading conditions. Figure 3.7 shows that the increase in compression ratio max-CP always increases for petroleum-based diesel & specific blends. However, it was observed that at the higher load conditions, max-CP of NOME blends were in close competition with POME blends at CR 18. This event was due to the increased cylinder temperature and oxygen availability, which improves NOME blends' viscosity. The initiation of combustion for biodiesel blends was delayed because of their higher densities than diesel. Similar reasons were reported by **Balamurugan** *et al.* **(2014)**. The ignition event for B20 (POME, NOME, WVOME) was the farthest among all tested biodiesel blends because of slow combustion.

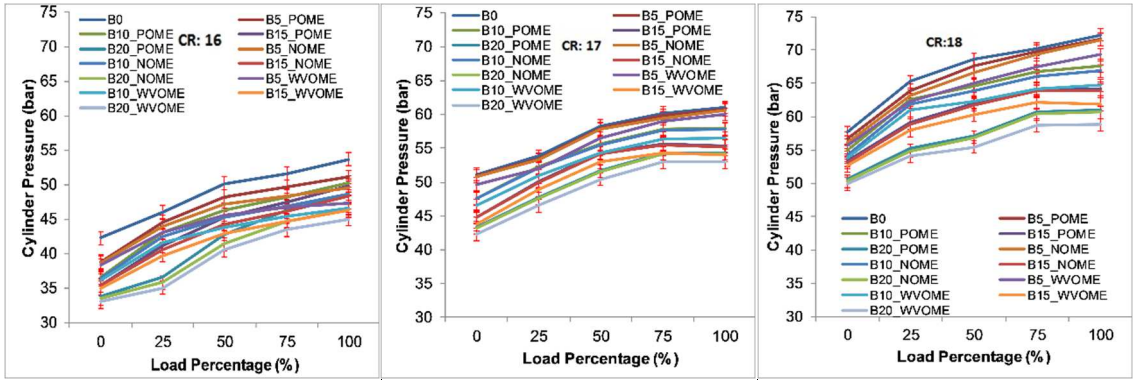

Figure 3.7: Peak cylinder pressure of different test fuels & blends at different CR (16, 17, 18) and different engine load conditions.

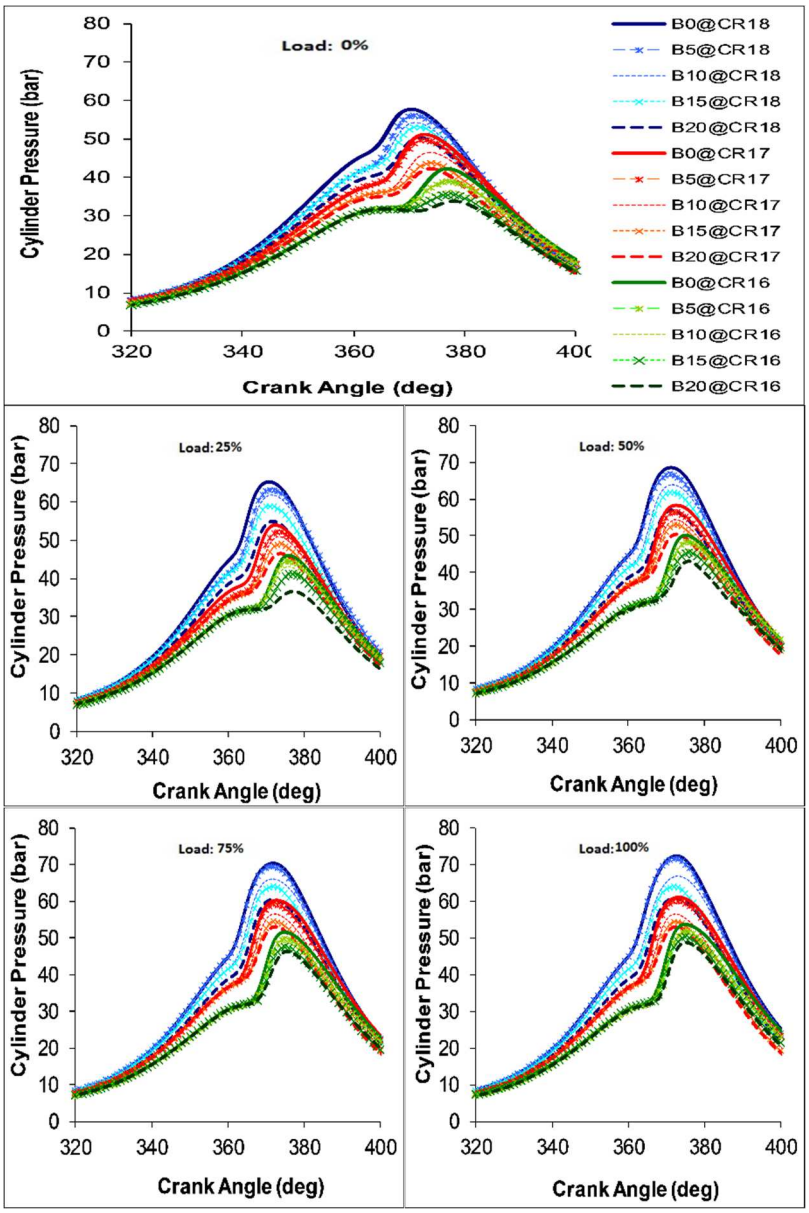

Figure 3.8: Graphical illustration of the Pressure versus CA variation using diesel & biodiesel-blend (B5, B10, B15, B20) with CR 18, 17 & 16 at different engine Load.

Figure 3.8 shows the impact of CR on CP of the engine fueled with petroleum-based diesel and biodiesel blends (B5, B10, B15, B20) at different engine loads. It was observed for CR 18; the peak CP decreased by 20% when utilizing B20 compared with B0 and about 3 CA delay. It might also be seen that B5 could compensate for this decrease in maximum pressure and longer ignition delay. Subsequently, it was noticed that the diesel fuel could be replaced by B5 fuel with a minimum amount of peak pressure loss. Bringing down the CR from 18 to 16 prompts a decrease in top CP from 72.29 to 53.68 bar (25%) for diesel, and from 69.29 to 47.38 bar (31%) for B5, 64.74 to 46.58 bar (28%) for B10, 61.89 to 46.24 bar (25%) for B15, and 58.80 to 45.03 bar (23%) for B20 biodiesel blend at peak engine load condition. The outcomes showed that peak CP improves with the increase in CR for all the test fuels and the effect of CR was higher in the B5 biodiesel blend than for petroleum diesel. Lower CR prompted lower gas temperature, and therefore longer ignition delay. Consequently, the Maximum CP moves further from TDC, showing an increment in ignition delay. Similar result was presented by **Selvan** *et al.* **(2009)**.

3.4.3 Impact of biodiesel blends on Ignition delay

Fuel's essential properties are viscosity and flash point, which influence the ignition delay. Viscosity influenced atomization and vaporization of fuel, influencing fuel-air mixture preparation (**Muralidharan** *et al.***, 2011**). From the experimental results, it was observed that with increase in blending percentage the SOC decreased at each load, but at the same time with increase in engine load the SOC increased for specific test fuels. If SOC increased in terms of BTDC that mean ignition delay reduced as the injection of fuel was taken place at fixed CA. Ignition delay reduced with an increase in the engine load. This phenomenon directly resulted from the increased in engine load, leading to heat incremented inside the chamber that enabled the fuel-air to ignite sooner. This pattern was reported by **Behera** *et al. (***2013**). At full load, the impact of tested biodiesel blends on the chamber gas temperature was more because of longer

ignition delay than diesel fuel. The phenomenon happened because higher viscosity fuel influences atomization and vaporization, influencing the fuel-air preparation and unsatisfactory spray formation for tested biodiesel blends. Figure 3.9 represents the change of SOC in before TDC (BTDC) with increased Engine loads for diesel and POME biodiesel blends. The SOC for diesel, POME blends (B5, B10, B15, B20) at full load and CR 18 was about 23°, 22°, 21°, 21° and 20° (degree BTDC) respectively because all the biodiesel blends had higher viscosity in correlation with petroleum-based diesel.

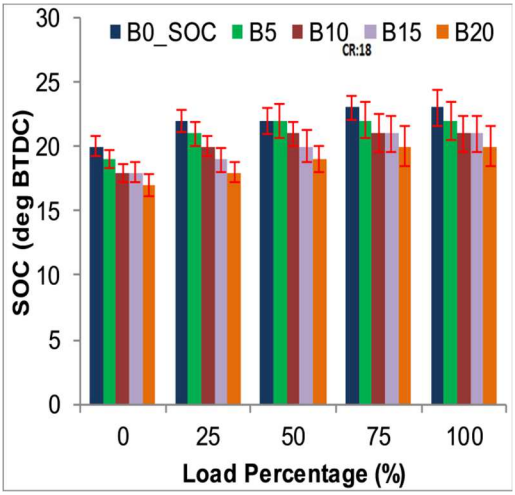

Figure 3.9: Graphical illustration of the Start of combustion at different loading conditions (CR 18).

3.4.4 Impact of compression ratio on Ignition delay

Figure 3.10 represent SOC's change with increased engine loads for diesel and different biodiesel blends (B5, B10, B15 & B20) at different compression ratios. It was observed that the SOC decreased with compression ratio hence increment in ignition delay. Lower CR prompted lower gas temperature, and therefore longer ignition delay.

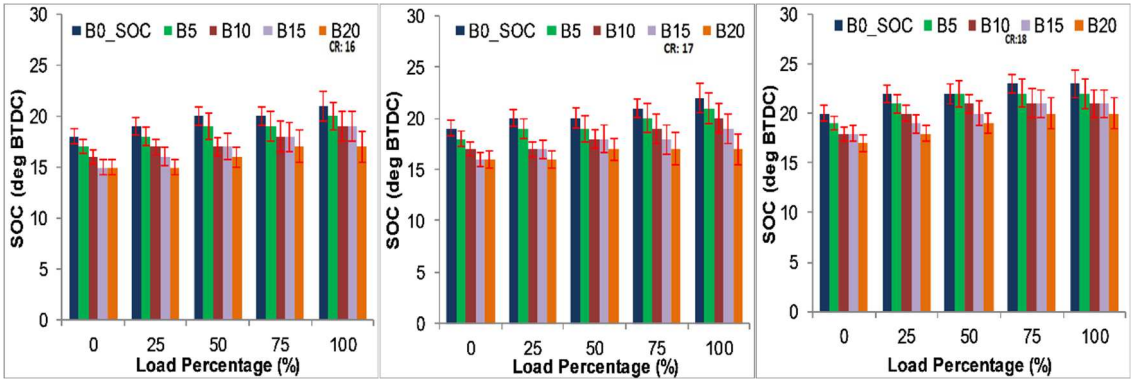

Figure 3.10: Start of combustion at different loading conditions (CR 16,17 &18).

3.4.5 Impact of biodiesel blends on Net Heat Release

From experiment results it was observed that at CR 16 the peak NHR differences was noticeable between engine load 0% to 50%. Where at CR 18 the peak NHR among test fuel was marginal for all engine load conditions. The NHR rate relied upon the SOC, ignition delay, fuel mass burned in the premixed phase at separate CR, and change in different fuel ignition rates. It was observed in the figures that the peak NHR was observed to be lower for all the biodiesel blends compared with petroleum-based diesel at 0% to 50% engine loads at various CR. The higher NHR for diesel was associated with its better mixture development and higher calorific value. Ignition delay and high fuel density was the cause of lowermost NHR for biodiesel blends at lower engine load. At higher engine load the peak NHR differences among test fuels were marginal. Similar observation was reported by **Elango and Senthil** (**2011**) for the Jatropha blends utilized as a fuel in an unmodified diesel engine.

Figure 3.11, 3.12, 3.13 portrays the change of the net heat release (NHR) rate with the CA plot for various POME at CR 18. 17 and CR 16 biodiesel blends (B5, B10, B15, B20) and diesel at various engine load conditions.

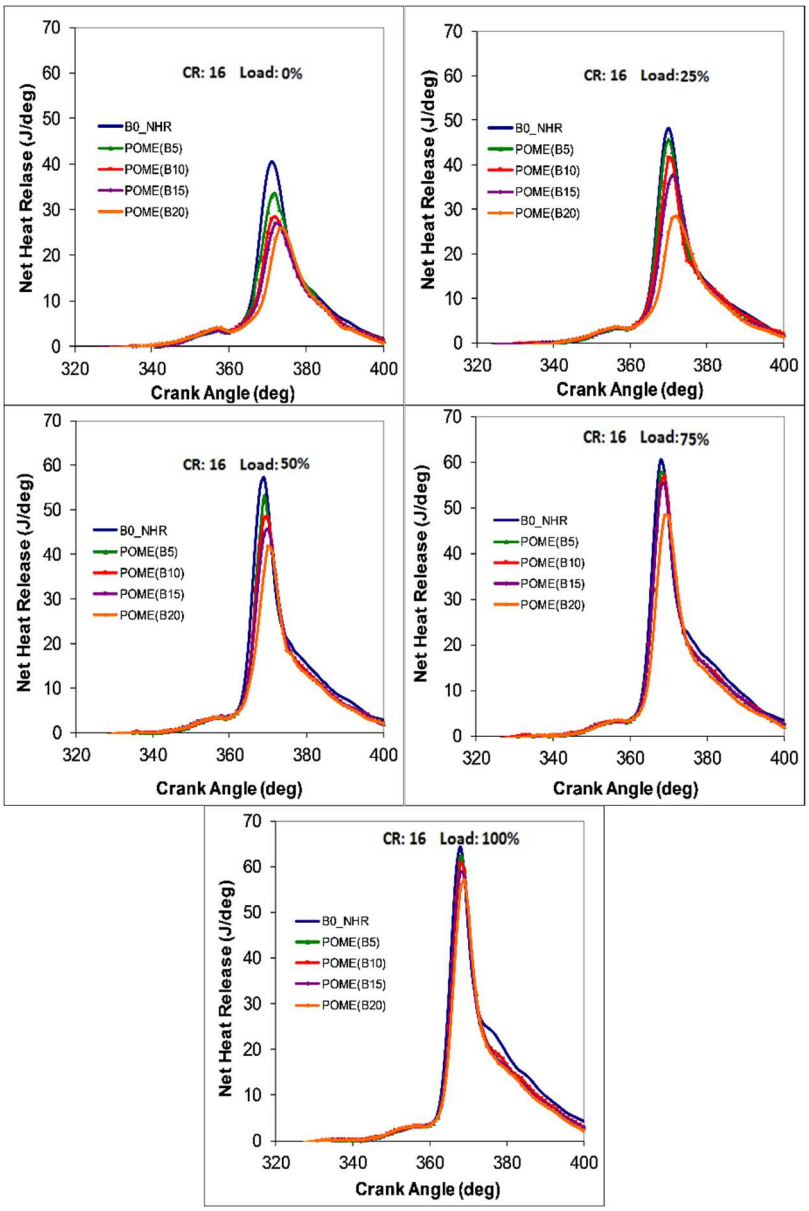

Figure 3.11: Graphical illustration of the NHR versus CA variation using diesel (B0), POME blends (B5, B10, B15 & B20) with CR 16:1 at 0% Load to 100% Load.

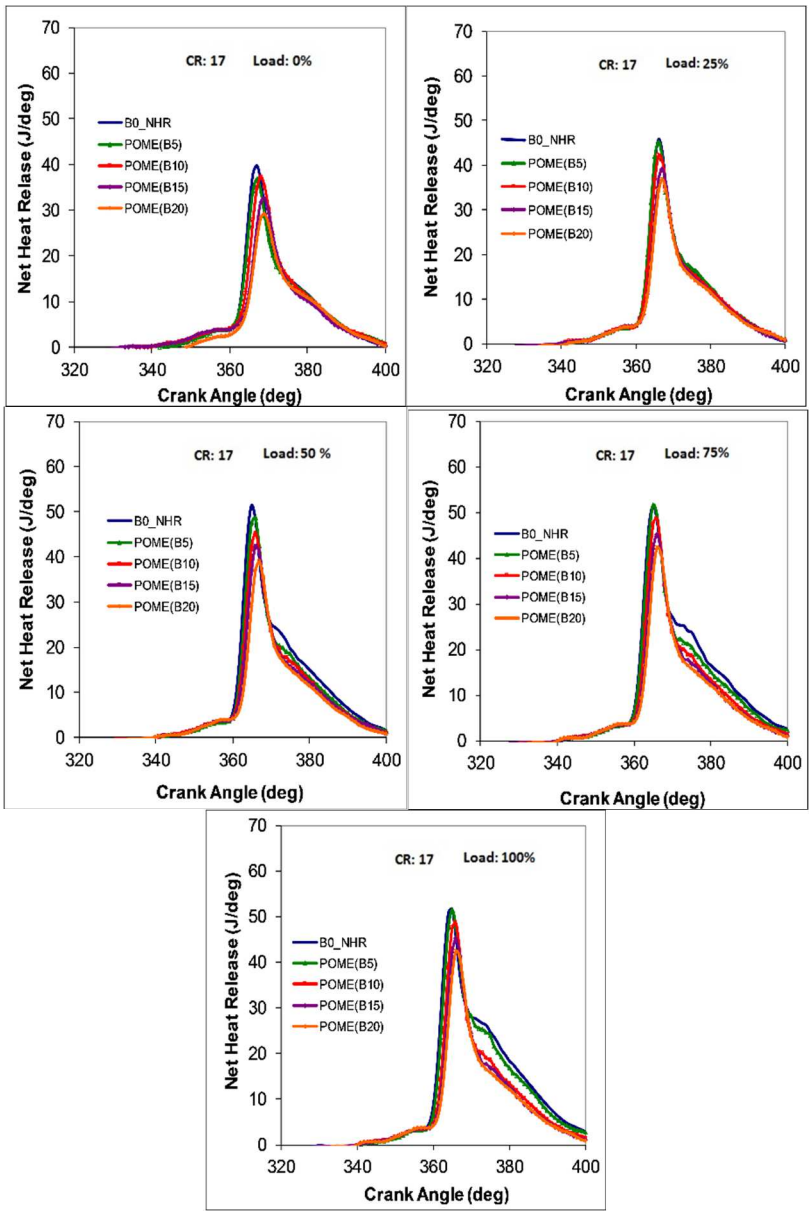

Figure 3.12: Graphical illustration of the NHR versus CA variation using diesel (B0), POME blends (B5, B10, B15 & B20) with CR 17:1 at 0% Load to 100% Load.

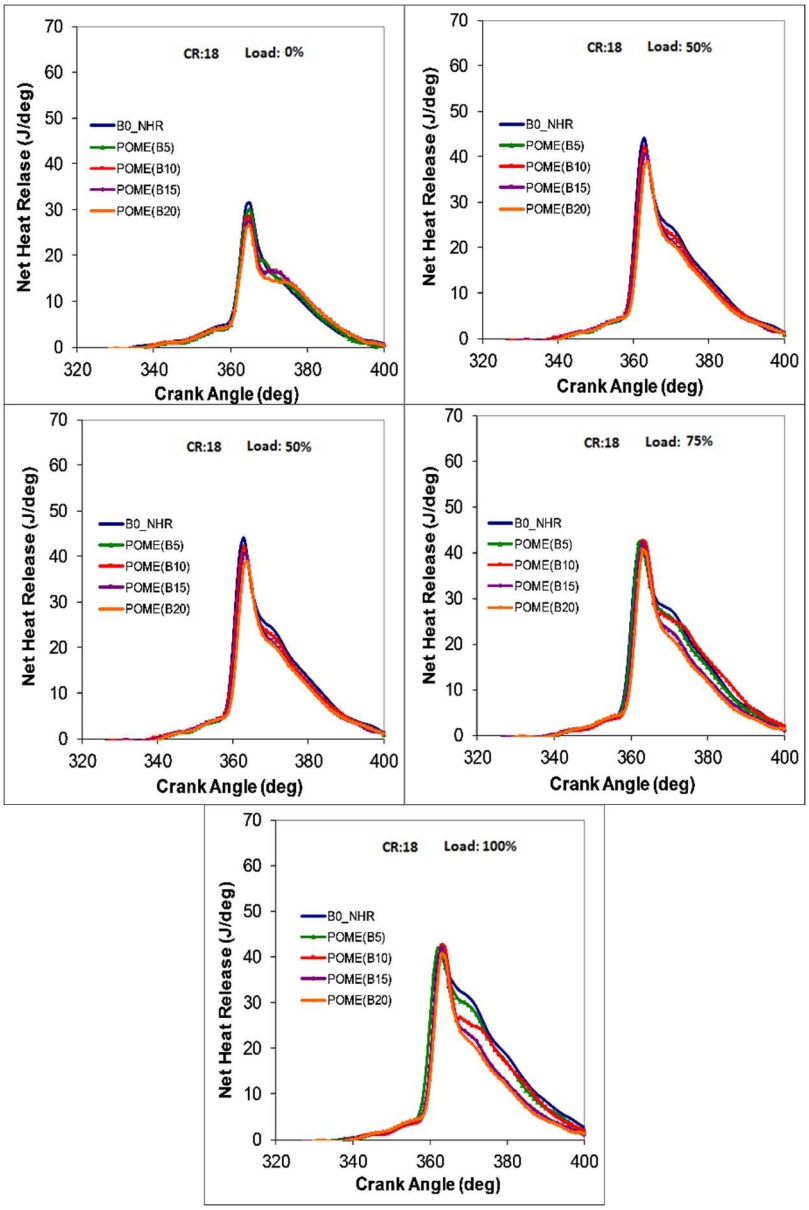

Figure 3.13: Graphical illustration of the NHR versus CA variation using diesel (B0), POME blends (B5, B10, B15 & B20) with CR 18:1 at 0% Load to 100% Load.

3.4.6 Impact of compression ratio on Net Heat Release

The impact of CR on NHR for diesel and biodiesel blends combustion is appeared in figure 3.11, figure 3.12, and figure 3.13, individually for different CR. A slight delay in top NHR & SOC with a reduction in CR was noticed for both petroleum-based diesel and biodiesel blends (B5, B10, B15 & B20). An increase in peak NHR, from 41.8 to 64.27 J/CA (53%) with a reduction in CR from 18 to 16, was seen for diesel. An increase in top NHR, from 40.49 to 56.88 J/CA (40%) with a change in CR from 18 to 16, was observed on B20 activity at peak engine load condition. This phenomenon had happened cause of the accumulation of more fuel in the combustion chamber and longer ignition delay with lower in-chamber gas temperature. Similar pattern was reported by **Hariram** *et al.* **(2015)**. On account of engine activity with biodiesel blends in the current investigation, higher NHR than diesel was seen at CR 18, particularly at higher CR settings. This event demonstrated a quicker ignition rate, perhaps because of the oxygen particle present in biodiesel atoms. Reducing the CR from 18 to 16 prompted a increase in the peak NHR. Likewise, this event could be because of high viscosity leading to poor atomization in biodiesel blends, at lower compression ratio due to longer ignition delay and more fuel accumulated. It was the reason behind the peak NHR value at lower CR.

3.4.7 Impact of biodiesel blends on Combustion duration

CD is the time between SOC to EOC. From the NHR curve, the CA where there was an abrupt rise in heat release was taken as the SOC. EOC was determined from the cumulative heat release rate. The EOC value was defined using the probable heat release rate's moving average in the data retrieval system. EOC point could be represented as the early point when the average heat release rate dropped below zero. The rapid rise in combustion pressure & NHR occurred in the event of rapid combustion with ignition delay. SOC was spotted concerning CA when the NHR was increased from zero to a positive value.

Figure 3.14 portrays the variety of the combustion duration (CD) as for different engine loads. It tended to be seen from the figure that CD incremented with an increase in the engine loads for all the biodiesel blends and diesel. This phenomenon happened because of the increase in fuel injected into the combustion chamber. Increasing the biodiesel percentage in biodiesel blends brings about a longer CD span. Since biodiesel was a more viscous fuel, which would require more effort for the burning, this resulted in slow combustion, which resulted longer CD length.

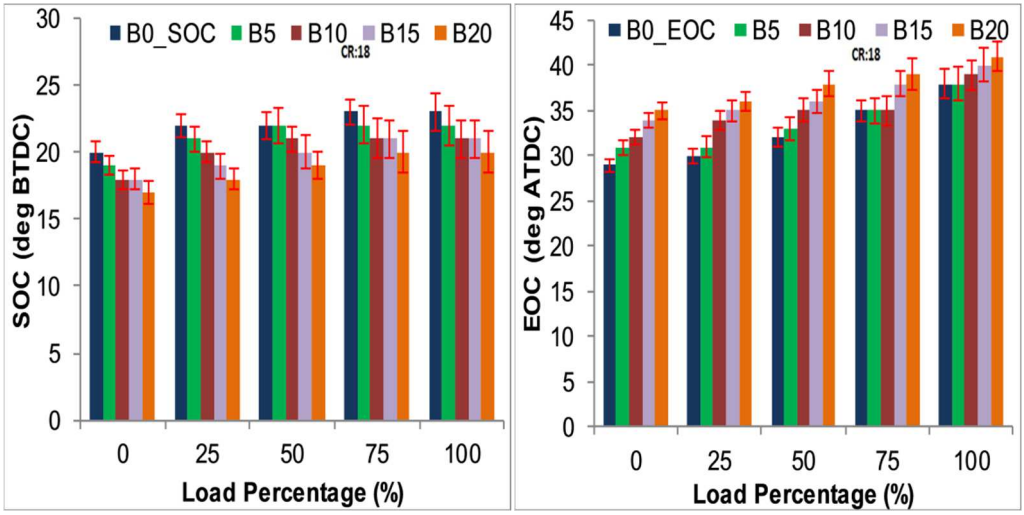

Figure 3.14: Graphical illustration of the Start of combustion (SOC) & End of Combustion (EOC) at different loading conditions (POME) (CR 18).

3.4.8 Impact of biodiesel blends on Mass fraction burned

Figure 3.15 portrays the variety of MFB with engine loads plot for diesel and biodiesel blends. The MFB of B5, B10, B15 & B20 blends displayed a similar pattern compared to diesel. It was observed that 5% and 10% MFB for all the tested biodiesel blends seem to be later than diesel at different engine load. This event was expected due to the higher viscosity in all biodiesel

blends fuel. Variation in MFB (mass burned fraction 5% & 10%) in the combustion chamber for all the test fuels are illustrated in figure 3.15. The MFB results were collected in the 'Engine soft' software interface developed by Apex Innovation Pvt. Ltd. In diesel (B0), the 5% & 10 % MFB amount was slightly higher than the B5 and B10 biodiesel blends at all loading conditions. This phenomenon happened because of the proper atomization of petroleum diesel. Also, it was observed that the value of 5% & 10 % MFB decreased with an increase in load due to higher evaporation. The 10 % MFB was calculated and plotted based on the after TDC (ATDC) crank angle. In experimental results, completion of 10 % mass fraction burned for B5 & B10 blends were very close to TDC point. That was why 10% of MFB value was almost nil for B5 & B10 blends in figure 3.15.

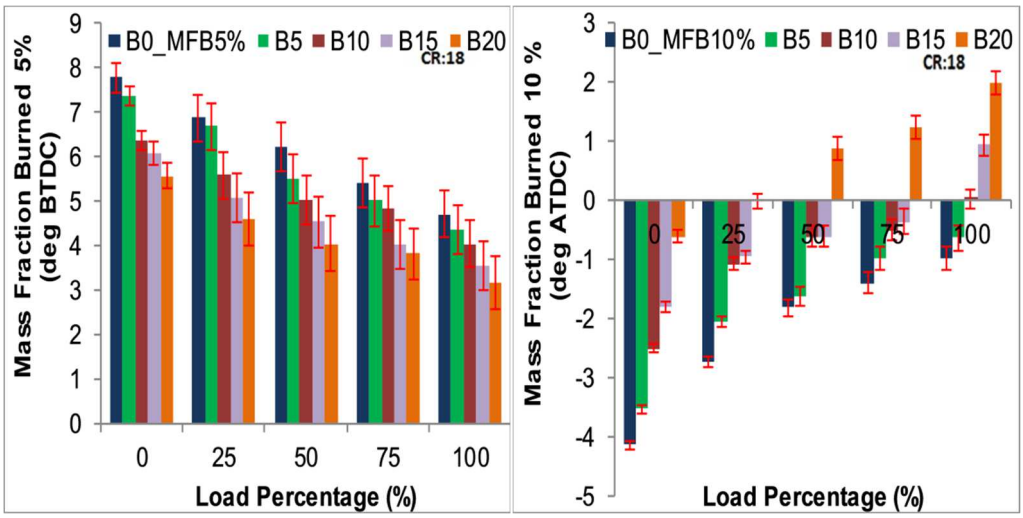

Figure 3.15: Graphical illustration of the Mass fraction Burned (5% & 10%) at different loading conditions (POME).

3.4.9 Impact of biodiesel blends on Brake thermal efficiency

It tended to be seen from the figure that the brake thermal efficiency (BTE) of all the tested fuel increased with increment in engine load. The BTE for diesel was observed to be maximum in this investigation. Since diesel had a higher LHV and appropriate air-fuel ratio, that outcomes complete ignition. It was observed from the figure that B5 and B10 show higher BTE at full engine load, contrasted with that of B15 and B20. This phenomenon resulted from the fuel's extra lubricity because of possibly higher viscosity and sulfur present in the blends. For B15 and B20, the BTE was lower than that of B5 and B10 cause of more density, lower LHV at full engine load. Similar results were reported by **Elango** *et al.* **(2011)**.

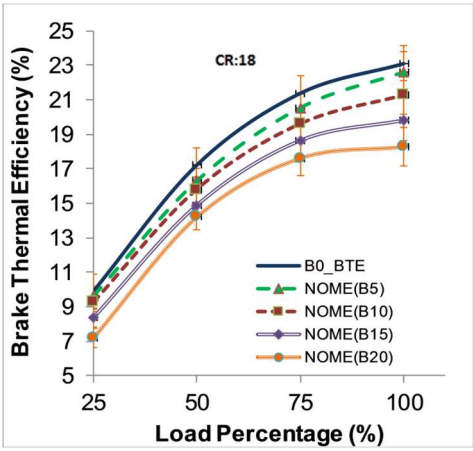

Figure 3.16: Brake thermal efficiency at different loading conditions (Diesel & NOME blends)

Figure 3.16 portrays the variety of BTE w.r.t engine load for diesel and all the test fuel blends in this investigation. It might be seen from the figure that the BTE increased with increment in the engine load for diesel and all the test fuel blends. The estimations of the BTE at full Load were 23.12%, 22.6%, 21.27%, 19.83%, and 18.27% for diesel, and the NOME B5, B10, B15, B20 blends individually. It was seen that the BTE of B5, B10, B15 & B20 blends (NOME) were lower

than that of diesel by about 2%, 8%, 14%, and 20% separately, at peak load. The phenomenon happened because of their lower calorific value and higher density contrasted with that of diesel. It was observed that rapid rise in BTE was between 0% to 75% engine load.

Figure 3.17 portrays BTE increased with increment in the Engine load for diesel and all the test POME fuel blends. The estimations of the BTE (POME) at full Load were 23.12%, 22.92%, 22.31%, 19.88%, and 18.37% for diesel, and the POME B5, B10, B15, B20 blends individually. With increase in engine load from 0% to 75% a sharp rise in BTE was observed for all the test fuels and at 0% to 25% load conditions, BTE of all test fuels were very close to each other. Similar observation was found in WVOME blends, but at peak load condition the BTE differences was noticeable compared to diesel.

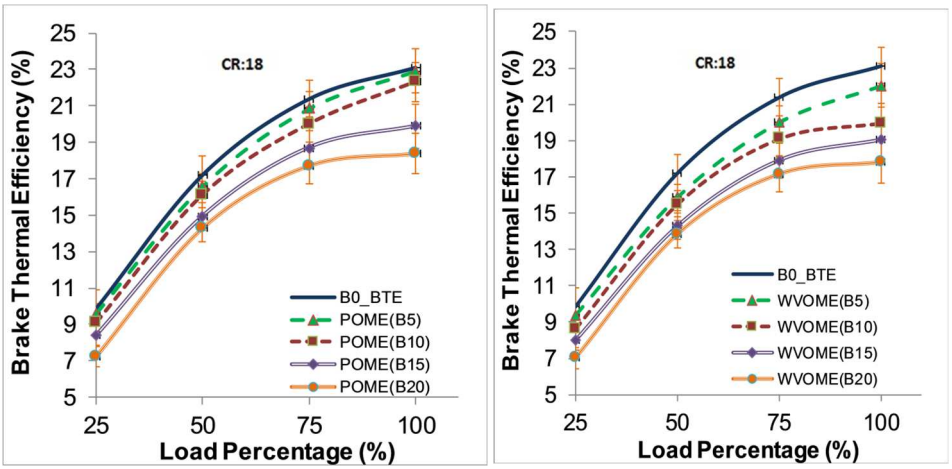

Figure 3.17: Brake thermal efficiency at different loading conditions (Diesel, POME & WVOME blends)

It was seen that with the increase in load, at first, BTE was increased, and with the further increase in load, BTE had followed a downturn. The observed development in the BTE was clarified with the support of BMEP. As the engine load expanded, BMEP increased because of more fuel burning. This event resulted in an increment in the BTE at first. However, it was seen

that after a 75% engine load, the BTE curve presented descending pattern. This phenomenon was because the time taken to complete the combustion reduced when the increase of load past the 75% engine load at high temperature and BMEP bringing about more fuel inflow and more energy necessity. It was seen that BTE reduced with the increase in the biodiesel content in the fuel. The components influencing this aspect were viscosity and fuel LHV. With the increase in the biodiesel content, the heating value decreased, bringing about less force produced; therefore, BTE reduced. With the increment in biodiesel content, there was an increment in the viscosity of fuel, which brought about poor atomization of fuel injector and low power output, making low BTE.

3.4.10 Impact of compression ratio on Brake thermal efficiency

Figure 3.18 illustrates the variety of BTE for diesel, B5, B10, B15, B20 blends at peak engine load at CR 16, 17, and 18. It was seen that increase in the CR, the BTE increased. This phenomenon was a result of the increase in BMEP with the increase in CR.

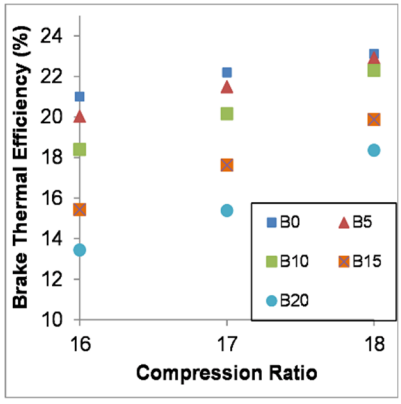

Figure 3.18: Brake thermal efficiency at different CR (Diesel & biodiesel blends)

With the increase in CR, the BMEP estimations increased because of high CP and temperature assuring a superior burning to occur, bringing about high BTE. For the most part, BTE reduced with the increase in the biodiesel content. However, at CR 18:1, it was seen that BTE was high

for B5 & B10 in comparison with petroleum-based diesel. This aspect was because of the high temperature and CP developed in the chamber at CR 18:1 and because of the higher oxygen content in the biodiesel. The most increased BTE was noted at the peak engine load condition for diesel as 23.12% (CR 18:1).

3.4.11 Impact of biodiesel blends on Brake specific fuel consumption

The variety of NOME BSFC with the engine load is portrayed in figure 3.19 (a). It was observed from the figure the BSFC same pattern was followed for diesel, and all biodiesel blends test fuel. The BSFC of B5, B10, B15, and B20 was higher than diesel at all engine loads. The more density and lower LHV were the cause behind the higher BSFC. Similar outcomes were reported by **Altun** *et al.* **(2008)**. The BSFC of diesel was discovered to be the least, which was about 0.37 kg/kW-h. Also, the estimations of BSFC B5, B10, B15, and B20 (NOME) were observed to be about 0.39, 0.42, 0.46, and 0.51 kg/kW-h, separately, at full engine load.

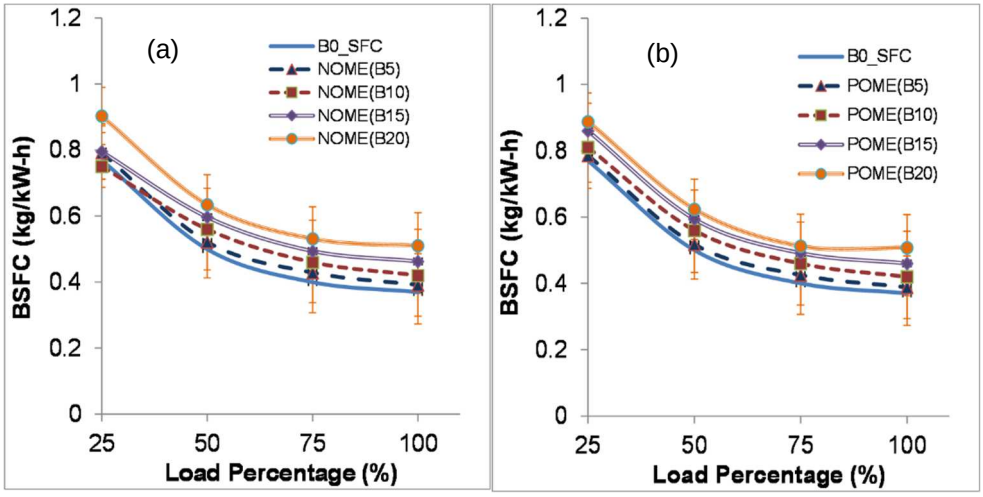

Figure 3.19: (a) Graphical illustration of the BSFC at different loading conditions (Diesel & NOME blends), **(b)** BSFC at different loading conditions (Diesel & POME blends)

The variety of POME BSFC with the engine load is portrayed in figure 3.19 (b). The BSFC of B5, B10, B15, and B20 (POME) were observed to be about 0.38, 0.42, 0.46, and 0.50 kg/kW-h, separately, at full engine load.

The variety of WVOME BSFC with the engine load is portrayed in figure 3.20. At full engine load, the BSFC values of B5 and B10 were 0.42 and 0.45, whereas the brake specific fuel consumption of B15 and B20 were about 0.46 and 0.53 kg/kW-h. The BSFC differences were marginal for all the test fuels between 0% to 50% load conditions. However, at peak load conditions, the BSFC differences were noticeable for B20 compared to other test fuels.

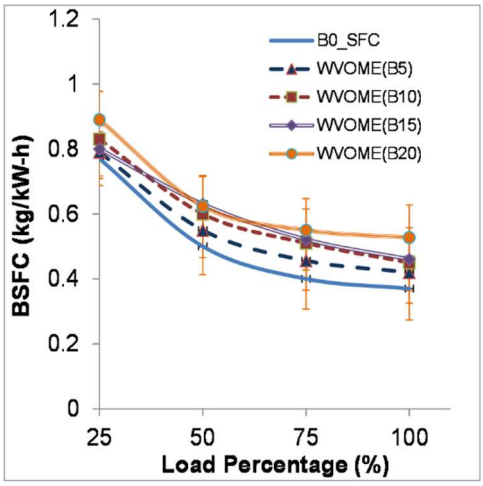

Figure 3.20: Graphical illustration of the BSFC at different loading conditions (Diesel & WVOME blends)

BSFC was calculated as the ratio of fuel consumption in kg/h to the brake power(kW). It was seen that the BSFC was higher for the test fuels with high biodiesel content. This aspect could be clarified with the assistance of LHV and the density of test fuels. As the LHV decreased with the biodiesel content, the fuel consumption to deliver a unit power increased, resulting in an

increment in the BSFC values. Another factor affecting BSFC was the density of the test fuel (**Datta and Mandal, 2017**). The densities were seen to be increasing with the biodiesel content. This event increased the fuel mass flow rate since more injected fuel for a similar load. With the increase in density, the fuel injector's atomization would be unsatisfactory, bringing about less effective burning and less power output. The BSFC values were seen to be decreasing with the load. This pattern was the same for petroleum-based diesel, B5, B10, B15, and B20 biodiesel blends.

3.4.12 Impact of Compression Ratio on Brake specific fuel consumption

There was an increase in fuel utilization with the increase in load; however, the engine power produced exceeded the fuel utilization, which brought reduced BSFC. Acceleration in CR up to 18:1 from the CR 16:1 has appeared in figure 3.21. The diagram shows the variety of BSFC with CR at top engine load conditions.

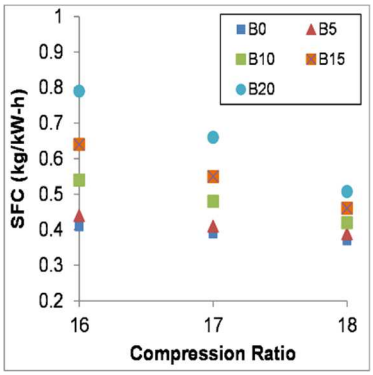

Figure 3.21: Graphical illustration of the BSFC (Diesel & biodiesel blends) at different CR (16:1, 17:1 and 18:1)

With the increase in CR, the BSFC values decreased. The reason behind this pattern was because BMEP expanded with CR increase. This event came about with more power development and less BSFC values.

3.4.13 Impact of compression ratio and biodiesel blends on energy analysis

The transformation of fuel energy into heat energy was analyzed at CR 16, 17, 18 at 100% engine load. The VCR engine was considered for this investigation; CR's impact on different energy circulations under different biodiesel blends was calculated at the average and is illustrated in figures 3.22. The energy in the shaft and cooling water, reduced by 4% and 6%, separately, for change in CR from 18:1 to 17:1 and The energy in the shaft and cooling water, reduced by 9% and 16%, separately, for change in CR from 18:1 to 16:1. For similar settings, energy diverted by exhaust gases and the unaccounted loss incremented by 21% and 11%, individually for change in CR from 18:1 to 17:1 and 33% and 19% for change CR from 18:1 to 16:1.

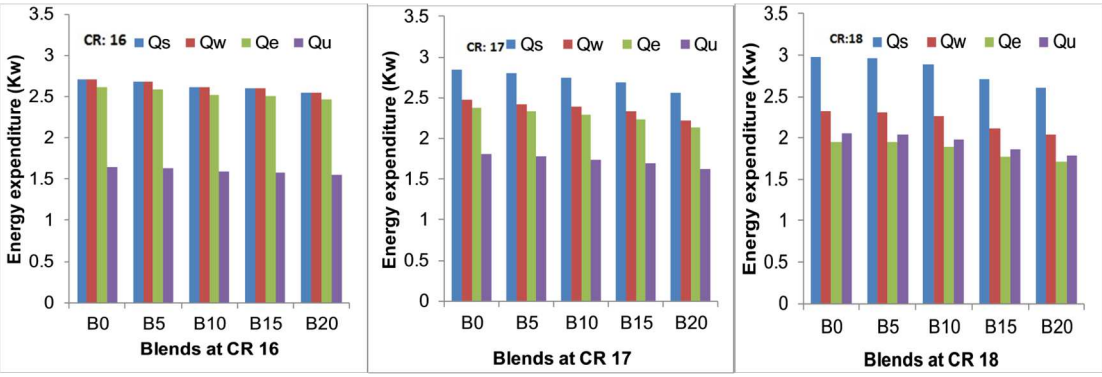

Figure 3.22: Graphical illustration of Energy distribution of diesel and biodiesel blends at CR 16,17,18

The reason was because of the quick distribution of temperature at higher CR. The energy transformation of tested blends (B15 and B20) decreased because of its poor volatility nature and

ignition delay (**Zheng** *et al.,* **2012**). Increasing CR from 16:1 to 18:1, power output increment was observed.

3.4.14 Impact of biodiesel blends on exergy analysis

The exergy analysis of the test engine for the test fuels was considered on exergetic efficiency, which was the exergy ratio of shaft work to the sum of exergy of incoming air and fuel. It is noticeable in figure 3.23 that the exergetic efficiency and fuel exergy were increased with an increase in load due to high fuel consumption at higher load.

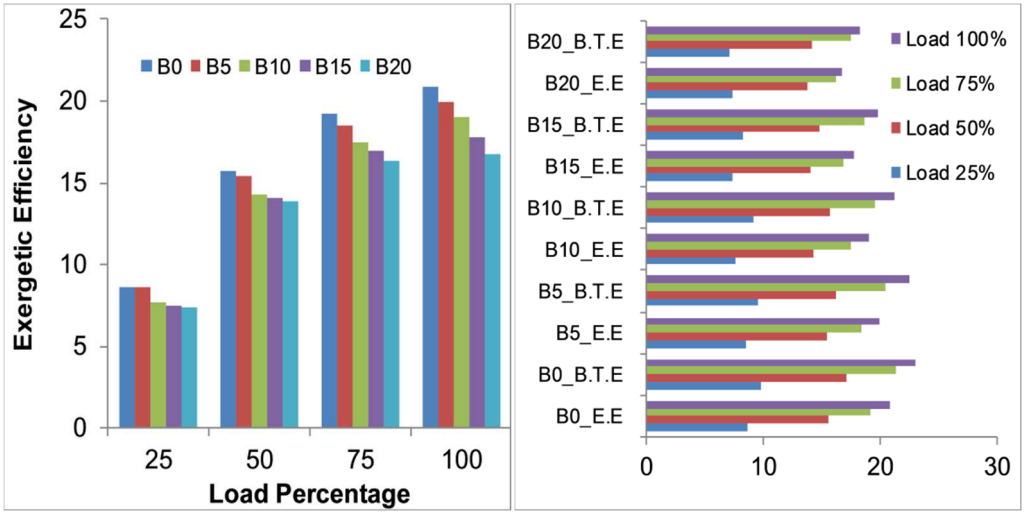

Figure 3.23: Graphical illustration of the exergetic efficiency at different loading conditions & Comparison of exergy efficiency and brake thermal efficiency at different loading conditions.

Compared with petroleum diesel (B0), a noticeable reduction in biodiesel blends' exergetic efficiency was observed. This phenomenon happened cause of the lower heating value of test fuel and the low shaft exergy. The exergetic efficiency correlated the actual engine systems with a theoretical consideration, and operating under the same circumstances. Figure 3.23 illustrates

different loads at CR 18 on the engine with exergetic efficiency of an unmodified diesel engine fueled with Diesel (B0) and Diesel-biodiesel blends (B5, B10, B15, B20). From the right-side figure of figure 3.23, it was observed that the increase in exergetic efficiency along with engine load matches the trend of brake thermal efficiency. Also, it was noticeable that the brake thermal efficiency was slightly higher than exergetic efficiency. The reason might be the cause of thermodynamic irreversibility.

3.4.15 Impact of biodiesel blends on emission

The high emission of CO was because of the poor ignition of fuel-air due to inadequate air present around fuel atoms or lacking time in the cycle for complete combustion. The CI engine gives low emission of CO as they generally work with a lean fuel-air ratio at low engine load. The variety of CO emissions with engine load for all tested fuels is portrayed in figure 3.24.

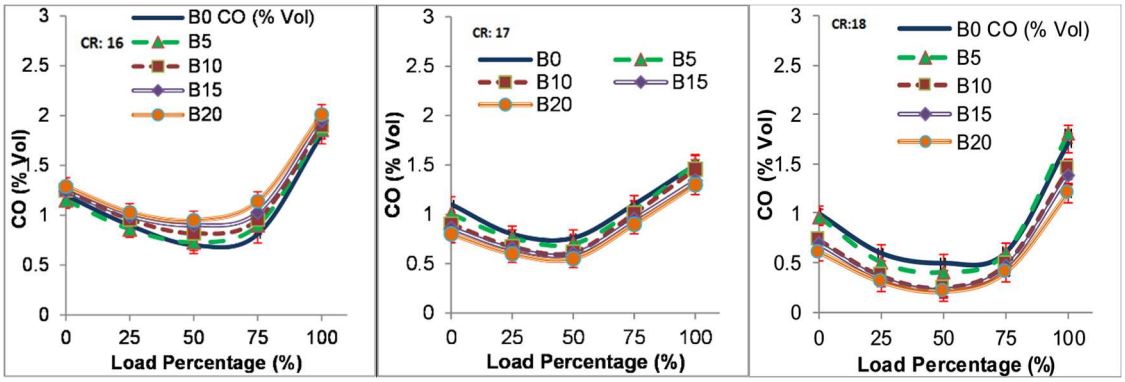

Figure 3.24: Graphical illustration of the Carbon Monoxide emission at different loading conditions and at different CR (16, 17, 18). (POME)

It was observed from the figure that the emission of CO was the least for B20, compared with other test fuels individually at different load conditions. The reason was the presence of more oxygen. Emission of CO happened on account of incomplete fuel ignition in the CI engine. At first, the CO emissions decreased up to 50% engine load and afterward abruptly increased at higher engine load. At 50% engine load, the decreased in CO emission was because of the burning

of the more lean fuel-air mixture. The excess fuel-air proportion was prompted to produce more smoke and prevented oxidation of CO to CO_2; therefore, emission increased. The emission of CO was observed to be lower in B20 fuel than other test fuels. At peak load condition and 17:1 CR, the noticed CO emission decreased by about 13% for B20 compared to diesel. With increasing CR (17:1 to 18:1), the emission of CO was evaluated in B20 fuel activities. For instance, at peak load, the CO emanations in B20 fuel decreased by about 23% when the CR was increased from 17:1 to 18:1.

The impact of CR on CO emission has appeared in figure 3.24. Emission of CO exceptionally relies upon the burning temperature and accessibility of oxygen. A decrease in CR from 18 to 16 prompted an increase in CO emissions by 40% for B20, while it was observed higher emission of CO at B20 blend in CR to 16 compared to petroleum diesel. The reason was more fuel accumulated at CR 16. Also, lower emission of CO was recorded under engine activity with CR settings 17:1 and 18:1. Biodiesel blends recorded lower CO emissions at CR 17 & 18 cause of oxygen present in the biodiesel structure.

Figure 3.25 portrays the emission of NOx outcome of different engine loads at different CR. Emission of NOx was fundamentally made with dissociation of the climatic nitrogen at high adiabatic flame temperature conditions. It was strongly developed with maximum ignition temperature, oxygen presence, and NOx formation time. It was observed that at higher engine load, NOx increased with expanding engine load. This event directly resulted from the considerable fuel consumed at higher engine load, followed by high CP and temperature, and consequently, NOx increased. Also, the emission of NOx development was higher at CR 17 for all the tested biodiesel blends than diesel. This increased NOx discharge was because of the oxygen presence with biodiesel blends, specifically B20.

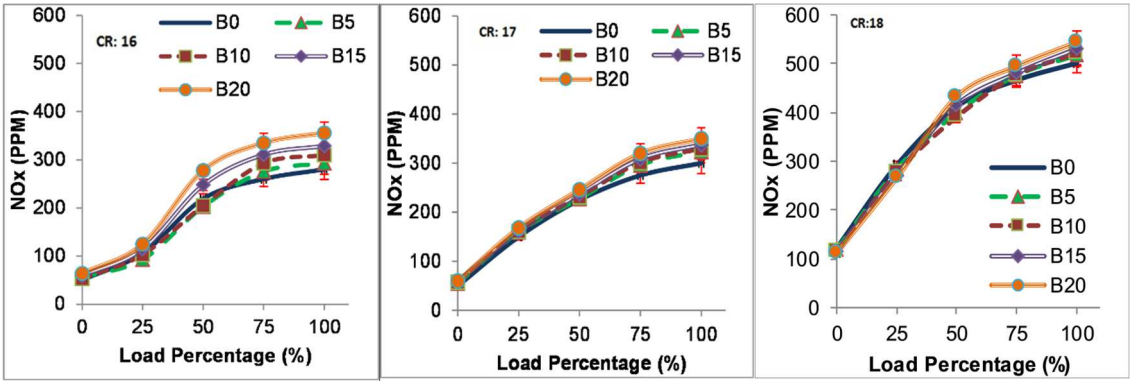

Figure 3.25: Graphical illustration of the Oxides of Nitrogen emission at different loading conditions and at different CR (16, 17, 18). (POME)

Figure 3.25 also portrays CR's impact on NOx development during the combustion cycle for engine activity with diesel and biodiesel blends. The outcomes showed that NOx emissions' arrangement was more delicate to CR on account of engine activity with biodiesel blends than with petroleum diesel. On decreasing the CR from 18 to 16, NOx emission was reduced by around 33% for B20. However, it was also observed that at lower CR and peak load conditions, the differences in NOx emission among the test fuels were noticeable.

Figure 3.26 portrays the variety of HC emissions with engine load for diesel and biodiesel blends (B5, B10, B15, B20). The outcomes presented that the HC discharges incremented with expanding engine load. At 17 CR and zero engine load, the evaluated HC discharge was 25 ppm for diesel, but it increased to 43 ppm at peak engine load. However, at CR 16, the HC emission was marginally higher for biodiesel blends at peak load conditions cause by more fuel accumulation at the ignition delay period. The expanded emission of HC at higher engine load was because of oxygen inadequacy; leaner fuel-air burning offers lower HC emissions. Like this, the HC emissions decreased with tested biodiesel blends at all engine loads as for diesel at CR (17:1 and 18:1). It had occurred cause of improved oxygen content in tested biodiesel blends,

which prompted complete fuel burning. With expanding CR (17:1 to 18:1), HC's emission were reduced for B15 and B20 because higher CR offers high CP and temperature, which improves fuel burning.

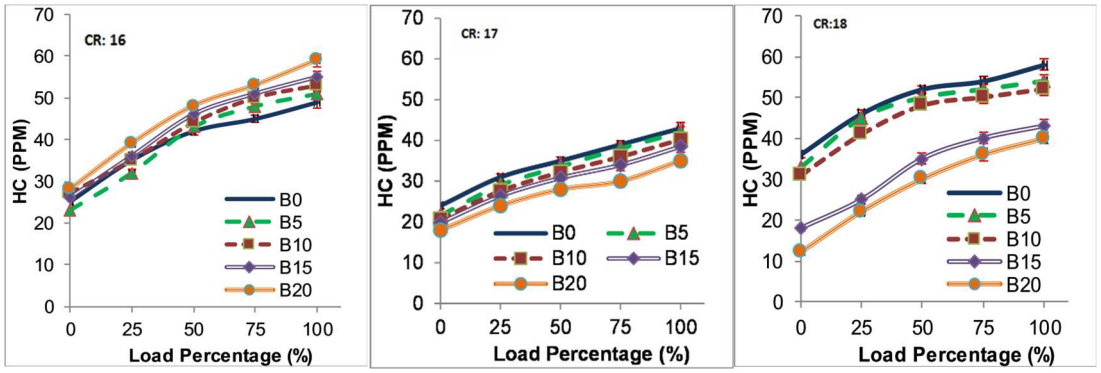

Figure 3.26: Graphical illustration of the Unburnt Hydrocarbon emission at different loading conditions and at different CR (16, 17, 18). (POME)

3.5 Closure

To sum up, in this chapter, the engine could run on biodiesel blends successfully up to B20 without any significant engine modification, but B5 and B10 gave a better performance with overall lower emission than B20. The advantages of recommended high compression ratio engine operation were discussed. In the case of POME, NOME, and WVOME tested blends, marginal differences were observed, though POME blends perform better than the other two. In this regard, the next chapter concentrated on developing a thermodynamic single-zone CI engine model fueled with biodiesel blends. The single-zone engine model was validated with obtained experimental results.

Chapter 4

Modeling of Biodiesel-blend fueled Compression Ignition Engine

4.1 Introduction

This chapter discusses the development of the biodiesel blend powered compression ignition (CI) engine model. The model had been created considering a single zone thermodynamic boundaries by some species' properties present in the combustion chamber during the cycle. The chapter deals with the formulation and validation of the biodiesel blend fired diesel engine using a crank slider, cylinder pressure, and heat release model incorporated with a modified Weibe function reported by **Stone (1994)**. The developed model was validated with the experimental results from an unmodified engine fuelled with biodiesel blends (B5 & B10). Simulation of the engine was developed considering the impact of bore, stroke, connecting rod length, crank radius, compression ratio, equivalence ratio, thermodynamic relations during combustion, and variable specific heat on the general engine operation (**Abu Nada *et al.*, 2006; Abu Nada *et al.*, 2007**). The in-house developed code was utilized in these investigations with a sequentially approved thermodynamic, single-zone computational model. Although the model was initially produced for the spark-ignition engine, it tended to be stretched out and adjusted to maintain compression ignition engine activities. The activity and performance examination of CI and SI engines was fundamentally the same as from a thermodynamic perspective, yet the principal distinction was embedded in the heat release model. The CI engine model comprised the accompanying sub-models, and it incorporates the following assumptions:

- The cylinder charge (intake air) and combustion product mixture were assumed as an ideal gas.
- The cylinder charge (intake air) and combustion product mixture were assumed to be homogeneous.
- Chemical equilibrium existed among the gaseous species inside the combustion chamber.
- The specific heats of the gaseous species varied with the local temperature.
- Variations in specific heats had been considered with the crank rotation change due to change in temperature and composition.
- Heat added to the cycle based on the mass fraction of the fuel burnt as a crank angle function using modified Weibe function.
- Heat transfer loss was assumed as a fraction of total heat generated during combustion (**Lin *et al.*, 2008**).
- There was no effect on the combustion chamber design but a flat topped piston was utilized in the model development.
- The chemical formula was assumed for diesel $C_{14}H_{25}$ and biodiesel $C_{17.20}H_{32.31}O_2$ for emission modeling (**Yesilyurt, 2020**).
- The engine load change was considered based on actual fuel consumption and equivalence ratio from the experimental results at the same engine load and speed.

A computer program was written on the FORTRAN program for the presented thermodynamic model. Fortran is a computer programming language that is extensively used in numerical, scientific computing. FORTRAN, in full 'Formula Translation', a computer programming language created in 1957 by John Backus that shortened the process of programming and made computer programming more accessible (Backus, 1981). Fortran is a relatively small language that is surprisingly easy to learn and use.

4.2 Crank Slider Model

The engine geometry calculation has appeared in figure 4.1. The relation between the chamber volume and the crank angle was the capacity of compression ratio, bore, stroke and connecting rod length. The compression ratio (CR) of engine was presented as:

$r_c = \frac{(V_d + V_c)}{V_c}$ Where, V_d was the displaced or swept volume and V_c was the clearance volume.

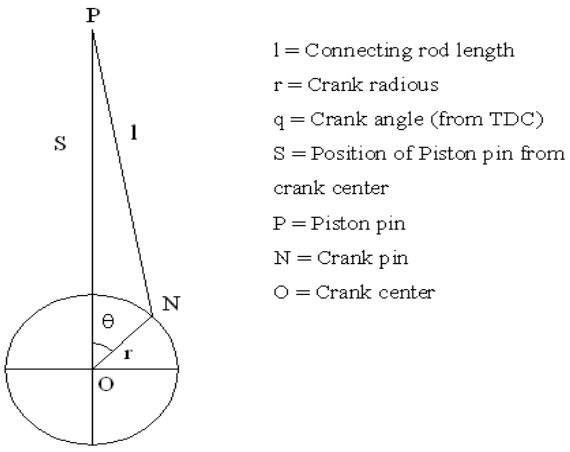

Figure.4.1: Engine cylinder and piston arrangement

In figure 4.1, expression for Scould be obtained as

$$S = r\cos\theta + \sqrt{l^2 - r^2 \sin^2\theta} \tag{4.1}$$

The vertical piston position relative to the Top Dead Center (TDC) could be expressed as,

$$z(\theta) = l + r(1 - cos\,\theta) - \sqrt{l^2 - r^2\,sin^2\,\theta} \tag{4.2}$$

The cylinder volume V at any crank position θ was obtained by

$$V = V_c + (\pi/4)B^2(l + r - S) \tag{4.3}$$

Here, V = cylinder volume, V_c= clearance volume, B = bore of engine cylinder, S = stroke

R =ratio of connecting rod length to crank radius.

Instantaneous volume with respective to crank angle were presented as (**Pulkrabek, 2004**):

$$V = V_c + (\pi/4)B^2 \times S/2 \times \left[\left(1 + R - cos\,\theta - \sqrt{R^2 - sin^2\,\theta}\right)\right] \tag{4.4}$$

The derivative of the combustion chamber volume with respect to crank angle could now be calculated by differentiating with respect to θ

$$\frac{dV}{d\theta} = \frac{\pi B^2}{4} \cdot 2z \cdot \frac{dz}{d\theta} \tag{4.5}$$

$$\frac{dV}{d\theta} = \frac{\pi B^2}{2} \cdot \left(l + r(1 - cos\,\theta) - \sqrt{l^2 - r^2\,sin^2\,\theta}\right) \cdot \left(r\,sin\,\theta\left(1 + r\,cos\,\theta\,(l^2 - r^2\,sin^2\,\theta)^{-1/2}\right)\right) \tag{4.6}$$

These equations (4.1 to 4.6) described the relation between cylinder volume and crank angle in an internal combustion engine.

Engine average piston speed or mean piston speed was obtained by

$$\overline{\vartheta_{pis}} = 2SN \tag{4.7}$$

Where, N was the rpm.

Cross sectional area of a cylinder and surface area of a flat topped piston was calculated according to **Pulkrabek (2004).**

$$A = A_{ch} + A_p + \frac{\pi BS}{2}[R + 1 - cos\,\theta - \sqrt{R^2 - sin^2\,\theta}] \quad (4.8)$$

Where, A_{ch} was the surface area of cylinder head, A_p was the cross sectional area of a flat topped piston.

4.3 Cylinder Pressure Model

According to the First law of thermodynamics (**da Silva, 1993; Caton, 2001**),

$$\Delta U = Q - W \quad (4.9)$$

ΔU = change in internal energy of a closed system, Q = quantity of heat supplied to the system, W = work done by the system.

Combustion model was developed based on the conservation principle applied to a combustion chamber as the control volume.

The relation from ideal gas law and its differential form,

$$PV = mR_gT \; and \; \frac{dV}{V} + \frac{dP}{P} = \frac{dT}{T} \quad (4.10)$$

The relation from conservation of energy could be expressed in differential form and applied to a control volume, the equation becomes:

$$\frac{d(mu)}{d\theta} = \dot{Q}^{cyl} - \dot{W}^{cyl} \quad (4.11)$$

Here, m = mass flow rate, u = internal energy

$$\Rightarrow \frac{d(mu)}{d\theta} = \frac{dQ}{d\theta} - \frac{dW}{d\theta} \quad (4.12)$$

$$\Rightarrow m\frac{du}{d\theta} + u\frac{dm}{d\theta} = \frac{dQ}{d\theta} - \frac{dW}{d\theta} \quad (4.13)$$

$$\Rightarrow m\frac{du}{d\theta} = \frac{dQ_g}{d\theta} - \frac{dQ_{ht}}{d\theta} - \frac{dW}{d\theta} \tag{4.14}$$

[Q_g =Apparent gross heat release, Q_{ht} =Heat transferred to the cylinder wall]

and net heat release rate was

$$\frac{dQ_n}{d\theta} = \frac{dQ_g}{d\theta} - \frac{dQ_{ht}}{d\theta} = m\frac{du}{d\theta} + P\frac{dV}{d\theta} \tag{4.15}$$

Since $u = c_v T$ and $du = c_v dT$

$$\frac{dQ_n}{d\theta} = mc_v\frac{dT}{d\theta} + P\frac{dV}{d\theta} \tag{4.16}$$

Rearranging equations (4.10 and 4.16),

$$\frac{dQ_n}{d\theta} = mc_v\left[\frac{T}{V}\frac{dV}{d\theta} + \frac{T}{P}\frac{dP}{d\theta}\right] + P\frac{dV}{d\theta} \tag{4.17}$$

$$\Rightarrow \frac{dQ_n}{d\theta} = P\frac{dV}{d\theta} + \frac{c_v P}{R}\frac{dV}{d\theta} + \frac{c_v V}{R}\frac{dP}{d\theta} \tag{4.18}$$

$$\Rightarrow \frac{dQ_n}{d\theta} = \left(1 + \frac{c_v}{R}\right)P\frac{dV}{d\theta} + \frac{c_v V}{R}\frac{dP}{d\theta} \tag{4.19}$$

$$\Rightarrow \frac{dQ_n}{d\theta} = \left(\frac{k}{k-1}\right)P\frac{dV}{d\theta} + \left(\frac{1}{k-1}\right)V\frac{dP}{d\theta} \tag{4.20}$$

Where,$R = c_v(k-1)$ and k =adiabatic index = $\frac{c_p}{c_v}$

Equation (4.20) was the simplified pressure model which could be rearranged as

$$\frac{dP}{d\theta} = \frac{k-1}{V}\frac{dQ_n}{d\theta} - \frac{kP}{V}\frac{dV}{d\theta} \tag{4.21}$$

The $\frac{dV}{d\theta}$ could be determined from equation (4.6) and$\frac{dQ_n}{d\theta}$ was obtained by using the Wiebe function.

The net heat term had both heat added and heat loss in case of combustion

$Q_n = Q_{in}x_b - Q_l$ Where, Q_{in} indicated total heat input and x_b as fraction of heat release,

$$\Rightarrow \frac{dQ_n}{d\theta} = Q_{in}\frac{dx_b}{d\theta} - \frac{dQ_l}{d\theta} \tag{4.22}$$

The heat loss could be obtained as,

$$\Rightarrow \frac{dQ_n}{d\theta} = Q_{in}\frac{dx_b}{d\theta} - \frac{dQ_l}{d\theta} \tag{4.23}$$

$$\frac{dQ_l}{d\theta} = \frac{hA}{\omega}(T_w - T_g) \tag{4.24}$$

Where, h = heat transfer coefficient, ω = rotation speed (rad /sec), A = area of cylinder wall, T_w= temperature of cylinder wall.

The pressure variation during the intake and exhaust stroke could be obtained as (**Ganesan, 2013**):

$$\frac{dP}{dt} = kP\left(\frac{1}{M}\frac{dM}{dt} - \frac{1}{V}\frac{dV}{dt}\right) \tag{4.25}$$

The equation (4.26) required mass flow rate dM/dt, which was to be found from the equations of fluid mechanics. For the intake stroke, mass flow rate could be obtained as:

$$\frac{dM_{in}}{dt} = AP\sqrt{\frac{2k}{RT(k-1)}\left(\frac{P_{in}}{P}\right)^{\frac{k-1}{k}}\left[\left(\frac{P_{in}}{P}\right)^{\frac{k-1}{k}} - 1\right]} \tag{4.26}$$

[When (Pin/P)<PRcrit]

$$\frac{dM_{in}}{dt} = AP\sqrt{\frac{k}{RT}\left(\frac{2}{k+1}\right)^{(k+1)/(k-1)}} \tag{4.27}$$

[When(Pin/P)>PRcrit]

The critical pressure ratio that defines the two regimes was called $PR_{crit}$and depended only on the value of k of the gas.

$$PR_{crit} = (\frac{k+1}{2})^{\frac{k}{k-1}} \tag{4.28}$$

Where P_{in} was the intake manifold pressure and P was the cylinder pressure.

Similarly for the exhaust stroke there was a little change in the mass flow rate equation which was mentioned below.

$$\frac{dM_{ex}}{dt} = AP \sqrt{\frac{2k}{RT(k-1)}(\frac{P}{P_{ex}})^{\frac{k-1}{k}}\left[(\frac{P}{P_{ex}})^{\frac{k-1}{k}} - 1\right]} \tag{4.29}$$

[When (P/Pex)<PRcrit]

$$\frac{dM_{ex}}{dt} = AP\sqrt{\frac{k}{RT}(\frac{2}{k+1})^{(k+1)/(k-1)}} \tag{4.30}$$

[When (P/Pex)>PRcrit]

Where P_{ex} was the exhaust manifold pressure and P was the cylinder pressure.

Where valve area could be obtained as:

$$A = A_{in}(|sin\,\theta|)^{1/3} \tag{4.31}$$

Where A_{in} was the wide-open valve area.

4.4 Heat release model

Ferguson (1986) suggested that the addition of heat might be a prescribed function of crank angle.

$$x_b = \frac{1}{2}[1 - cos\{\pi(\frac{\theta - \theta_s}{\Delta\theta})\ \}] \tag{4.32}$$

Here, x_b was the fraction of heat release, θ refers to crank angle, θ_S was the start of heat release and $\Delta\theta$ was the duration of heat release during $\theta_S < \theta < \theta_S + \Delta\theta$.

Ivan Ivanovitch Wiebe was a Russian engineer and scientist from the Urals of German decent who introduced this function (**Ghojel, 2010**). The emission characteristics of diesel engines are strongly correlated to the in-cylinder combustion processes. The engine combustion characteristics are mainly understood through the apparent heat release rate (AHRR) that is determined from the measured cylinder pressure data as a function of crank angle (θ) (**Rakopoulos et al., 2006**). The burn fraction or burn rate of a combustion process are normally characterised using Wiebe equation (4.33), which was introduced more than 60 years ago (**Ghojel et al., 2010**). The Wiebe equation presents the relationship between the burn fraction (x_b) and the three main combustion parameters, that is., (i) the instant at which heat release rate becomes positive, θs; (ii) instantaneous crank angle, θ; and (iii) the duration of combustion, Δθ.

The function generally used was

$$x_b = 1 - exp\{-a(\frac{\theta - \theta_s}{\Delta\theta})^n\} \quad (4.33)$$

The burn fraction is strongly dependent on the values of efficiency (a) and form (n) factors, so it is important to use accurate values for these constants. Different ranges of values have been suggested in the literature for a and n values, the value for a has been chosen arbitrarily without any physical reasoning, in most of the work the value of a is 5 (**Kumar et al., 2004**) or 6.908 (**Liu et al.,1997**). According to (**Kim, 2013**), the values for a and n are 5 and 2 respectively.

The mass fraction of fuel burned in an internal combustion engine could be expressed as a function of crank angle using the Wiebe function, and that was:

$$x_b(\theta) = 1 - exp\{-a(\frac{\theta - \theta_s}{\Delta\theta})^n\} \quad (4.34)$$

The S-shape characteristic of mass fraction burned form the CI engine model is shown in figure 4.2.

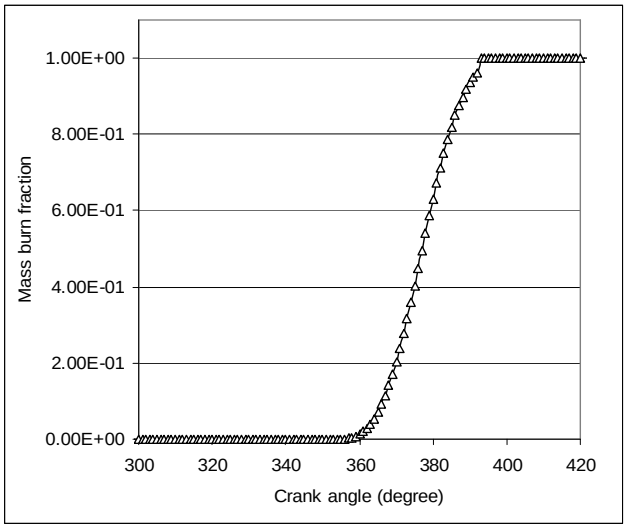

Figure.4.2: Burned mass fraction characteristic (from model)

And burn fraction for compression ignition engine was calculated as follows:

Before ignition $x_b = 0$

During combustion, burn fraction could be expressed as:

$$x_b = 1 - exp(-a\lambda^n) \tag{4.35}$$

$$\lambda = \frac{\theta - \theta_s}{\Delta\theta} \tag{4.36}$$

Now, according to **Stone (1994)** for compression ignition engine,

$$x_b = \alpha f_1(\lambda) + (1-\alpha) f_2(\lambda) \tag{4.37}$$

α =pre-mixed diffusion combustion parameter for compression ignition engine,

$f_1(\lambda)$ =pre-mixed phase, $f_2(\lambda)$ =diffusion burning phase

$$\alpha = 1 - 0.875\frac{\varphi^{0.350}}{{\tau_{id}}^{0.375}} \tag{4.38}$$

φ =equivalence ratio.

$$\tau_{id} = \frac{3.52\, exp(\,{}^{2100}/_{t_{id}})}{({}^{p_{id}}/_{100})^{1.022}} \tag{4.39}$$

τ_{id}=ignition delay, t_{id}=temperature at ignition delay=$t_{id} = t_1 r_c^{k-1}$, p_{id}=pressure at ignition delay=$p_{id} = p_1 r_c^{k}$.

Here, k =adiabatic index=$\frac{c_p}{c_v}$

Rearranging above equations

$$\text{So, } f_1(\lambda) = 1 - (1 - \lambda^{K1})^{K2} \text{ and } f_2(\lambda) = 1 - exp(-K3 \times \lambda^{K4}) \tag{4.40}$$

The K value were defined as,

$$K1 = 2 + 1.25 \times 10^{-8}(\tau_{id} N)^{2.4} \tag{4.41}$$

Where, N = r.p.m

$$K2 = 5000 \tag{4.42}$$

$$K3 = \frac{14.2}{\varphi^{0.644}} \tag{4.43}$$

$$K4 = 0.79(K3)^{0.25} \tag{4.44}$$

Now, by differentiating,

$$\frac{df_1}{d\lambda} = K1 \times K2 \times \lambda^{(K1-1)} \times (1 - \lambda^{K1})^{(K2-1)} \tag{4.45}$$

$$\frac{df_2}{d\lambda} = K3 \times K4 \times \lambda^{(K4-1)} \times (1 - f_2) \quad (4.46)$$

$$\frac{dx_b}{d\theta} = \frac{\alpha}{\Delta\theta}\frac{df_1}{d\lambda} + \frac{1-\alpha}{\Delta\theta}\frac{df_2}{d\lambda} \quad (4.47)$$

So, the heat release and mass burn fraction were related as

$$\frac{dQ_n}{d\theta} = Q_{in}\frac{dx_b}{d\theta} - \frac{dQ_l}{d\theta} \quad (4.48)$$

Net heat input (Q_{in}) could be expressed as:

$$Q_{in} = m_f Q_{LHV} \quad (4.49)$$

Where, m_f was the mass of fuel inside the combustion chamber and Q_{LHV} was the lower heating value of fuel. Quantity of mass of fuel was taken from experimental results.

4.5 Thermodynamic Properties of intake air and Combustion product

It was assumed that the compression ignition engine model could predict the engine performance fueled with biodiesel. This model might not be accurate for the biodiesel conditions, but it could predict results close to experimental results.

In heat release calculation for the engine, the specific heat ratio was the essential thermodynamic factor. **Gatowski *et al.* (1984**) had developed a single zone heat release model based on the 1st law of thermodynamics. It was widely used and had proposed a specific heat ratio model using a mass burned fraction to calculate the specific heat of the burned and unburned mixture. In this compression ignition engine model, it was assumed that the specific heats of the gaseous species varied with the engine cylinder temperature. The variation of specific heats of air was found in the literature (**Abu Nada *et al.*, 2007**).

The following equation calculated it.

$$C_p = 2.506 \times 10^{-11} T_g^2 + 1.454 \times 10^{-7} T_g^{1.5} - 4.246 \times 10^{-7} T_g + 3.162 \times 10^{-5} T_g^{0.5} + 1.3303 - 1.512 \times 10^{4} T_g^{-1.5} + 3.063 \times 10^{5} T_g^{-2} - 2.212 \times 10^{7} T_g^{-3} \quad (4.50)$$

It was assumed that the air was an ideal gas and the mixture contained 78.1% nitrogen, 20.95% oxygen, 0.92% argon and 0.03% carbon dioxide (molar basis). In a practical case, specific heats of all the reactants and the combustion products were temperature dependent. Generally, the standard combustion products available from Biodiesel blend fuel were carbon dioxide, carbon monoxide, water vapour, nitrogen, oxygen, hydrogen, and Oxides of nitrogen. Some of those products had specific heats that were strongly dependent on temperature. In contrast, specific heats of other products were less dependent on temperature. The most practical approach was to calculate the specific heats of reactants and combustion product individually and then calculate the summation of individual species-specific heats. In the present work, the specific heat of clearance volume due to exhaust gas residue recirculation was also calculated and added with the reactant's specific heat. This model assumed that the clearance volume was filled with exhaust gas after each engine cycle and that exhaust gas residue was circulated again with fresh charge in the next engine cycle. The molar specific heat was calculated at constant pressure as

$$C_{pmix} = \sum_{i=1}^{n} C_{pi}\, Y_i \quad (4.51)$$

C_{pi} were the molar specific heats and Y_i were the mole fraction .

Thus, the specific heat of combustion product could be calculated as:

$$C_{p-mix_{product}} = C_{pCO_2} Y_{CO_2} + C_{pCO} Y_{CO} + C_{pH_2O} Y_{H_2O} + C_{pH_2} Y_{H_2} + C_{pO_2} Y_{O_2} + C_{pN_2} Y_{N_2} + C_{pN_2} Y_{NO} \quad (4.52)$$

The specific heat of clearance volume due to exhaust gas recirculation was calculated as:

$$C_{p-clearence-vol} = \sum_{i=1}^{n} V_{ci} \times C_{pi-volumetric} \quad (4.53)$$

V_{ci} were the individual volume of exhaust gas residue at clearance volume of combustion chamber.

$C_{pi-volumetric}$ were the individual volumetric specific heats of exhaust gas residue.

The specific heat of reactant air could be calculated as:

$$C_{p-mix_{reactant\_AIR}} = C_{pair} Y_{air} + C_{p-clearence-vol} \quad (4.54)$$

During the combustion, it was assumed that the flame front travel throughout the combustion chamber and the gases ahead of the flame were unburned and had the same properties as an intake air. The gases behind the flame front were assumed burned, and it had the properties of the combustion product. Thus, the specific heat of the mixture could be calculated as:

$$C_{p-mix} = C_{p-mix_{reactant\_AIR}} \times (1 - x_b) + C_{p-mix_{product}} \times (x_b) \quad (4.55)$$

x_b was the burned mass fraction. figure 4.3 shows the variation of specific heats and specific heats ratio and crank angle rotation in the present model to predict the performance parameters. Both the specific heats were increased with the increase in temperature during compression and power stroke. However, the specific heat ratio had fallen successively that had been accounted for in the present model.

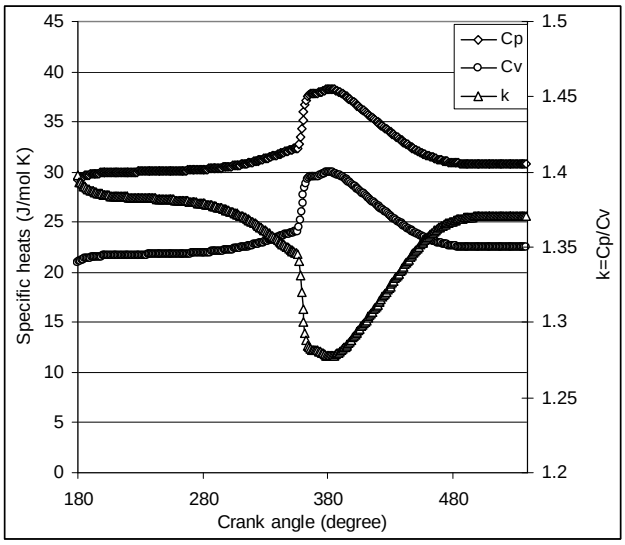

Figure 4.3: Variation of specific heats and specific heats ratio along crank angle rotation (from model)

In the present work, it was assumed that there were only seven species ($CO, CO_2, H_2O, O_2, H_2, N_2, NO$) in the combustion product. The chemical reaction for combustion could be written as,

$$C_xH_yO_l + \rightleftarrows \frac{a}{\varphi} \cdot (O_2 + 3.76 \cdot N_2) \rightarrow n_1 \cdot CO + n_2 \cdot CO_2 + n_3 \cdot H_2O + n_4 \cdot O_2 + n_5 \cdot H_2 + n_6 \cdot N_2 + n_7 \cdot NO \quad (4.56)$$

Where, $\frac{a}{\varphi} = \frac{x+\frac{y}{4}-\frac{l}{2}}{\varphi}$

This chemical reaction was valid for stoichiometric ($\varphi = 1$), rich ($\varphi > 1$) and lean ($\varphi < 1$) mixture. It was assumed that there was no carbon monoxide (CO) for Lean fuel-air mixture, and for the rich fuel-air mixture, there was no oxygen in the combustion product. The value of $n_1, n_2, n_3, n_4, n_5, n_6, n_7$ denoted the number of mole of individual combustion product and value

of x, y, l, a denoted the mole number of individual reactant. The solution of seven unknowns ($n_1, n_2, n_3, n_4, n_5, n_6, n_7$) required seven equations. The balancing of carbon, oxygen, hydrogen and nitrogen atoms provided four equations.

Total of all combustion product mole fractions was considered as 1.

Chemical equilibrium of CO_2, H_2O, CO, H_2 known as water gas shift reaction had been considered for the combustion.

$$CO + H_2O \Leftrightarrow CO_2 + H_2 \tag{4.57}$$

The equilibrium constant (k_p) of this reaction was temperature dependent, and it also could be calculated from moles of respective species, as:

$$k_p = \frac{n_2 \times n_5}{n_1 \times n_3} \tag{4.58}$$

The value of equilibrium constant could be calculated from the change in Gibbs function between the gaseous constituents in the combustion product and reactants at the combustion zone temperature.

$$k_p = exp(-\frac{g^0_{CO_2}}{RT} - \frac{g^0_{H_2}}{RT} + \frac{g^0_{CO}}{RT} + \frac{g^0_{H_2O}}{RT}) \tag{4.59}$$

Also, hypothetical equation considered presented as follow,

$$\frac{1}{2}N_2 + \frac{1}{2}O_2 \Leftrightarrow NO \tag{4.60}$$

And equilibrium constant for hypothetical reaction could be written as:

$$k_{NO} = \frac{n_7}{\sqrt{n_6} \times \sqrt{n_4}} \tag{4.61}$$

From those seven equations, seven unknown values were calculated.

4.6: Model validation with experimental results

Experimental results were taken from a VCR, 661.1 cc single cylinders Kirloskar diesel engine (Table 4.1) to validate the thermodynamic simulation single-zone model, using diesel, B5

& B10 biodiesels (POME) at zero load conditions. The heating value of the B100 POME biodiesel fuel was measured as 37.06 MJ/kg, and this was considered in the developed model.

Table 4.1. Test Engine setup specifications

Engine	4 stroke, single combustion chamber, CI engine
Fuel	Diesel (biodiesel blends B5 & B10 during experiment)
Bore	0.0875m
Stroke	0.110m
Displacement Volume	661.1 cc
Compression ratio	18:1

Predicted results and experimental results were compared (figure 4.4) at operating condition 35˚ crank angle (CA) burning duration and fuel injection time 11˚ (CA) Before Top Dead Center (BTDC) at zero load conditions.

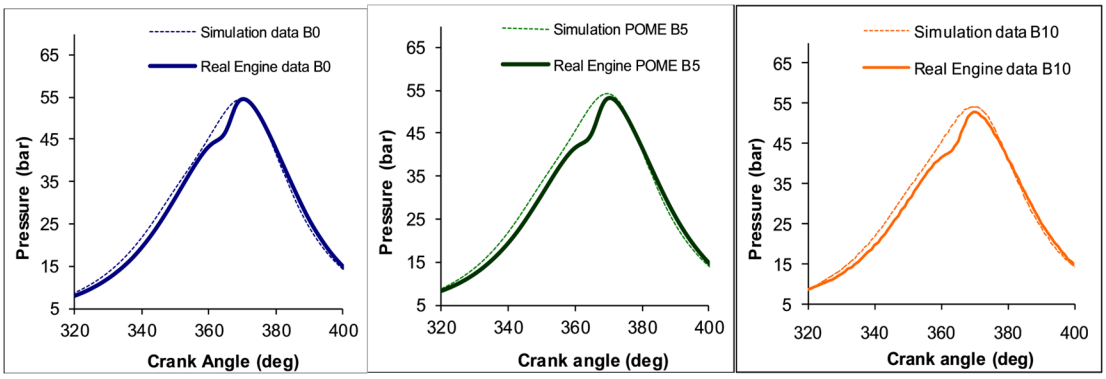

Figure 4.4: Comparison of simulation and experimental Cylinder pressure versus CA variation using B0, B5 & B10

The comparison indicated a very close alignment with the experimental data for B0 and POME B5 & B10 biodiesel blends. The ‘a’ and ‘n’ value was taken as 4.5 and 3.3 in Weibe function to

curve fit experimental data. Figure 4.5 shows the comparison regarding the burned mass fraction between the prediction models with the experimental results. It was observed between the experimental and simulation outcomes no or least difference during the flame development (Crank angle in the middle of 10% MFB to 50% MFB) and had a recognizable difference during the initial & final flame development (Crank angle in the middle of 0% MFB to 10% MFB and 50%MFB to 90% MFB). The simulated pressure crank angle differences were relatively well validated with the experimental results. Major pressure differences were observed between 360° - 370° CA, specifically at 364° CA. The reason was the pressure drop caused by the evaporation of fuel in actual engine. This result indicates that the thermodynamic simulation could finely illustrate in-cylinder combustion.

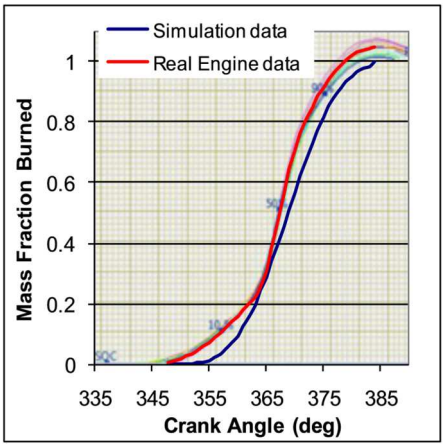

Figure 4.5: Comparison of simulation and experimental Mass burned fraction relative to CA for B0.

4.7: Analysis of performance prediction with different biodiesels

Figure 4.6 shows that the cylinder pressure developed during combustion has been portrayed at zero, 25, 50, 75, 100 percent load conditions.

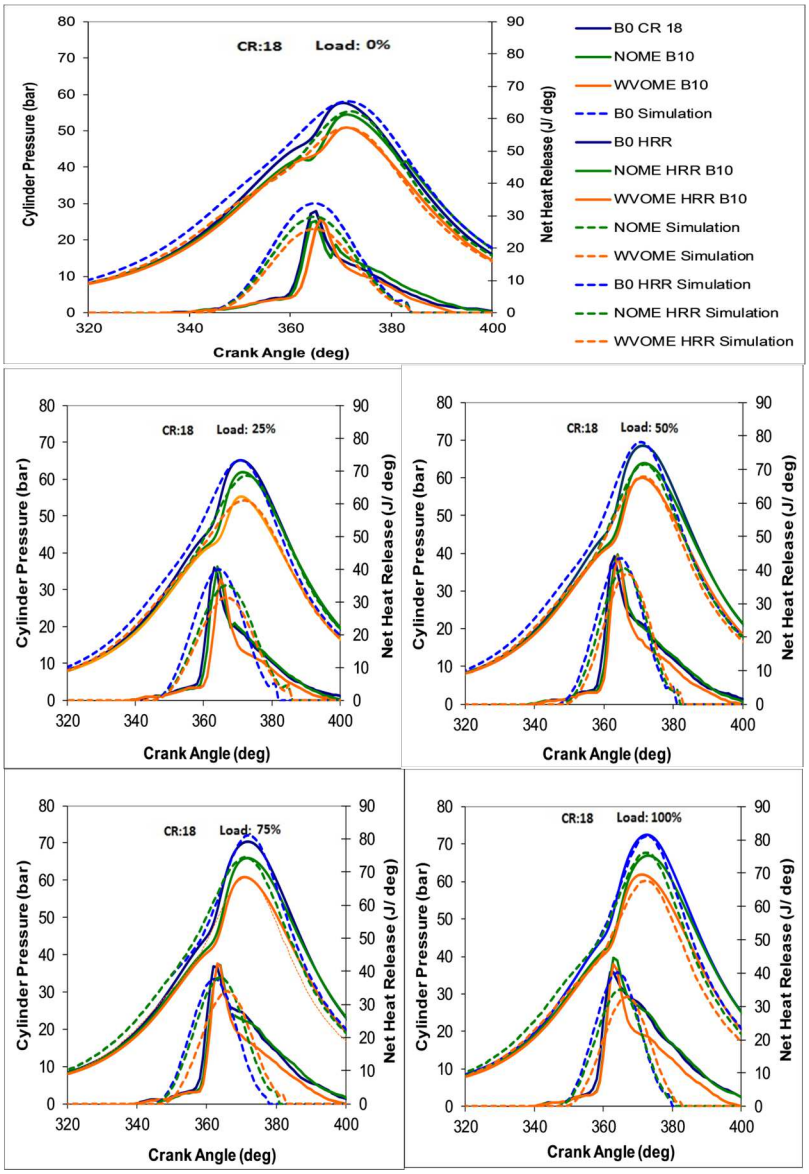

Figure 4.6: Comparison of simulation and experimental Cylinder pressure and NHR results versus CA variation using diesel (B0), NOME blend (B10) & WVOME blend (B10) with CR 18:1 at 0% to 100% Load.

In this model, the engine load change was considered based on actual fuel consumption and equivalence ratio from the experimental results at the same engine load and speed (1500 rpm). The fuel consumption and equivalence ratio increased as the engine load advanced from zero, and the engine speed remained constant during engine operation. The maximum cylinder pressure developed after TDC (360° CA) along with the thermodynamic simulation combustion pressure versus CA (crank angle) results were compared with experimental results at respective loads for test fuels as petroleum Diesel (B0), NOME-Diesel Blend (NOME B10), and WVOME-Diesel blend (WVOME B10). The comparison indicated a very close understanding of all the test fuels' experimental data in this research work. The accuracy of the NHR models of CI engines was strongly dependent on the ratio of the specific heat. In an actual engine, specific heats ratio depended on actual cylinder temperature, and the cylinder temperature depended on flame speed apart from other parameters during combustion. In this model, NHR was calculated based on the single-zone model from literature as a function of cylinder pressure, volume, specific heats ratio, and crank angle. However, flame speed was not considered for simplification. This consideration might be why NHR simulation differs from the NHR of experimental data in the early part of combustion. Deviation in NHR (net heat release) of B0, NOME B10 & WVOME B10 test fuel at different loading conditions are presented in figure 4.6 (Secondary Y-axis) along with the thermodynamic simulation. NHR versus CA results was compared with experimental results at respective loads for test fuels. NHR relied on various factors like consumption rate, lower heating value, equivalence ratio, and fuel combustion quality. The topmost NHR was observed after TDC and in-between 360-370 degree CA for different loading conditions. It was observed that at zero percent load condition, maximum NHR was obtained for Diesel (B0) compared to NOME B10 & WVOME B10; this might be because of fuel type and the fuel consumption amount. Nevertheless, at higher loading conditions, the NHR profile for B0, NOME B10 & WVOME B10 was very similar, resulting in high fuel consumption for biodiesel blends.

Figure 4.7 and figure 4.8 Indicated thermal efficiency and Indicated SFC are presented separately, obtained from the simulated thermodynamic model. The trend matched the direction of BTE and BSFC of an actual engine. It was observed that the differences in simulated ITE and ISFC and was marginal between 0% to 25% engine loading conditions among B0, B5 and B10. Also, the rise in ITE was very sharp between 0% to 25% load conditions. Where the drop of ISFC was noticeable between 50% to 100% load conditions.

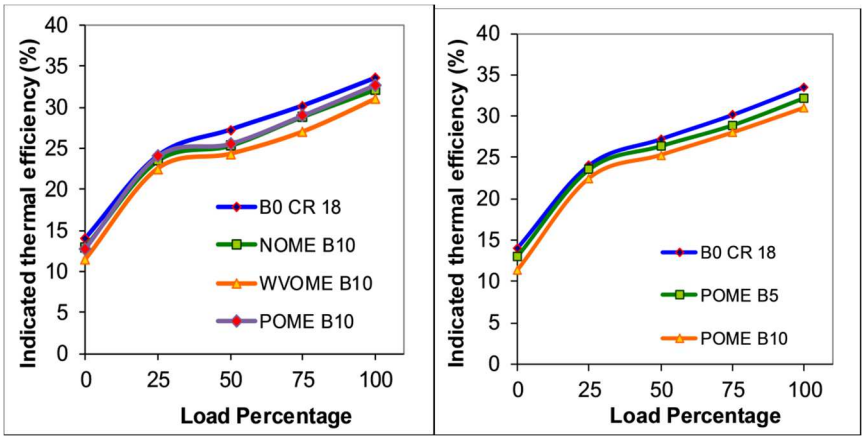

Figure 4.7: Graphical illustration of the simulated Indicated thermal efficiency at different loading

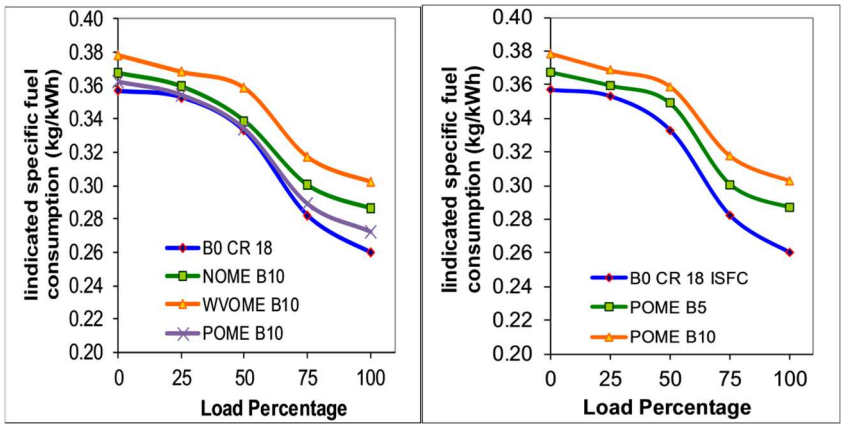

Figure 4.8: Graphical illustration of the simulated Indicated SFC at different loading conditions.

4.8: Prediction on emission using different biodiesel blends

The simulated mole fraction of carbon monoxide (CO) emission as the combustion products are presented in figure 4.9. In the simulation model for the lean fuel-air mixture, there was no carbon monoxide (CO), and for rich fuel-air mixture, there was no oxygen in the combustion product. At 25% load condition, the equivalence ratio for only diesel and B5 POME blend was more significant, the value was greater than one (rich fuel-air mixture), but for B10 POME blend, the equivalence ratio was less than one (lean fuel-air mixture). These equivalence ratio values were taken from experimental data. That was why the CO mole fraction values of the B10 POME blend was zero at 25% load condition. At 25% load condition, the equivalence ratio for only diesel was greater than one (rich fuel-air mixture), but for NOME and WVOME, the equivalence ratio was less than one (lean fuel-air mixture). These equivalence ratio values were taken from experimental data. That was why the CO mole fraction values for NOME & WVOME were zero at 25% load condition.

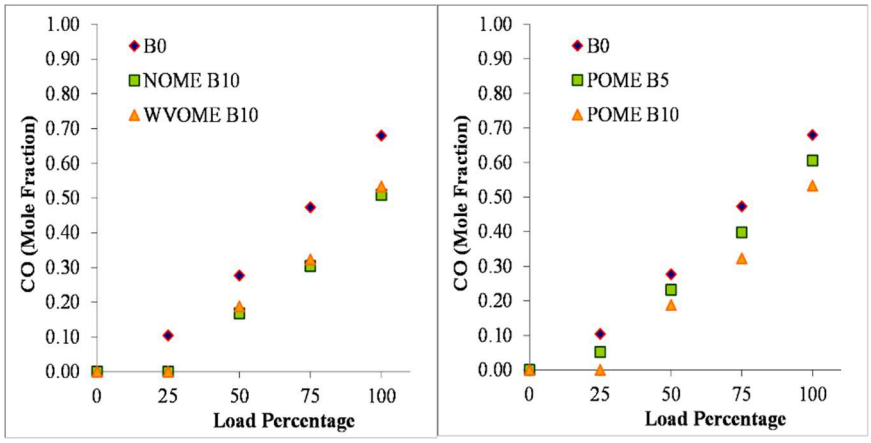

Figure 4.9: Graphical illustration of the simulated Carbon Monoxide emission at different loading conditions.

The simulated mole fraction of oxides of nitrogen (NOx) emission as the combustion products are presented in figure 4.10. However, the NOx mole fraction values for diesel and POME blends (B5 & B10) were not zero at zero load conditions. The mole fraction values were about 0.0007, 0.0005, and 0.0004, respectively, for NOx. Also, the equilibrium constant value for oxides of nitrogen formation was taken as a function of the highest combustion temperature. The peak temperature available from the simulated results for POME blends was low compared to diesel. That was why the simulated mole fraction values for NOx emission were shallow and near zero, but it was relatively more at peak load conditions. Though the NOx mole fraction values for NOME & WVOME were not zero at 25% load condition. The mole fraction values were about 0.0007 and 0.0003, respectively, for NOx. The equilibrium constant value for oxides of nitrogen formation was taken as a function of the highest combustion temperature, and the peak temperature available from the simulated results for biodiesel blends was low compared to diesel. That was why the simulated mole fraction values for NOx emission were low compared to diesel.

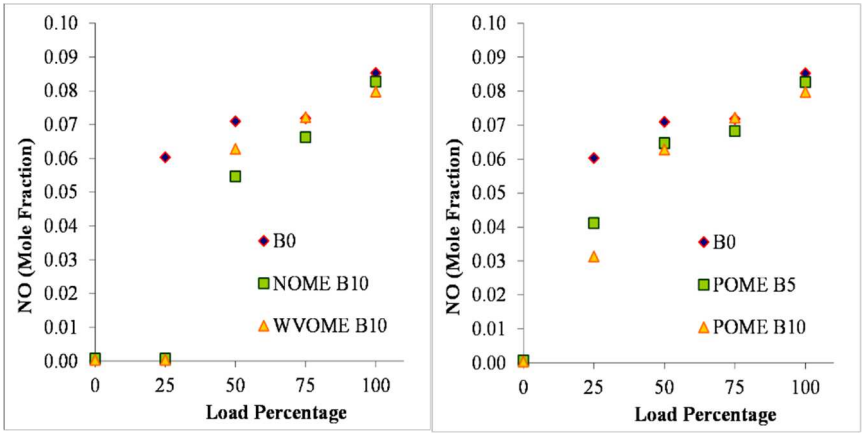

Figure 4.10: Graphical illustration of the simulated Oxides of Nitrogen emission at different loading conditions.

4.9 Closure

The emission prediction model's purpose was to deal only with the gas phase combustion products produced from hydrocarbon fuel combustion, containing carbon, hydrogen, oxygen atoms, and air. As the single-zone model implies, the combustion product was assumed in a single temperature and pressure for the entire combustion product mass. Also, the combustion products available from diesel and biodiesel blend fuel were assumed in mole fraction as carbon dioxide, carbon monoxide, water vapour, nitrogen, oxygen, hydrogen, and oxide of nitrogen. Therefore, direct quantitative comparisons had not been done with experimental results but trend of qualitative variation of different emission species at different loading conditions were well predicted.

Chapter 5

Conclusion and Future Scope

5.1 Conclusion

Biodiesel has stood out as a feasible, sustainable power source because of its lower ozone-depleting substance emission and its capability to decrease reliance on imported petroleum derivatives and satisfy the worldwide energy need. Generally, biodiesel has been delivered from edible oils because of their low FFA. However, their utilization has raised a few issues, such as food versus fuel and numerous different issues that have influenced their financial suitability. Hence, investigation of inedible and waste oils may decrease biodiesel's expense, particularly in developing nations that can scarcely manage the cost of the significant expense of edible oils. This research intended to deliver biodiesel from some expected edible, inedible feedstocks and waste oil. These oils incorporate; refined palm (Elaeis guineensis), unrefined neem (Azadirachta indica), and Waste Vegetable oils.

Biodiesel was derived from edible palm, inedible neem, and waste vegetable oil. The essential fuel properties were tested and also compared with the literature results. Critical parameters that influenced POME biodiesel yield were optimized using the L9 Taguchi method to achieve maximum yield. Also, the individual contribution of critical parameters was determined by ANOVA analytical method. Significant outcomes from this section are the following:

- The tested biodiesel properties (viscosity, calorific value, density, and flash point) revealed that POME, NOME, and WVOME were in close comparison except for heating

value. However, the tested properties were close to American and British biodiesel standard values.

- Optimum biodiesel yield was obtained as 86.2% with 1% catalyst concentration and 3 hours reaction time for POME using the Taguchi method.
- ANOVA computes Reaction time and percentage of Catalyst concentration were the utmost vital parameters, and its contributions were 38.67% and 31.85% for POME production. Contribution percentages of biodiesel production for M/O ratio and reaction temperature were 16.69% and 12.79%.

The edible and inedible oil biodiesel blends (B5, B10, B15, and B20) were tested in a variable compression ratio engine at three different compression ratios and five individual engine load conditions. Combustion, performance, and emission characteristics were studied. Also, energy in terms of shaft energy and associated energy loss and exergy as exergetic efficiency were analyzed based on experimental results. Notable analysis from this section are the following:

- The maximum CP and NHR for the tested biodiesel blends were lower, about 0.9% to 18% and 0.6% to 3%, at full load because of the lower calorific value compared to diesel.
- The peak NHR was lower for all the biodiesel blends than petroleum-based diesel at 0% to 50% engine loads at different CR; at CR 16, the peak NHR differences were noticeable among the test fuels.
- The engine could successfully run on the tested biodiesel blends with varying compression ratios, 16, 17, and 18. The increase in compression ratio max-CP was always raised in the case of all test fuels. However, at the higher load conditions, the max-CP of NOME blends was close to POME blends at CR 18 because of increased cylinder temperature and oxygen availability.

- B5 could replace the diesel fuel with a minimum peak pressure loss. Bringing down the engine's CR from the standard value of 18 to 16 incited a decrease in peak CP, and the effect of CR was higher (31%) in the B5 biodiesel blend compared to petroleum diesel (25%).
- The SOC decreased with compression ratio hence the increase in ignition delay. Lower CR prompted lower gas temperature and therefore longer ignition delay. It was observed that with the increase in blending percentage, the SOC decreased at each load, but at the same time, with the increase in engine load, the SOC increased for specific test fuels.
- There was a slight delay in peak NHR and the start of combustion with a drop in CR because of excess fuel accumulation in the combustion chamber due to longer ignition delay and lower in-chamber gas temperature at the beginning of combustion.
- Biodiesel blends (B5, B10, B15, and B20) in a diesel engine could perform with marginally lower brake thermal efficiency than diesel because of the higher density and lower calorific value.
- With an increase in the CR, the BTE increased because of increased BMEP. The rapid rise in BTE occurred between 0% to 75% engine load conditions. Also, with the expansion in CR, the BSFC values decreased.
- The shaft energy and energy loss in cooling water were decreased by 4% and 6%, separately, with a CR change from 18 to 17. Moreover, the shaft and cooling water's energy declined by 9% and 16%, separately, for change in CR from 18:1 to 16:1. Energy loss for exhaust gases and the unaccounted losses increased with CR reduction.
- The exergetic efficiency of inedible diesel-biodiesel blends (NOME B10 & WVOME B10) was comparatively inadequate rather than diesel (B0). B10 NOME blend produced better exergetic efficiency compared to B10 WVOME. Also, because of thermodynamic

irreversibility, noticeable higher brake thermal efficiency was observed compared to exergetic efficiency.

- The emission of CO was the least for B20 among the test fuels because of more oxygen presence. At first, the CO emission reduced up to 50% engine load and afterwards abruptly increased at higher engine load because more fuel produced more smoke and prevented oxidation of CO to CO_2; therefore, emission increased.
- The decrease in CR increased CO emissions because more fuel accumulated at lower CR. NOx emissions were more delicate to CR on engine activity with biodiesel blends than petroleum diesel. On decreasing the CR from 18 to 16, NOx emission was reduced by around 33% for B20.

A single-zone model was developed based on the crank slider, cylinder pressure, heat release, and combustion product models. The model's predicted combustion results were validated with the experimental results fueled with B5 and B10 biodiesel blends. The simulated model anticipated the indicated thermal efficiency and indicated fuel consumption. Engine emission CO and NO in terms of mole fraction were predicted from the model.

- The predicted MFB and the empirical data obtained from the engine analysis were in acceptable harmony.
- From the predicted pressure versus crank angle curve, it was evident that the introduced thermodynamic model's predictions were in appreciable agreement with the empirical data. The anticipated CP had a noticeable difference in the peak pressure (under ±5%) and the peak pressure position w.r.t crank angle (under ±5℃A). Subsequently, the introduced model was appropriate for thermodynamic cycle examination of a compression ignition engine for diesel and biodiesel blend (B5 & B10) fuel operation.

- The differences in simulated ITE and ISFC were marginal between 0% to 25% engine load conditions among B0, B5 and B10. Also, the rise in ITE was very sharp between 0% to 25% load conditions. Where the drop of ISFC was noticeable between 50% to 100% load conditions.
- The proposed exhaust emission model portrayed various assumptions impacts. The predicted results show that the model forecast was in terms of mole fraction to determine CO and NO emission from the engine. The simulated NO emission was found slightly lower at low load conditions but relatively more at peak load conditions.

Finally, the engine could run on biodiesel blends successfully up to B20 without any significant engine modification, but B5 and B10 gave a better performance with overall lower emission than B20.

5.2 Scope of future work

The present work on edible and inedible oil biodiesel production, experimentation on the unmodified engine, and development of a single-zone CI engine model fueled with biodiesel blends can be extended further to explore many other scopes. Some of them are as follows:

- Optimization of engine performance employing response surface methodology could be considered in future investigations.
- Impact of biodiesel blends on cumulative heat release.
- Engine performance utilizing added substances to improve these biodiesel engine performance and emission could be considered.
- Several non-specialized restricting variables of biodiesel creation could be considered by directing affectability investigation and life cycle analysis (LCA).

- The engine model boundaries, for example, equivalence ratio, combustion duration, and the start of combustion, were resolved experimentally. A detailed investigation of these boundaries could be considered which might prompt the demonstration of the combustion process with magnificent accuracy.
- The model could be supplanted by a two or three zone thermodynamic combustion model for critical upgrades in the outcomes.
- With necessary analysis and modifications, the current methodology could be reached out to predict turbocharged CI engines with higher biodiesel blends.

References

Abou Al-Sood, M.M., Ahmed, M. and Abdel-Rahim, Y.M.Rapid thermodynamic simulation model for optimum performance of a four-stroke, direct-injection, and variable-compression-ratio diesel engine, *International Journal of Energy and Environmental Engineering*, vol. **3**, **2012**. DOI:10.1186/2251-6832-3-13.

Abu Nada, E., Al hinti, I., AlSarkhi, A. and Akash, B., Thermodynamic analysis of spark-ignition engine using a gas mixture model for the working fluid. *Int. J. Energy Res*., vol. **31**, pp. 1031–1046, **2007**.

Abu-Nada, E., Al-Hinti, I., Al-Sarkhi, A. and Akash, B., Thermodynamic modeling of sparkignition engine: effect of temperature dependent specific heats, *International Communications in Heat and Mass Transfer*, vol. **33**, pp. 1264–1272, **2006**.

Adeyemi, N.A., Mohiuddin, A.K.M. and Jameel, A.T., Biodiesel production: a mini review. *International Energy Journal*, vol. **12**, pp. 15-28, **2011**.

Agarwal, A.K., Dhar, A., Gupta, J.G., Kim, W.I, Choi, K., Lee, C. S. and Park, S., Effect of fuel injection pressure and injection timing of Karanja biodiesel blends on fuel spray, engine performance, emissions and combustion characteristics, *Energy Conversion and Management*, vol. **91**, pp. 302–314, **2015**.

Agarwal, D. and Agarwal, A.K., Performance and emissions characteristics of jatropha oil (preheated and blends) in a direct injection compression ignition engine, *Applied Thermal Engineering*, vol. **27**, pp. 2314-2323, **2007**.

Ali, M.H., Mashud, M., Rubel, M.R. and Ahmad, R.H., Biodiesel from Neem oil as an alternative fuel for Diesel engine, *Procedia Engineering*,vol. **56**, pp.625 – 630, **2013**.

Altun, S., Bulut, H. and Cengiz, O., The comparison of engine performance and exhaust emission characteristics of sesame oil–diesel fuel mixture with diesel fuel in a direct injection diesel engine. *Renew Energy*, vol. **33**, pp. 1791–1795, **2008**.

Antonio PagánRubio, J., Vera-García, F., Hernandez Grau, J., Muñoz Cámara, J. and AlbaladejoHernandez, D., Marine Diesel Engine Failure Simulator Based On Thermodynamic Model, *Applied Thermal Engineering*, **2018**. DOI: https://doi.org/10.1016/j.applthermaleng.2018.08.096.

References

Araby, R., Amin, A., Morsi, A.K., Ibiari, N.N. and Diwani, G.I., Study on the characteristics of palm oil–biodiesel–diesel fuel blend. *Egyptian Journal of Petroleum, vol.* **27**, pp. 187–194, **2018**.

Ashraful, A.M., Masjuki, H.H., Kalam, M.A., Rizwanul Fattah, I.M., Imtenan, S., Shahir, S.A. and Mobarak, H.M. Production and comparison of fuel properties, engine performance, and emission characteristics of biodiesel from various non-ediblevegetable oils: a review. *Renew Sustain Energy Rev*, vol. **80**, pp. 202–228, **2014**.

Atabani, A. E., Silitonga, A. S., Ong, H. C., Mahlia, T. M. I., Masjuki, H. H., Badruddin, I. A. and Fayaz, H., Non-edible vegetable oils: A critical evaluation of oil extraction, fatty acid compositions, biodiesel production, characteristics, engine performance and emissions production. *Renewable and Sustainable Energy Reviews*, vol. **18**, pp. 211–245, **2013**. DOI:10.1016/j.rser.2012.10.013

Atadashi, I.M., Aroua, M.K. and Abdul Aziz, A., High quality biodiesel and its diesel engine application: A review, *Renewable and Sustainable Energy Reviews*, vol. **14**, pp. 1999-2008, **2010**.

Avhad, M.R., Sánchez, M., Peña, E., Bouaid, A., Martínez, M., Aracil, J. and Marchetti, J.M., Renewable production of value-added jojobyl alcohols and biodiesel using a naturally-derived heterogeneous green catalyst, *Fuel*, vol. **179**, pp. 332–338, **2016**.

Awad, S., Varuvel, E.G., Loubar, K. and Tazerout, M., Single zone combustion modeling of biodiesel from wastes in diesel engine, *Fuel*, vol. **106**, pp. 558–568, **2013**.

Aydın, S., Detailed evaluation of combustion, performance and emissions of ethyl proxitol and methyl proxitol-safflower biodiesel blends in a power generator diesel engine, *Fuel*, vol. **270**, **2020**. DOI:https://doi.org/10.1016/j.fuel.2020.117492.

Babatunde, E.O., Karmakar, B., Olutoye, M.A., Akpan, U.G., Auta, M. and Halder, G., Parametric optimization by Taguchi L9 approach towards biodiesel production from restaurant waste oil using Fe-supported anthill catalyst. *Journal of Environmental Chemical Engineering*, **2020**. DOI:10.1016/j.jece.2020.104288.

Baeyens, J. and Kang, Q., Appels L., Dewil R., Lv Y., Tan T., Challenges and opportunities in improving the production of bio-ethanol. *Prog. Energy Combust. Sci*., vol. **47**, pp. 60–88, **2015**. DOI:10.1016/j.pecs.2014.10.003.

Bala, B.K., Studies on biodiesel fuel from rapeseed oil as prepared in super critical methanol, *Fuel*, vol. **80**, pp. 693-708, **2001**.

Balamurugan, T. and Nalini, R., Experimental investigation on performance, combustion and emission characteristics of four stroke diesel engine using diesel blended with alcohol as fuel. *Energy*,vol. **78**, pp. 356–363, **2014**.

Balat, M. and Balat, H., Progress in biodiesel processing. *Applied Energy*, vol. **87**, pp. 1815-1835, **2010**.

Banković-Ilić, I.B., Stamenković, O.S. and Veljković, V.B., Biodiesel production from non-edible plant oils, *Renewable and Sustainable Energy Reviews*, vol. **16**, pp. 3621–3647, **2012**.

Baratta, M., Ferrari, A. and Zhang, Q., Multi-zone thermodynamic modeling of combustion and emission formation in CNG engines using detailed chemical kinetics, *Fuel*, vol. **231**, pp. 396–403, **2018**. DOI:10.1016/j.fuel.2018.05.088.

Barnwal, B.K. and Sharma, M.P., Prospects of biodiesel production from vegetable oils in India, *Renewable and Sustainable Energy Review*, vol. **9**, pp. 363-378, **2004**.

Bart, J.C.J., Palmeri, N. and Cavallaro, S., Biodiesel Science and Technology: From Soil To Oil: Woodhead Publishing Limited, **2010**.

Behera, P. and Murugan, S., Combustion, performance and emission parameters of used transformer oil and its diesel blends in a DI diesel engine. *Fuel*, vol. **104**, pp. 147–154, **2013**.

Backus, J., THE HISTORY OF FORTRAN I, II, AND III, HISTORY OF PROGRAMMING LANGUAGES, Academic Press, Inc. ISBN 0-12-745040-8, **1981**.

Bhatia, S.K., Bhatia, R.K. and Yang, Y.H., An overview of microdiesel—A sustainable future source of renewable energy. *Renew Sust Energy Rev,* vol. **79**, pp.1078–1090, **2017**.

Bhuiya, M.M.K., Rasul, M.G., Khan, M.M.K., Ashwath, N. and Azad, A.K., Prospects of 2nd generation biodiesel as a sustainable fuel—Part: 1 selection of feedstocks, oil extraction techniques and conversion technologies, *Renewable and Sustainable Energy Reviews*, vol. **55**, pp. 1109–1128, **2016**.

Bian, B., Bajracharya, S., Xu, J., Pant, D. and Saikaly, P.E., Microbial electrosynthesis from CO2: Challenges, opportunities and perspectives in the context of circular bioeconomy, *Bioresour Technol*, vol. **302**, **2020**. DOI:10.1016/j.biortech.2020.122863.

Biswas, P.K. and Pohit,S., What ailsIndia'sbiodieselprogramme?, *Energy Policy*, vol. **52**, pp. 789–796, **2013**.

Biswas, P.K., Pohit, S. and Kumar, R., Biodiesel from jatropha: can India meet the 20% blending target?, *EnergyPolicy*, vol. **38**, pp. 1477–1484, **2010**.

Bora, B.J. and Saha, U.K., Experimental evaluation of a rice bran biodiesel – biogas run dual fuel diesel engine at varying compression ratios, *Renewable Energy*, vol. **87**, pp. 782–790, **2016**.

Bravo, J.T., Silva, C.M. and Farias, T.L., Road vehicle simulation model for energy and environmental impact of petrodiesel and biodiesel, *International Journal of Energy for a Clean Environment*, vol. **8**, pp. 339–357, **2007**.

Capuano, D., Costa, M., Di Fraia, S., Massarotti, N. and Vanoli, L., Direct use of waste vegetable oil in internal combustion engines, *Renewable and Sustainable Energy Reviews*,vol. **69**, pp. 759–770, **2017**.

Caton, J.A., Comparisons of instructional and complete versions of thermodynamic engine cycle simulations for spark-ignition engines, *Int J Mech Eng Educ*, vol. **29**, pp. 283–306, **2001**.

Chapagain, B.P., Yehoshua, Y. and Wiesman, Z., Desert date (Balanites aegyptiaca) as an arid lands sustainable bioresource for biodiesel, *Bioresource Technology*, vol. **100**, pp. 1221-1226, **2009**.

Charpe, T.W. and Rathod, V.K., Biodiesel production using waste frying oil. *Waste Management*, vol. **31**, pp. 85–90, **2011**.

Chernova, N.I., Kiseleva, S.V. and Vlaskin, M.S., Biofuel production from microalgae by means of hydrothermal liquefaction: advantages and issues of the promising method, *International Journal of Energy for a Clean Environment*, vol. **18**, pp. 133-146, **2017**.

Cheung, C.S., Liu, M.A., Lee, S.C. and Pan, K.Y., Experimental study on emission characteristics of diesel engines with diesel fuel blended with dimethyl carbonate, *International Journal of Energy for a Clean Environment*, vol. **6**, pp. 239-253, **2005**.

Cipolat, D., The effect of fuel properties on the start of injection and energy release of a compression ignition engine fueled on dimethyl ether, *International Journal of Energy for a Clean Environment*, vol. **11**, pp. 51-63, **2010**.

D'Errico, G., Cerri, T. and Pertusi, G., Multi-objective optimization of internal combustion engine by means of 1D fluid-dynamic models, *Applied Energy*, vol. **88**, pp. 767-777, **2011**.

da Silva, L.L.C., Simulation of the thermodynamic processes in diesel cycle internal combustion engines, SAE technical paper series. *SAE International*, **1993**.

Das, M., Sarkar, M., Datta, A. and Santra, A. K., An experimental study on the combustion, performance and emission characteristics of a diesel engine fuelled with diesel-castor oil biodiesel blends, *Renewable Energy*,vol. **119**, pp. 174-184, **2018**.

Das, S., Kashyap, D., Kalita, P., Kulkarni, V. and Itaya, Y., Clean gaseous fuel application in diesel engine: A sustainable option for rural electrification in India, *Renewable and Sustainable Energy Reviews*, vol. **117**, **2020**. DOI:10.1016/j.rser.2019.109485.

Datta, A., and Mandal B.K., Engine performance, combustion and emission characteristics of a compression ignition engine operating on different biodiesel-alcohol blends, *Energy* , vol. **125**, pp. 470–483, **2017**.

Deka, D.C. and Basumatary, S., High quality biodiesel from yellow oleander (Thevetia peruviana) seed oil, *Biomass and Bioenergy*, vol. **35**, pp. 1797–1803, **2011**.

Demirbas, A., A Realistic Fuel Alternative for Diesel Engines, **2008**. DOI: 10.1007/978-1-84628-995-8.

Demirbas, A., Bafail, A., Ahmad, W. and Sheikh, M., Biodiesel production from non-edible plant oils. *Energy Exploration & Exploitation*, vol. **34**, pp. 290–318, **2016**.

Deng, X., Fang, Z., Liu, Y.H. and Yu, C.L., Production of biodiesel from Jatropha oil catalyzed by nanosized solid basic catalyst, *Energy*, vol. **36**, pp. 777-784, **2011**.

Descieux, D. and Feidt, M., One zone thermodynamic model simulation of an ignition compression engine, *Applied Thermal Engineering*, vol. **27**, pp. 1457–1466, **2007**.

Dhamodaran, G., Krishnan, R., Pochareddy, Y.K., Pyarelal, H.M., Sivasubramanian, H. and Ganeshram, A.K., A comparative study of combustion, emission, and performance characteristics of rice-bran-, neem-, and cottonseed-oil biodiesels with varying degree of unsaturation, *Fuel*, vol. **187**, pp. 296–305, **2017**.

Dhar, A., Kevin, R. and Agarwal, A. K., Production of biodiesel from high-FFA neem oil and its performance, emission and combustion characterization in a single cylinder DICI engine, *Fuel Processing Technology*,vol. **97**, pp. 118–129, **2012**.

Dhar, S. and Shukla, P.R., Low carbon scenarios for transport in India: Co-benefits analysis, *Energy Policy*, vol. **81**, pp. 186–198, **2015**. DOI: 10.1016/j.enpol.2014.11.02.

Elango, T. and Senthil, T.K., Combustion and emission characteristics of a diesel engine fuelled with Jatropha and diesel oil blends. *Therm Sci*, vol. **15**, pp. 1205–1214, **2011**.

Emiroğlu, A.O., Keskin, A. and Şen, M., Experimental investigation of the effects of turkey rendering fat biodiesel on combustion, performance and exhaust emissions of a diesel engine, *Fuel*, vol. **216**, pp. 266–273, **2018**.

Fathi, M., Jahanian, O., Ganji, D.D., Wang, S. and Somers, B., Stand-alone single- and multi-zone modeling of direct injection homogeneous charge compression ignition (DI-HCCI) combustion engines, *Applied Thermal Engineering*, vol. **125**, pp. 1181–1190, **2017**.

Feng, H., Zhang, C., Wang, M., Liu, D., Yang, X. and Chia-fon, L., Availability analysis of n-heptane/iso-octane blends during low-temperature engine combustion using a single-zone combustion model, *Energy Conversion and Management*, vol. **84**, pp. 613–622, **2014**.

Ferguson, C.R., Internal Combustion Engines–Applied Thermosciences, John Wiley & Sons, New York, **1986**.

Fernandes, A., Simon, A.T. and Lima, C.R.C., Study of the environmental and technical performance of a diesel engine with the alternative use of biofuel obtained from the reutilization of vegetable oil, *Procedia CIRP*, vol. **7,** pp. 335–340, **2013**.

Ganesan, D., Rajendran, A. and Thangavelu, V., An overview on the recent advances in the transesterification of vegetable oils for biodiesel production using chemical and biocatalysts. *Reviews in Environmental Science and Bio/Technology*, vol. **8**, pp. 367–394, **2009**.

Ganesan V., Internal combustion engine. Tata McGraw Hill Publication New Delhi, **2011**.

Ganesan, V., Computer Simulation of Compression-Ignition Engine Processes, Universities Press Private Limited, **2013**.

Gatowski, J.A., Balles, E.N., Chun, K.M., Nelson, F., Ekchian, J.A. and Heywood, F.B., A heat release analysis of engine pressure data. SAE Paper No: 841359, **1984**.

Genovese, A. and Ragona, R., Public transport and co_2 emission: a comparative assessment between conventional and innovative vehicles, *International Journal of Energy for a Clean Environment*, vol. **4**, Issue 3, **2003**.

Ghadge, S.V. and Raheman, H., Biodiesel production from mahua (Madhuca indica) oil having high free fatty acids. *Biomass and Bioenergy*, vol. **28**, pp.601–605, **2005**.

Ghojel, J. I., Review of the development and applications of Wiebe function: a tribute to the contribution of Ivan Wiebe to engine research. *International Journal of Engine Research*, Volume **11**, **2010**.

Gogoi, T. K., and Baruah, D. C., A cycle simulation model for predicting the performance of a diesel engine fuelled by diesel and biodiesel blends, *Energy*, vol. **35**, pp. 1317–1323, **2010**.

Guo, J., Sun, S. and Liu, J., Conversion of waste frying palm oil into biodiesel using free lipase A from Candida antarctica as a novel catalyst, *Fuel*, vol. **267**, **2020**. DOI:10.1016/j.fuel.2020.117323

Habibullah, M., Masjuki, H.H., Kalam, M.A., Rahman, S.M.A., Mofijur, M., Mobarak, H.M. and Ashraful, A.M., Potential of biodiesel as a renewable energy source in Bangladesh. *Renew. Sustain. Energy Rev.*, vol. **50**, pp. 819–834, **2015**. DOI:10.1016/j.rser.2015.04.149.

Hariram,V. and Vagesh Shangar, R., Influence of compression ratio on combustion and performance characteristics of direct injection compression ignition engine, *Alexandria Eng. J.*, vol. **54**, pp. 807-814, **2015**. DOI:10.1016/j.aej.2015.06.007.

Heywood, J.B., Internal combustion engines fundamentals. McGraw Hill Publications, 491–667, **1988**.

Hirkude, J. and Padalkar, A.S., Experimental investigation of the effect of compression ratio on performance and emissions of CI engine operated with waste fried oil methyl ester blend, *Fuel Processing Technology*, vol. **128**, pp. 367–375, **2014**.

Holser, R.A. and Kuru, R.H., Transesterified Milkweed (asclepias) seed oil as a biodiesel fuel, *Fuel*, vol. **85**, pp. 2106-2110, **2006**.

Huffman, G.D., Using the ideal gas law and heat release models to demonstrate timing in spark and compression ignition engines. *International Journal of Mechanical Engineering Education*, vol **28**, No 4, **1999**. DOI: 10.7227/IJMEE.28.4.1.

Ibragimov, A., Sidique, S.F. and Tey, Y.S., Productivity for sustainable growth in Malaysian oil palm production: A system dynamics modeling approach. *Journal of Cleaner Production*, **2019**. DOI:10.1016/j.jclepro.2018.12.113.

Ibrahim, T.N., Experimental study of vegetable oil diesel blends on the performance of compression ignition engine, *J Eng Sci*, vol. **4**, pp. 33–44, **2011**.

Ilkılıç, C., Aydın, S., Behcet, R. and Aydin, H., Biodiesel from safflower oil and its application in a diesel engine. *Fuel Processing Technology*, vol. **92**, pp. 356–362, **2011**.

Jain, S. and Sharma, M.P., Biodiesel production from Jatropha curcas oil, *Renewable and Sustainable Energy Reviews*, vol. **14**, pp. 3140-3147, **2010**.

Jamil, F., Al-Muhtaseb, A., Myint, M.T.Z., Al-Hinai, M. and Al-Haj, L., Baawain M, et al. Biodiesel production by valorizing waste Phoenix dactylifera L. Kernel oil in the presence of synthesized heterogeneous metallic oxide catalyst (Mn@MgO-ZrO2), *Energy Convers Manage*, vol. **155**, pp. 128-137, **2018**.

Janaun, J. and Ellis, N., Perspectives on biodiesel as a sustainable fuel, *Renewable and Sustainable Energy Reviews*, vol. **14**, pp. 1312-1320, **2010**.

Jena, P.C., Raheman, H., Prasanna, G.V.K. and Machavaram, R., Biodiesel production from mixture of mahua and simarouba oils with high free fatty acids, *Biomass and Bioenergy*, vol. **34**, pp. 1108-1116, **2010**.

Kalbande, S.R. and Vikhe, S.D., Jatropha and karanja bio-fuel: An alternative fuel for diesel engine, *ARPN Journal of Engineering and Applied Sciences*, vol. **3**, pp. 7-13, **2008**.

Kant Bhatia, S., Kant Bhatia, R., Jeon, J.M., Pugazhendhi, A., Kumar Awasthi, M., Kumar, D. and Yang, Y.H., An overview on advancements in biobased transesterification methods for biodiesel production: Oil resources, extraction, biocatalysts, and process intensification technologies. *Fuel*, vol. **285**, **2021**. DOI:10.1016/j.fuel.2020.119117

Kawaguchi, Y., Tamaki, N., Shimizu, M. and Hiroyasu, H., Experimental investigation on the waste oil combustion burner for energy saving and low-pollution, *International Journal of Energy for a Clean Environment*, vol. **5**, Issue 3, **2004**.

Kim, J., Bae, C., Kim, G., Simulation on the effect of the combustion parameters on the piston dynamics and engine performance using the Wiebe function in a free piston engine. *Applied Energy*; vol. **107**: pp. 446–455, **2013**.

Koelch, J. and Meyer, P.R., Food recycling oil-methyl ester: a biodiesel fuel for small diesel engines with SCR and oxidation catalysts, *International Journal of Energy for a Clean Environment*, vol. **6**, pp. 125-135, **2005**.

Komninos, N.P. and Rakopoulos, C.D., Modeling HCCI combustion of biofuels: a review, *Renewable and Sustainable Energy Reviews* ; vol. **16**, pp. 1588–610, **2012**.

Kotas, T.J., The Exergy Method of Thermal Plant Analysis; Elsevier: Amsterdam, The Netherlands, **2013**, ISBN-978-0-408-01350-5.

Kowalewicz, A., Eco-diesel engine fueled with rapeseed oil methyl ester and ethanol, *International Journal of Energy for a Clean Environment*, vol. **8**, pp. 373-387, **2007**.

Kumar, A., Shukla, S.K. and Tierkey, J.V., A Review of Research and Policy on Using Different Biodiesel Oils as Fuel for C.I. Engine, *Energy Procedia*, vol. **90**, pp. 292–304, **2016**.

Kumar, A., Tirkey, J.V. and Shukla, S.K., Comparative energy and economic analysis of different vegetable oil plants for biodiesel production in India, Renewable Energy, vol. **169**, pp. 266-282, **2021**.

Kumar, A.A., Biofuels (alcohols and biodiesel) applications as fuels for internal combustion engines. *Prog Energy Combust Sci*., vol. **33**, pp. 233–271, **2007**.

Kumar, R., Reader, G.T, Zheng, M., A Preliminary Study of Ignition Consistency and Heat Release Analysis for a Common-Rail Diesel Engine. *SAE* paper no. 2004-01-0932; **2004**.

Kumar, S. and Chaube, A.J., Critical review of jatropha biodiesel promotion policies in India. Energy Policy vol. **41**, pp. 775–781, **2012**.

Lesnik, L., Iijaz, J., Hribernik, A. and Kegl, B., Numerical and experimental study of combustion, performance and emission characteristics of a heavy-duty DI diesel engine running on diesel, biodiesel and their blends, *Energy Conversion and Management*, vol. **81**, pp. 534–546, **2014**.

Lim, S. and Teong, L.K., Recent trends, opportunities and challenges of biodiesel in Malaysia: An overview. *Renewable and Sustainable Energy Reviews*, vol. **14**, pp. 938–954. **2010**.

Lin, C.Y. and Lin, H.A., Diesel engine performance and emission characteristics of biodiesel produced by the peroxidation process, *Fuel*, vol. **85**, pp. 298-305, **2006**.

Lin, J.C. and Hou, S.S., Performance analysis of an air-standard Miller cycle with considerations of heat loss as a percentage of fuel's energy, friction and variable specific heats of working fluid, *International Journal of Thermal Sciences*, , vol. **47**, pp. 182–191, **2008**.

Liu, Z., Karim, G,A., Simulation of combustion process in gas-fuelled diesel engines. Part A, Journal of Power and Energy; 211(A2): pp. 159-169, **1997**.

Malaya, N., Meher, L.C., Naik, S.N. and Das, L.M., Production of biodiesel from high free fatty acid Karanja (Pongamia Pinnata) oil, *Biomass and Bioenergy*, vol. **32**, pp. 354-357, **2008**.

Mandolesi de Araújo, C. D., de Andrade, C.C., de Souza e Silva, E. and Dupas, F.A.,Biodiesel production from used cooking oil: A review,*Renewable and Sustainable Energy Reviews*, Elsevier, vol. **27**, pp. 445-452, **2013**.

Mani, M., Subash, C. and Nagarajan, G., Performance, emission and combustion characteristics of a di diesel engine using waste plastic oil. *Appl Therm Eng*, vol. **29**, pp. 2738–2744, **2009**.

Markov, V.A., Kamaltdinov, V.G., Zykov, S.A. and Sa, B., Optimization of the composition of blended biodiesel fuels with additives of vegetable oils, *International Journal of Energy for a Clean Environment*, vol. **20**, pp. 303-319, **2019**.

Martínez, G., Sánchez, N., Encinar, J.M. and González, J.F., Fuel properties of biodiesel from vegetable oils and oil mixtures. Influence of methyl esters distribution. Biomass and Bioenergy, vol. **63**, pp. 22–32, **2014**.

Masera, K. and Hossain, A. K., Production , Characterisation and Assessment of Biomixture Fuels for Compression Ignition Engine Application, *International Journal of Mechanical and Mechatronics Engineering*, vol. **11**, pp. 1857–1863. **2017**.

Mayeed, M.S. and Ghiaasiaan, S.M.,Waste energy recovery system for automobile engine exhaust gas and coolant, *International Journal of Energy for a Clean Environment*, vol. **18**, pp. 99-111, **2017**.

Meher, L.C., Vidya, S.S., Dharmagad, D. and Naik, S.N., Optimization of alkali catalyzed transesterification of Pongamia pinnata oil for production of biodiesel, *Bioresource Technology*, vol. **97**, pp. 1392-1397, **2006**.

Mendera, K.Z., Spyra, A. and Smereka, M., Mass fraction burned analysis. Journal of KONES Internal Combustion Engines, No. 3-4, ISSN 1231 - 4005, **2002**.

Mendow, G., Monella, F.C., Pisarello, M.L. and Querini, C.A., Biodiesel production from non-degummed vegetable oils: Phosphorus balance throughout the process. *Fuel Processing Technology*, vol. **92**, pp. 864–870, **2011**.

Misra, R.D. and Murthy, M.S., Blending of additives with biodiesels to improve the cold flow properties, combustion and emission performance in a compression ignition engine—A review. *Renew Sustain Energy Rev*, vol. **15**, pp. 2413-2422, **2011**.

Mujtaba, M.A., Kalam, M.A., Masjuki, H.H., Gul, M., Soudagar, M. E. M., Ong, H. C., Ahmed, Atabani, A.E., Razzaq, L. and Yusoff, M., Comparative study of nanoparticles and alcoholic fuel additives-biodiesel-diesel blend for performance and emission improvements, *Fuel*, vol. 279, **2020**. DOI: 10.1016/j.fuel.2020.118434.

Muralidharan, K. and Vasudevan, D., Performance, emission and combustion characteristics of a variable compression ratio engine using methyl esters of waste cooking oil and diesel blends. *Applied Energy*, vol. **88**, pp. 3959–3968, **2011**.

Nabi, M.N., Hoque, S.M.N. and Uddin, M.S., Production of biodiesel in Bangladesh from inedible renewable pithraj oil (aphanamixis polystachya) and experimental investigation of methyl esters as biodiesel on C.I. engine. *International Energy Journal,* vol. **11**, pp. 73-80, **2010**.

Nabi, M.N., Rahman, M.M., Islam, M.A., Hossain, F.M., Brooks, P., Rowlands, W.N., Tulloch, J., Ristovski, Z.D. and Brown, R. J., Fuel characterisation, engine performance, combustion and exhaust emissions with a new renewable Licella biofuel, *Energy Conversion and Management*, vol. **96**, pp. 588–598, **2015**.

Naylor, R.L. and Higgins, M. M., The political economy of biodiesel in an era of low oil prices. *Renewable and Sustainable Energy Reviews*, vol. **77**, pp. 695–705, **2017**.

Neto Da Silva, F. and Arriscado De Oliveira, A., Technical assessment of diesel fuel-oleic sunflower methyl ester blends utilization in a large diesel engine, *International Journal of Energy for a Clean Environment*, vol. **7**, pp. 29-41, **2006**.

No, S-Y., Inedible vegetable oils and their derivatives for alternative diesel fuels in CI engines: a review, *Renew Sustain Energy Rev.*,vol. **15**, no.1, pp. 131–149, **2011**.

Ogunkunle, O. and Ahmed, N.A., A review of global current scenario of biodiesel adoption and combustion in vehicular diesel engines, *Energy Reports*, vol. **5**, pp. 1560–1579, **2019**.

Ogunkunle, O. and Ahmed, N.A., Performance Evaluation of a Diesel Engine Using Blends of Optimized Yields of Sand Apple (Parinari polyandra) Oil Biodiesel. *Renewable Energy*, **2018**. DOI:10.1016/j.renene.2018.09.040.

Oyelade, J.O., Idowu, D.O., Oniya, O.O. and Ogunkunle, O., Optimization of biodiesel production from sandbox (Hura crepitans L.) seed oil using two different catalysts. *Energy Sources, Part A: Recovery, Utilization, and Environmental Effects*, vol. **39**, pp. 1242–1249, **2017**.

Panigrahi, N., Mohanty, M.K., Mishra, S.R. and Mohanty, R.C., Energy and Exergy Analysis of a Diesel Engine Fuelled with Diesel and Simarouba Biodiesel Blends, *J. Inst. Eng. India,* Ser. C, vol. **99**, pp. 9–17, **2018**.

Park S.H., Robust Design and Analysis for Quality Engineering. Chapman & Hall, London. **1996**.

Paul, A., Panua, R. and Debroy, D., An Experimental study of Combustion, Performance, Exergy and Emission characteristics of a CI engine fueled by Diesel-Ethanol-Biodiesel Blends, *Energy*, **2017**. DOI: 10.1016/j.energy.2017.09.137.

Payri, F., Olmeda, P., Martín, J. and García, A., A complete 0D thermodynamic predictive model for direct injection diesel engines. *Applied Energy*, vol. **88**, pp. 4632–4641, **2011**.

Phadke M.S., Quality Engineering Using Design of Experiments, Quality Control, Robust Design, and the Taguchi Method. Wadsworth & Books, *Pacific Grove*.**1988**.

Piaszyk, J., Animal fat (tallow) as fuel for stationary internal combustion engines. University of Birmingham, **2012**.

Pohit, S,. Biswas, P.K., Kumar, R. and Goswami,A.,Pricing model for biodiesel feedstock: a case study of Chhattisgarh in India, *Energy Policy*, vol. **38**, pp. 7487–7496, **2010**.

Pulkrabek, W., Engineering fundamentals of the internal combustion engine, second ed.Pearson Prentice-Hall, Upper Saddle River, New Jersey, USA, **2004**.

Puna, J.F., Gomes, J.F., Bordado, J.C., Correia, M., Joana N. and Dias, A.P.S., Screening heterogeneous catalysts for transesterification of triglycerides to biodiesel, *International Journal of Energy for a Clean Environment*, vol. **12**, pp. 45-54, **2011**.

Rakopoulos, C.D. and Giakoumis, E.G., Simulation and Analysis of a Natural Aspirated IDI Diesel Engine under Transient Conditions Comprising The Effect of Various Dynamic and Thermodynamic Parameters, *Energy Convers. Mgmt*, vol. **39**. pp. 465-484, **1998**.

Rakopoulos, C.D, Antonopoulos, K.A, Rakopoulos, D.C, Giakoumis, E.G., Study of combustion in a divided chamber turbocharged diesel engine by experimental heat release analysis in its chambers, **Applied Thermal Engineering**, vol. **26**: pp. 1611–20, **2006.**

Ramadhas, A., Jayaraj, S. and Muraleedharan, C., Use of vegetable oils as IC engine fuels—a review, *Renew Energy*,vol. **29**, no. 5, pp. 727–742, **2004**.

Ramadhas, A.S., Jayaraj, S. and Muraleedharan, C., Theoretical modeling and experimental studies on biodiesel-fueled engine, *Renewable Energy*, vol. **31**, pp. 1813–1826, **2006**.

Reitz R.D., Directions in internal combustion engine research. *Combustion and Flame*, vol. **160**, pp. 1–8, **2013**. DOI:10.1016/j.combustflame.2012.11.002.

Robbio, R.D., Cameretti, M.C. and Tuccillo, R., Ignition and combustion modelling in a dual fuel diesel engine, *Propulsion and Power Research*, vol. **9**, pp. 116-131, **2020**.

Rodrigo A.A. Munoz, David M. Fernandes, Douglas Q. Santos, Tatielli G.G. Barbosa and Raquel M.F. Sousa, Biodiesel: Production, Characterization, Metallic Corrosion and Analytical Methods for Contaminants, Biodiesel - Feedstocks, *Production and Applications, Zhen Fang, IntechOpen*, **2012**, DOI: 10.5772/53655.

Rosha, P., Mohapatra, S. K., Mahla, S. K., Cho, H., Chauhan, B. S. and Dhir, A., Effect of compression ratio on combustion, performance, and emission characteristics of compression ignition engine fueled with palm (B20) biodiesel blend, *Energy*, vol. **178**, pp. 676-684, **2019**.

Saario, A., Makiranta, R., Backlund, A. and Oksanen, A., Optimization methods in minimization of emissions from combustion, *International Journal of Energy for a Clean Environment*, vol. **12**, pp. 15-29, **2011**.

Sakhrieh, A., Abu-Nada, E., Al-Hinti, I., Al-Ghandoor, A. and Akash, B., Computational thermodynamic analysis of compression ignition engine, *International Communications in Heat and Mass Transfer*, vol. **37**, pp. 299–303, 2010.

Saravanan, A.P., Mathimani, T., Deviram, G., Rajendran, K. and Pugazhendhi, A., Biofuel policy in India: A review of policy barriers in sustainable marketing of biofuel, *Journal of Cleaner Production*, **2018**. DOI:10.1016/j.jclepro.2018.05.033

Sarin, A., Arora, R., Singh, M.P., Sarin, R., Malhotra, R.K. and Kundu, K., Effect of blends of Palm-Jatropha-Pongamia biodiesels on cloud point and pour point. *Energy*, vol. **34**, pp. 2016-2021, **2009**.

Sathish, R.K, Optimization of biodiesel production from Manilkarazapota (L.) seed oil using Taguchi method. *Fuel*, vol. **140**, pp. 90–96, **2015**.

Sayin, C. and Gumus, M., Impact of compression ratio and injection parameters on the performance and emissions of a DI diesel engine fueled with biodiesel-blended diesel fuel. *Appl Therm Eng*,vol. **31**, pp. 3182–3188, **2011**.

Scarlat, N., Dallemand, J.-F., Monforti-Ferrario, F., Banja, M. and Motola, V., Renewable energy policy framework and bioenergy contribution in the European Union – An overview from National Renewable Energy Action Plans and Progress Reports. *Renewable and Sustainable Energy Reviews*, vol. **51**, pp. 969–985, **2015**. DOI:10.1016/j.rser.2015.06.062.

Selvan, V.A.M., Anand, R.B. and Udayakumar, M., Combustion characteristics of diesohol using biodiesel as an additive in a direct injection compression ignition engine under various compression ratios, *Energy Fuels*, vol. **23**, pp. 5413-5422, **2009**. DOI:10.1021/ef900587h.

Semwal, S., Arora, A.K., Badoni, R. and Tuli, D.K., Biodiesel production using heterogeneous catalysts. *Bioresource Technology*, vol. **102**, pp. 2151–2161, **2011**.

Sendilvelan, S. and Bhaskar, K., Experimental analysis of pilot injection-assisted premixed charge compression ignition to reduce emissions with jatropha oil methyl ester in a diesel engine, *International Journal of Energy for a Clean Environment*, vol. **17**, pp. 67-80, **2016**.

Senthil, M.K., Ramesh, A. and Nagalingam, B., Complete vegetable oil fueled dual fuel compression ignition engine. *SAE*: paper no: 2001-28-0067.

Setyawan, D., The Impacts of the Domestic Fuel Increases on Prices of the Indonesian Economic Sectors, Energy Procedia, vol. **47**, pp. 47 – 55, **2014**.

Shahid, E.M. and Jamal, J., Production of biodiesel: A technical review. *Renewable and Sustainable Energy Reviews*, vol. **15**, pp. 4732-3745, **2011**.

Sharma, A. and Murugan, S., Potential for using a tyre pyrolysis oil-biodiesel blend in a diesel engine at different compression ratios, *Energy Conversion and Management*, vol. **93**, pp. 289–297, **2015**.

Sharma, Y.C. and Singh, B., Development of biodiesel: Current scenario. *Renewable and Sustainable Energy Reviews*, vol. **13**, pp. 1646-1651, **2009**.

Sharon, H., Karuppasamy, K., Soban Kumar, D.R. and Sundaresan, A., A test on DI diesel engine fueled with methyl esters of used palm oil. *Renewable Energy*, vol. **47**, pp. 160–166, **2012**.

Singh Pali, H., Sharma, A., Singh, Y. and Kumar, N., Sal biodiesel production using Indian abundant forest feedstock, *Fuel*, vol. **273**, **2020**. DOI:10.1016/j.fuel.2020.117781.

Singh, D., Sharma, D., Soni, S.L., Sharma, S. and Kumari, D., Chemical compositions, properties, and standards for different generation biodiesels: A review, *Fuel,* vol. **253**, pp. 60–71, **2019**.

Singh, J. and Gu S., Commercialization potential of microalgae for biofuels production, *Renew Sustain Energy Rev*, vol. **14**, pp. 2596–2610, **2010**.

Singh, S.P. and Singh, D., Biodiesel production through the use of different sources and characterization of oils and their esters as the substitute of diesel: A review, *Renewable and Sustainable Energy Reviews,* vol. **14**, pp. 200-216, **2010**.

Song, E., Shi, X., Yao, C. and Li, Y., Research on real-time simulation modelling of a diesel engine based on fuel inter-zone transfer and an array calculation method, *Energy Conversion and Management*, vol. **178**, pp. 1–12, **2018**. DOI:10.1016/j.enconman.2018.10.014.

Stone, R., Introduction to Internal Combustion Engines–Second Edition, Society of Automotive Engineers, Inc., Warrendale, PA, **1994**.

Suresh, M., Jawahar, C.P. and Richard, A., A review on biodiesel production, combustion, performance, and emission characteristics of non-edible oils in variable compression ratio diesel engine using biodiesel and its blends, *Renewable and Sustainable Energy Reviews,* vol. **92**, pp. 38-49, **2018**.

Swaraz, A.M., Satter, M.A., Rahman, M.M., Asad, M.A., Khan, I. and Amin, M.Z., Bioethanol production potential in Bangladesh from wild date palm (Phoenix sylvestris Roxb.): An experimental proof. *Industrial Crops and Products*, vol. **139**: 111507, **2019**. doi:10.1016/j.indcrop.2019.111507.

Szulczyk, K.R. and Khan, A.R., The Potential and Environmental Ramifications of Palm Biodiesel: Evidence from Malaysia. *Journal of Cleaner Production*. **2018**. doi:10.1016/j.jclepro.2018.08.241.

Tamilselvan, P., Nallusamy, N. and Rajkumar, S., A comprehensive review on performance, combustion and emission characteristics of biodiesel fuelled diesel engines, *Renewable and Sustainable Energy Reviews,* vol. **79**, pp. 1134–1159, **2017**.

Tang, D., Wei, J., Wu, Y. and Li, N., Simulation and experimental study of the combustion and injection characteristics of small non-road diesel engine fueled with diesel/bio-diesel blends, *International Journal of Energy for a Clean Environment*, vol. **15**, pp. 1-18, **2014**.

Uslu, S. and Aydin, M., Effect of operating parameters on performance and emissions of a diesel engine fueled with ternary blends of palm oil biodiesel/diethyl ether/diesel by Taguchi method, *Fuel*, vol. **275**, **2020**. DOI:10.1016/j.fuel.2020.117978.

Vasudevan, D., Muralidharan, K. and Sheeba, K.N., Performance, emission and combustion characteristics of biodiesel fuelled variable compression ratio engine, *Energy*, vol. **36**, pp. 5385–5393, **2011**.

Veljkovic, V.B., Lakicevic, S.H., Stamenkovic, O.S., Todorovic, Z.V. and Lazic, M.L., Biodiesel production from Tobacco (Nicotiana Tabacum L.) seed oil with high content of free fatty acids, *Fuel*, vol. **85**, pp. 2671-2705, **2006**.

Venkatesan, H., Seralathan S. and Micha Premkumar, T., Recovery, Utilization, and Environmental Effects, *Energy Sources*, Part A, vol. **39**, pp. 2065-2071, **2017**.

Wan Ghazali, W.N.M., Mamat, R., Masjuki, H.H. and Najafi, G., Effects of biodiesel from different feedstocks on engine performance and emissions: A review. *Renewable and Sustainable Energy Reviews*, vol. **51**, pp. 585-602, **2015**.

Wang, R., Hanna, M.A., Zhou, W.W., Bhadury, P.S., Chen, Q., Song, B.A. and Yang, S., Production and selected fuel properties of biodiesel from promising non-edible oils: Euphorbia lathyris L., Sapium sebiferum L. and Jatropha curcas L. *Bior- esour Technol*, vol. **102**, pp. 1194–1199, **2011**.

Xiao, S., Sun, W., Du, J. and Li, G., Application of CFD, Taguchi Method, and ANOVA Technique to Optimize Combustion and Emissions in a Light Duty Diesel Engine, *Mathematical Problems in Engineering*, **2014**. DOI: 10.1155/2014/502902.

Yamaki, Y., Mori, K., Kamikubo, H., Kohketsu, S., Mori, K. and Kato, T., Application of common rail fuel injection system to a heavy duty diesel engine. SAE paper 942294; **1994**.

References

Yesilyurt, M.K., A detailed investigation on the performance, combustion, and exhaust emission characteristics of a diesel engine running on the blend of diesel fuel, biodiesel and 1-heptanol (C7 alcohol) as a next generation higher alcohol, *Fuel*, vol. **275**, **2020**. DOI:10.1016/j.fuel.2020.117893.

Yıldız, M. and AlbayrakCeper, B., Zero-dimensional single zone engine modeling of an SI engine fuelled with methane and methane-hydrogen blend using single and double Wiebe Function: A comparative study, *International journal of hydrogen energy*, **2017**. DOI:http://dx.doi.org/10.1016/j.ijhydene.2017.07.016.

Zahan, K.A. and Kano, M., Biodiesel Production from Palm Oil, Its By-Products, and Mill Effluent: A Review, *Energies*, vol. **11**, **2018**. DOI:10.3390/en11082132.

Zheng, J. and Caton, J.A., Second law analysis of a low temperature combustion diesel engine: effect of injection timing and exhaust gas recirculation, *Energy*, vol. **38**, pp.78–84, **2012**.

Annexure 1: Photographs of instruments

Figure A1.1: Flashpoint tester, hydrometer and Specific gravity bottle

Figure A1.2: Viscometer

Figure A1.3: Bomb calorimeter

(Picture Courtesy Chemical Engineering laboratory, Jadavpur University)

Annexure 2

Technical Specification of the Instruments

Sl. No.	Description	Unit	Data
	Technical specifications of the diesel engine		
1	Model type	-	Kirloskar TV1, Single-cylinder, 4-stroke
2	Type of injection	-	Direct
3	Rated power	kW	3.5
4	Rated speed	rpm	1500
5	Bore x Stroke	mm	87.5 x 110
6	Compression ratio	-	CR 17.5, Modified to VCR engine CR range 12 to 18
7	Method of cooling	-	Water cooled
8	Piston type	-	Bowl-in-piston
9	Connecting Rod Length	mm	234
10	Type of fuel injection	-	Pump-line-nozzle injection system
11	Number of valves	-	2
12	Start of injection	◦CA bTDC	23
13	Nozzle opening pressure	bar	210
14	Inlet valve opening	◦CA bTDC	4.5
15	Inlet valve closing	◦CA aBDC	35.5
16	Exhaust valve opening	◦CA bBDC	35.5
17	Exhaust valve closing	◦CA aTDC	4.5

Annexure 2: Technical Specification of the Instruments

Sl. No.	Description	Unit	Data
	Technical specifications of the Dynamometer		
1	Model type		Technomech, model TMEC10
2	Range		10BHP@1500- 5000 RPM
3	Dynamometer Loading unit		Model AX-155 (Apex). Type constant speed, Supply 230V AC.
	Technical specifications of the Piezo sensor		
1	Model type		Model S111A22 (PCB Piezotronics), Diaphragm stainless steel type & hermetic sealed
2	Pressure Range	psi	0- 5000
3	Sensitivity (± 0.1 mV/psi)	mV/psi	1.0
4	Temperature Range (Operating)	°C	-73 to +135
5	White coaxial Teflon cable		Model 002C20 (PCB piezotronics), Length 20 ft, Connections one end BNC plug and another end 10-32 micro
6	Piezo powering unit		Make-Apex, Model AX-409.

Annexure 2: Technical Specification of the Instruments

Technical specifications of the other sensors, device and component

Sl. No.	Description	Data
1	Crank angle sensor	Make Kubler, Model 8. KIS40.1361.0360 Clamping/Synchro flange, 6x12.5mm shaft, Supply= 5VDC Termination: 2m long axial cable
2	Temperature sensor	Make Radix Type K, Ungrounded, Sheath Dia.6mmX110mmL, SS316, Connection 1/4"BSP (M),
3	Temperature transmitter	Make ABUSTEK, Model: Fr Block, Thermocouple (K), Range: 0 To 1200ºC, Output: 4-20 mA, Power supply: 24 V DC, Pre-calibrated to 1200 Deg C
4	Temperature sensor	Make Radix, Type Pt100, Sheath Dia.6mmX110mmL, SS316, Connection 1/4"BSP(M),
5	Temperature transmitter	Make ABUSTEK, Model: Fr Block, Input: PT-100, Range: 0 To 100ºC, Output: 4-20 mA, Power supply: 24 V DC, Pre-calibrated to 100 Deg C
6	Data acquisition device	NI USB-6210 Bus Powered M Series Multifunction DAQ Device, NI DAQmx driver Software

Annexure 2: Technical Specification of the Instruments

7	Propeller shaft	Make Hindustan Hardy Spicer, Model 1260, Type A
Sl. No.	**Description**	**Data**
8	Manometer	Make Apex, Model MX-104, Range 100-0-100 mm, Type U tube,
9	Fuel measuring unit	Make Apex, Glass, Model: FF0.012
10	Redwood Viscometer	Working Temperature 99 ◦C Electrically Heated Immerssion Heater 1 Sample Capacity.
11	Pensky-Martens closed cup flash point tester	Temperature Range Ambient To 370°C, Manually Controlled Ramp, 430 W Power, Size 280 X 350 X 250 mm.
12	Bomb calorimeter	Static Jacket Calorimetry, 2 Tests Per Hour, Operator Time Per Test is 25 Minutes, Manual Oxygen Fill, Manual Bucket Fill, Manual Bomb Wash.
13	Load sensor	Make Sensotronics Sanmar Ltd., Model 60001, Type S beam, Universal, Capacity 0-50 kg
14	Load indicator	Make ABUS, model SV8-DC10, 85 to 270VAC, retransmission output 4-20 mA
15	Power supply	Make Meanwell, model NES-15-24, O/P 24 V, 0.7 A
16	Fuel flow transmitter	Make Yokogawa, Model EJA110E-JMS5J-912NN, Calibration range 0-500 mm H2O, Output linear
17	Air flow transmitter	Make WIKA, Model SL-1-A-MQA-ND-ZA4Z-ZZZ,

		output 4-20 mA, supply 10-30 Vdc, conn. 1/2"NPT(M), Range (-)25 - 0 mbar.
18	Rotameter	Make Eureka Model PG 5, Range 25-250 lph, Connection ¾" BSP vertical, screwed
19	Rotameter	Make Eureka Model PG 6, Range 40-400 lph, Connection ¾" BSP vertical, screwed
20	Water Pump	Make Kirloskar, Model Mini 18S, HP 0.5, Size 1" x 1", Single ph 230 V AC
21	Engine software	'ICEngineSoft_9_0' engine combustion and performance analysis software